



# Recent developments of supported and magnetic nanocatalysts for organic transformations: an up-to-date review

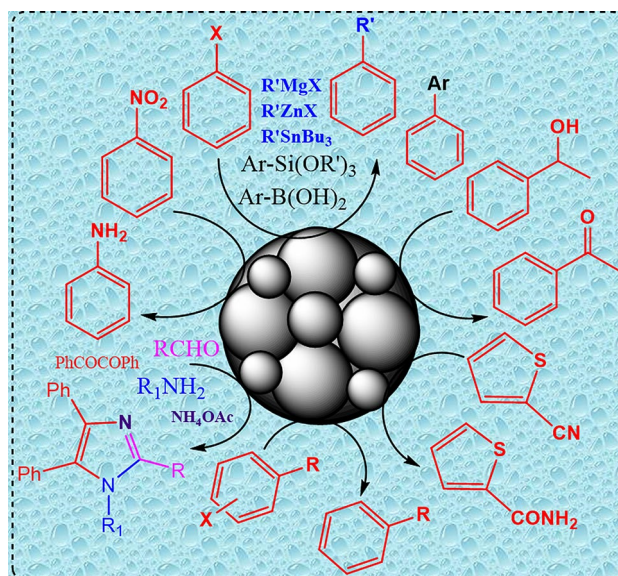
Shushay Hagos Gebre<sup>1</sup>

Received: 5 December 2020 / Accepted: 8 May 2021 / Published online: 27 May 2021  
© King Abdulaziz City for Science and Technology 2021

## Abstract

Designing and building an ideal catalyst for organic reactions is needed to increase the efficiency, reaction conditions, and to reduce its environmental impacts. The growth of nanotechnology is realized in the production of various nano-level catalysts for different applications. The as-synthesized nanocatalysts are easily manipulated to a desired shape and size with a high surface area to volume ratio, which is their critical property of the interaction of the nanomaterials with the substrates. These days, a vast array of catalysts (nanocatalysts) such as metals, metal oxides, magnetic, and alloyed/mixed nanocatalysts are applied in organic reactions to synthesize important chemicals in industries and pharmaceutical sectors with a high yield, selectivity, and reusability via reduction/hydrogenation, oxidation, condensation, C–C coupling, cyclization, and more. Consequently, this present review highlights the application of various nanocatalysts in organic reactions by combining certain proposed reaction mechanisms that have shown the impact of nanoparticles on the reactions. The factors influencing nanocatalyst performances are also discussed. Finally, the conclusion and future prospects are conveyed.

## Graphic abstract



**Keywords** Nanoparticles · Organic synthesis · Catalytic activity · Nanocatalyst · Heterogeneous catalyst

✉ Shushay Hagos Gebre  
shushayhagos@gmail.com

<sup>1</sup> Department of Chemistry, College of Natural and Computational Science, Jigjiga University, P.O Box, 1020 Jigjiga, Ethiopia

## Introduction

The continuous advancements in chemical transformation in recent decades have contributed vastly to chemical processing efficiencies using cost-effective precursors and catalysts to contribute some aspects of greenness (Varma 2016). In this regard, catalyst plays a central role where various chemical industries transform organic substrates into useful fine chemicals, pharmaceutical drugs, agrochemicals, cosmetics, and more (Amirmahani et al. 2020; Gao et al. 2021). Importantly, the continuous growth of nanotechnology has paramount importance in improving efficiency as the size of the catalytic particle plays a strong influence on the activity of the heterogeneous and homogeneous catalysis routes. Therefore, the concept of nanocatalyst is a hot issue for researchers due to its efficiency and selectivity, along with the environmental friendly synthetic approach, easily recycle and inexpensive material (Beletskaya and Tyurin 2010; Das 2016).

Nanomaterials in various forms possess distinct and unique physicochemical properties in relation to the bulk materials from which they are manufactured. This is due to the corollaries of their sizes, shapes, and synergistic effects (Holade et al. 2015). Recently, the synthesis of metals, metal oxides, magnetic and hybrid nanomaterials has undergone extensive nanotechnology studies for various applications. For instance, palladium nanoparticle (NPs), the most versatile element is used in organic reaction via alloying, decorating, or assisted with organic stabilizers, dendrimers, polymers, and iron having the advantage of magnetically recoverable and recyclable nanocatalysts. The development and innovation of novel nanocatalysts for organic synthesis are not only to increase the efficiency of the catalytic activity, but also to reduce the risks of environmental pollution (Kann 2010; Varma 2014; Tanna et al. 2016; Basavegowda et al. 2017; Mohammadparast et al. 2019; Dong et al. 2021). The nano-level materials may be designed in the form of NPs, nanocomposites, polymer-encapsulated NPs, nanorods, nanotubes, nanotemplates, nanowires, quantum dots, nanoflowers, etc. should be designed from the green chemistry point of view, free of phosphine, suitable for green solvents such as ionic liquids (ILs), supercritical fluids, water, fluorinated phases, etc. and from the green chemistry principle (atom saving, dematerialization, energy-saving, raw material diversification and more) (Nacci and Cioffi 2011). Separation of the catalyst from the reaction medium is another important event; however, in some cases, their appearance in nanoscale is difficult for their recovery. The nanocatalyst separation from the reaction mixture via filtration, extraction, or centrifugation strategies is tedious and time-consuming, or sometimes impossible. In recent times, the nanocatalysts

are acting as a bridge between heterogeneous and homogeneous catalysts which provides a large surface area for an increased rate of reaction and ease of their recovery from the reaction mixtures (Fig. 1). Particular attention is given to the heterogeneous magnetic nanocatalysts (MNCs) because of their insoluble and paramagnetic nature, which can be recovered by an external magnet without time-consuming procedures (Gross et al. 2015; Abu-dief and Abdel-fatah 2017; Ghobadi et al. 2021).

Today, the catalytic activity of the nanocatalyst represents a driving force and rich resource for chemical processes, used in both industries and in academia (Gawande et al. 2016). The NPs ranging from 1 to 100 nm are highly interesting and attracting researchers to use them in a wide range of technological applications (Gebre and Sendeku 2019). The catalytic efficiency, high yield, conversion, reusability, easily separated, and selectivity of the nanocatalyst is due to the small size, high surface area, shape, composition, the arrangement of the nanocatalyst as well as their interaction with the supporting materials. The nanostructured materials are designed by introducing inorganic or organic supporting materials to prevent agglomeration, modify their functional groups, improving the recyclability of the nanocatalyst, retain their magnetism and stability during the synthesis. For instance, free Au cannot be recycled as well as its catalytic activity depends on its size and morphology; therefore, size and morphology control synthesis of Au NPs applying appropriate supporting materials is a prime interest (Sharma et al. 2016a; Qin et al. 2019; Astruc 2020). In another case, MNCs such as  $\text{Fe}_3\text{O}_4$  and  $\gamma\text{-Fe}_2\text{O}_3$  can lose their magnetism due to fast oxidation in air and coating their surface via biopolymers/ILs like polyvinylpyrrolidone (PVP), polyethylene glycol (PEG), polyvinyl alcohol (PVA), dextran, cellulose, amino acids, etc. keep them magnetized. The coating of MNCs with large molecules which are sterically

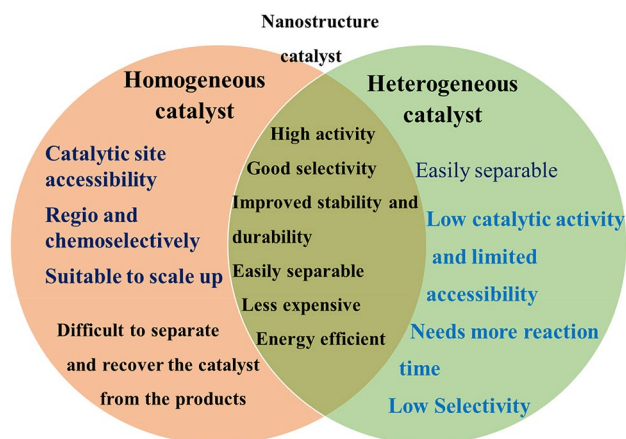


**Fig. 1** Comparison of the nanocatalysts with homogeneous and heterogeneous catalysts

crowded, charged and functional polymers can also protect the agglomeration and improve their stability in aqueous media (Rossi et al. 2014; Díaz-hernández et al. 2018; Chen et al. 2020; Escoda-torroella et al. 2021; Gebre 2021). Indeed, the attached ligands have multiple functions which offered additional benefit such as increasing activity at the core of the metal, synergistic effect, and their binding ability towards the metal is crucial for the long-term stability of the nanocatalyst. For example, carboxyl and hydroxyl groups have a strong binding affinity for iron oxide NPs, while thiols have a high affinity for gold-bearing surfaces (Heuer-jungemann et al. 2019). A weak bond between the supporters and the metal core leads to sintering and leaching of the metal during applications. Therefore, the use of magnetically recyclable nanocatalysts in an aqueous medium is a prime choice for chemists due to its availability, safe, economically feasible, environmentally benign, and easily handle with better product yields (Gawande et al. 2013). It should be noted here that most of the MNCs are superior to the other in terms of their stability (negligible leaching), less catalyst load required, and ease of separation (Sharma et al. 2016b). Nanocatalyst with a large surface area plays a major role in various organic reactions such as hydrogenation, reduction, oxidation, carbon–carbon (C–C), nitrogen–nitrogen (N–N), and carbon–nitrogen (C–N) coupling reactions, cyclization, condensation, and more as demonstrated in Fig. 2 (Chng et al. 2013). The increased surface area provides the advantage of increasing the reaction rate (Govan and Gun'ko 2014). Immobilization of a homogeneous metal complex on solid supports is a common method for producing heterogeneous molecular catalysts. Among various types of solid catalysts, transition metal complexes supported on metal–organic frameworks (M@MOFs) represent one of the most important groups, owing to their advantages such as high surface area, defined pore size, and tunable structure in their framework (Alamgholiloo et al. 2019, 2020). It has been confirmed that, the high surface area exhibited to increase the catalytic activity (yield and conversion) while modifying or blocking some part of the catalytic site or increasing the surface crowdedness binds the complex reactant molecule to the specific site without

competing for other reaction pathways lead to increase the selectivity and specificity of the reaction (Jin et al. 2017).

Given the growing interest in research and promising potential applications in their catalytic properties, it is ideal and timely to offer a comprehensive overview of the latest developments of nanocatalysts. In this review, the potential application of the nanocatalyst in the coupling, oxidation, reduction, condensation, heterocyclic synthesis, and dehalogenation reactions is summarized based on their efficiency, recyclability, yield, stability, and environmental concerns. Finally, the major challenges are highlighted and the conclusion is offered based on the latest developments in the field of the catalyst. I hope this review will provide guidance for researchers to rationally design various noncatalytic structures with unique morphologies and sizes for organic synthesis. Meantime, excellent articles from (Sharma et al. 2015; Zhang et al. 2019b; Bhaskaruni et al. 2020) were published on the basis of different aspects of the synthesis and applications of nanocatalysts. Despite the availability of literature reviews, they specifically focus on the synthesis approaches, or specific to MNCs for heterocyclic scaffolds, none of the recent reviews compiles broad applications of the nanomaterials. This review is exhaustive on a variety of nanocatalysts for various organic responses with their efficiency, stability, and recyclability. It is specifically aimed at compiling, discussing, and summarizing the recent trends on the nanocatalyst applications in organic reactions by addressing mechanistic aspects and characterizations. I hope this paper is an updated literature review on the varieties of nanomaterials for organic reaction applications.

## Applications of nanocatalyst in organic reactions

### Carbon–carbon coupling reactions

Cross-coupling reactions are some of the most studied reactions in modern chemistry using metal catalysts in recent decades (Pechtl et al. 2010; Niakan et al. 2021). Very important compounds for pharmaceuticals, agrochemicals, polymers, biologically active natural products, intermediates, fine chemicals, and high-technology materials, etc. can be obtained by the C–C, C–N, S–S, C–O linkage reactions (Hong et al. 2020; Sharma et al. 2020; Sun et al. 2020). Palladium-catalyzed C–C coupling reactions of aryl halides, such as Suzuki cross-coupling reactions also called Suzuki–Miyaura, Stille, Heck cross-coupling or refereed as Mizoroki–Heck reactions, Ullmann reactions, etc. (Fig. 3b), are powerful reactions for joining of biaryl or coupling of unsaturated and saturated alkyl structures into organic reactions (Narayanan 2010; Chen et al. 2015). The oxidizing addition of the organic electrophile leads to the formation

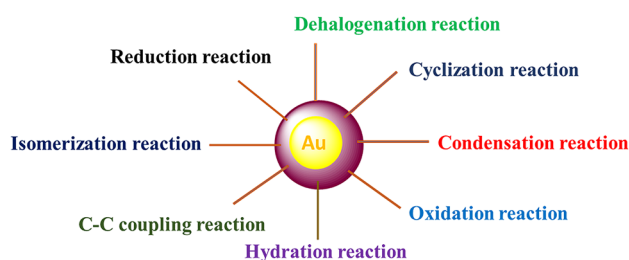
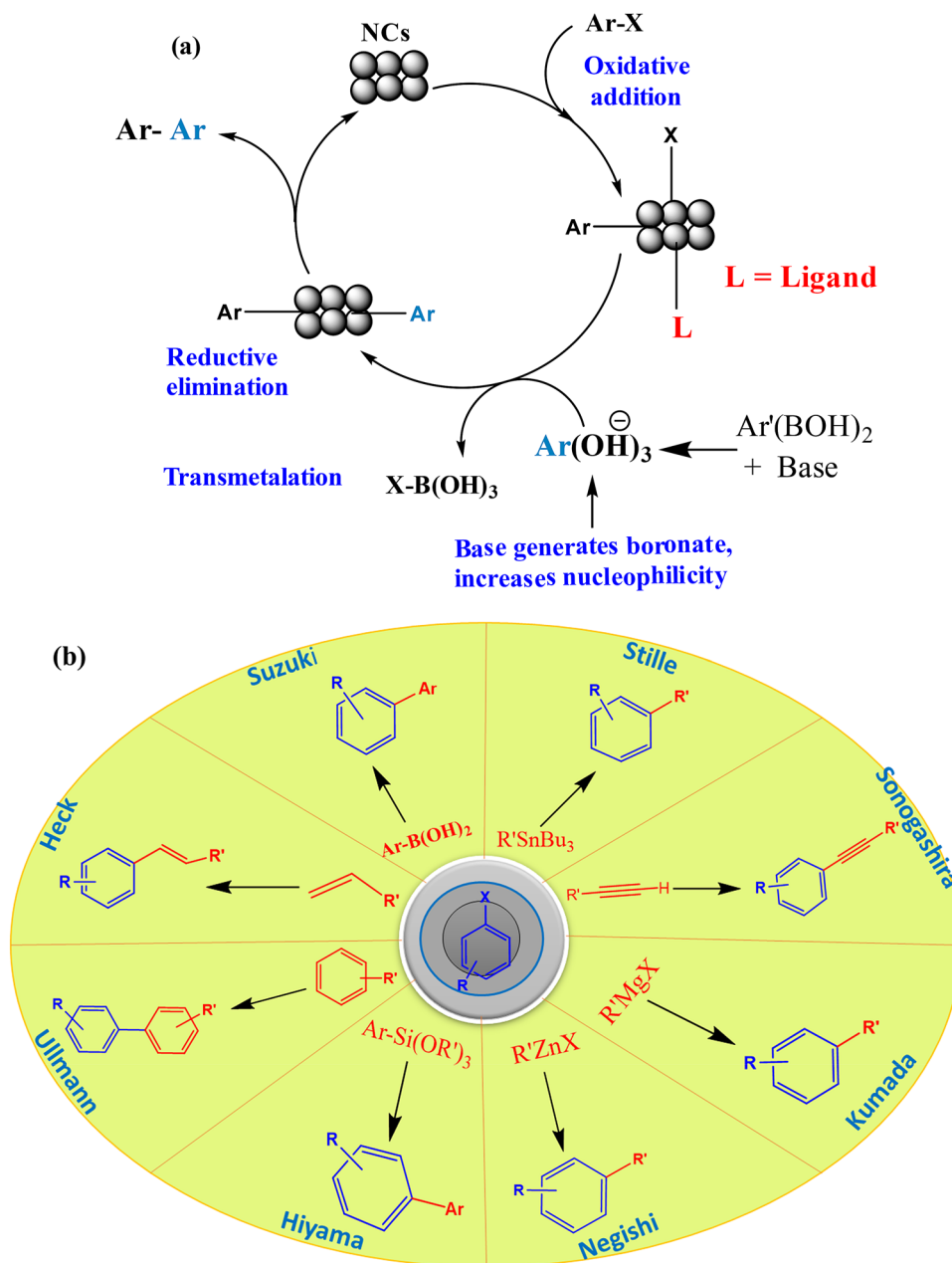


**Fig. 2** Application of nanoparticles in organic reactions

**Fig. 3 a** General reaction mechanism of C–C coupling reaction by the nanocatalyst **b** C–C bond-forming cross-coupling reactions (where X = Cl, Br, or I)



of the unsaturated metal nanocatalyst complex. The reduction elimination terminates the coupling products with the regeneration of the nanocatalyst for further reuse as shown in Fig. 3a. The application of bulk metals for C–C coupling is not common except for some metals such as bulk Pd due to their low catalytic activity, non-recyclable, and environmentally unfavorable activity. However, metals at the nano-level are highly efficient and active for the C–C coupling reaction in aqueous solutions with highly selective, recyclability, and take place under normal conditions (Holz et al. 2019; Jani and Bahrami 2020). In the coupling reaction, both the electron-rich and electron-deficient aryl halides are coupled to produce moderate efficiency, high selectivity, and

conversion. Less reactive aryl halides were performed at higher temperatures to meet the conversion. The yield of the product depends on the presence of electron-withdrawing and releasing groups in the aromatic derivatives (Goonesinghe et al. 2020). Ayad et al. (2019) engineered green and water-soluble Pd NPs supported on phosphonic acids for the Suzuki Miyaura, Sonogashira, and Heck cross-coupling reactions. The NP prepared environmentally friendly showed promising catalytic activity with high turnover frequencies (TOF) reached with low Pd NP load without any addition of toxic solvents.

Venkatesan and Santhanalakshmi (2010) developed Au/Ag/Pd trimetallic nanoparticle (TNP)-based catalysts for

Sonogashira coupling reactions between phenylacetylene and iodobenzene. Thus, the trimetallic NPs was highly active and catalyzed the reaction with a small amount of dose [0.5 mol% of Au–Ag–Pd (1:1:1)] to achieve 99.5% of 1,2-diphenylethyne yield and conversion; however, the Pd and Au–Pd NP yield 94% and 96%, respectively, under the same reaction condition (dimethylformamide (DMF))–H<sub>2</sub>O solvent, K<sub>2</sub>CO<sub>3</sub>, 120 °C reaction temperature, and 2 h). Cu NP was used for the synthesis of chromene derivatives using aromatic aldehydes, 4-hydroxy coumarins, and malononitrile reactants mixed together and allowed to stir on a magnetic stirrer at the 70 °C upon adding the Cu NPs. The reaction progression was controlled using thin-layer chromatography (TLC) using *n*-hexane: ethyl acetate (8:2) as an eluent. The catalyst was removed by adding ethanol, heating it, and then filtering it out of the reaction mix. The products were elucidated using Proton Nuclear Magnetic Resonance (<sup>1</sup>H NMR), Fourier Transform Infrared (FTIR), Mass Spectrometry (MS), and the melting point of the product was compared with authentic samples from the literature (Tanna et al. 2016). In addition, the catalyst did not lose its catalytic activity even after five consecutive cycles, indicating the stability and proper reuse of the nanocatalyst in the reaction model. The attachment of Cl, Br, and CN substituents at

the para position of the aldehyde (benzaldehyde) increases the yield of the chromene derivatives to 90, 93, and 95% yields, respectively, in 65–70-min reaction time (Balou et al. 2019). In another study, Chitosan functionalized Fe<sub>3</sub>O<sub>4</sub> NPs was used for 2-amino-4H-chromene synthesis using a one-pot strategy (Fig. 4). The MNCs was designed to produce a 99% yield of the product under ultrasound irradiation in a short time (20 min). Furthermore, the MNCs were recovered using a magnet and reused five times without noticeable loss. Only a 2% yield was decreased in the fourth run (Safari and Javadian 2015).

Suramwar et al. (2016) synthesized Cu NPs (40–80 nm) using a reduction method applying sodium borohydride and starch as reducing and stabilizing agents. The as-synthesized NP was checked in the Ullman reaction for the synthesis of biphenyl from iodobenzene and the NPs has been performed a 92% yield of the product (biphenyl); however, the reaction taking place using normal copper powder yields only 40% of biphenyl at the same reaction conditions (Fig. 5a). In a recent study, phenanthroline-functionalized polyacrylonitrile fiber (PANF) with Pd(0) NPs was reported for the Heck reaction. The fiber-stabilized Pd(0) NPs (PAN<sub>Phen</sub>F-Pd(0)) catalyst was used to synthesize cinnamic acid from iodobenzene and acrylic

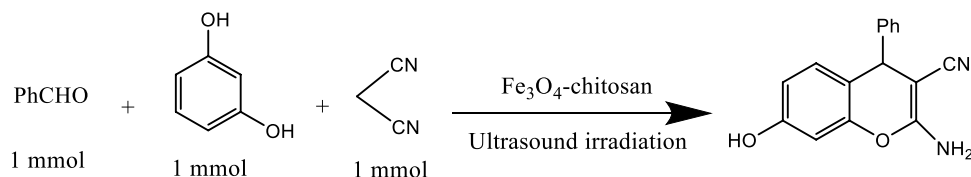


**Fig. 4** One-pot synthesis of 2-amino-4H-chromenes catalyzed by Fe<sub>3</sub>O<sub>4</sub>-chitosan nanoparticles under ultrasound irradiation at 50 °C (Safari and Javadian 2015) © Elsevier, reproduced with permission

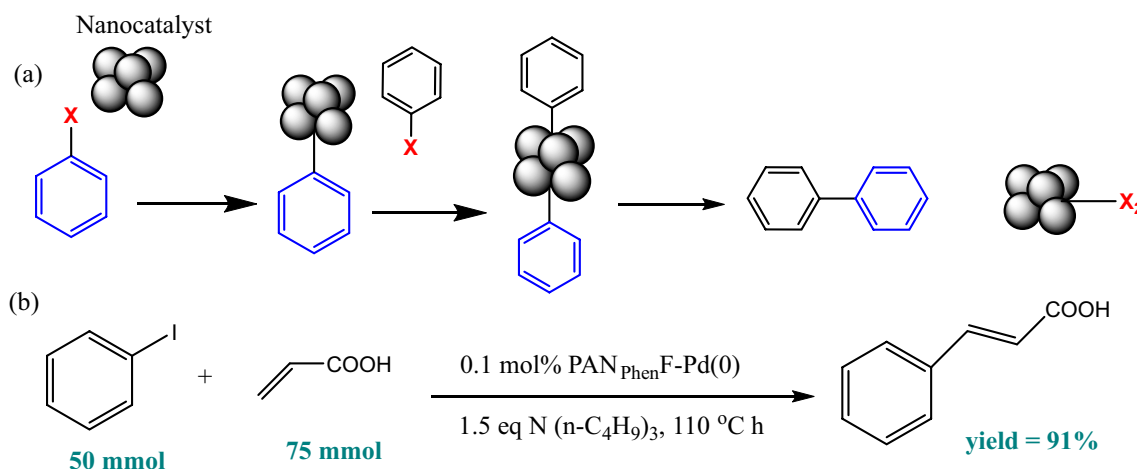


**Fig. 5** **a** Formation of biphenyl **b** Gram-scale experiment of Heck reaction catalyzed by PAN<sub>Phen</sub>F-Pd(0) (Xiao et al. 2021) © Elsevier, reproduced with permission

acid with excellent catalytic activity (Fig. 5b). The fiber-based catalyst was removed by a tweezer from the reaction and washed with ethyl acetate and dried. It was reused for six consecutive series and a slight decrease of yield from 96 to 87% was recorded in the sixth run (Xiao et al. 2021).

Qiu et al. (2018) synthesized Pd NPs with narrow particle size distribution ( $1.8 \pm 0.2$  nm) for Suzuki–Miyaura coupling catalytic activity. The NP was prepared using organic molecular cages as a template to resist agglomeration and to control the size of the catalyst. The NPs exhibited greater catalytic activity than the normal Pd(PPh<sub>3</sub>)<sub>4</sub> in the Suzuki–Miyaura coupling reaction with a yield greater than >99% summarized in Table 1.

Kardanpour et al. (2014) synthesized highly disperse and reusable Pd NPs supported on amino-functionalized metal–organic framework for the Suzuki cross-coupling reaction. The Pd/Uio-66-NH<sub>2</sub> NP was used in the Suzuki coupling reaction between an aryl halide and phenylboronic acid to give good yields of biphenyl derivatives as shown in Table 2 below. Furthermore, the NPs were filtered, washed with water and DMF, and dried at 60 °C,

and further reused until the fifth cycle without significant loss of their initial activity.

In another study, Mallikarjuna et al. (2017) used a bioinspired method to synthesize Pd NPs using *fenugreek* tea extracts as a reducing and stabilizing agent. The PdNPs@FT catalyst was used in the Suzuki–Miyaura coupling reaction between bromobenzene and phenylboronic acid, and an excellent yield (96%) of the product was obtained as confirmed by the <sup>1</sup>H NMR and UV–vis spectrum. Puthiaraj and Ahn (2015) studied Pd NPs immobilized on NH<sub>2</sub>-MIL-125 (Pd@NH<sub>2</sub>-MIL-125) for the purpose of Suzuki coupling between aryl chlorides and aryl boronic acids under K<sub>2</sub>CO<sub>3</sub> (1.5 mmol), MeOH (3 mL), Pd@NH<sub>2</sub>-MIL-125 (0.9 mol% of Pd) for 22 h as summarized in Table 3 below.

A recently published study by Ahadi et al. (2019) revealed the synthesis of Pd containing bipyridium chloride (liquid ionic-based) periodic mesoporous organosilica (Pd@Bipy-PMO) as a hybrid catalyst for Suzuki–Miyaura cross-coupling reaction in water taking 4-bromoacetophenone with phenylboronic acid as a model of the reaction. Excellent result up to 98% isolated yield was obtained. The reusability of the catalyst has been checked up to the 6th

**Table 1** Suzuki–Miyaura coupling of various aryl halides using Pd NP@3a and Pd(PPh<sub>3</sub>)<sub>4</sub> (reaction conditions: <sup>a</sup>aryl halide (0.057 mmol), phenylboronic acid (0.087 mmol),

Na<sub>2</sub>CO<sub>3</sub>(0.17 mmol), Pd catalyst (0.57 mmol, 1.0 mol%), <sup>b</sup>yields are based on <sup>1</sup>H NMR analysis of the crude products) (Qiu et al. 2018) © Royal Society of Chemistry, reproduced with permission

Entry	Aryl halide	Product	Yield (%)	
			Pd NP@3a	Pd(PPh <sub>3</sub> ) <sub>4</sub>
1			99	86, (99 <sup>c</sup> , 98 <sup>d</sup> , 22 <sup>e</sup> )
2			>99	81
3			96	85
4			>99, >99 <sup>f</sup>	78, 40 <sup>f</sup>
5			>99	73
6 <sup>g</sup>			99±0.4	75, (78 <sup>c</sup> , 72 <sup>d</sup> , 20±2.4 <sup>e</sup> )

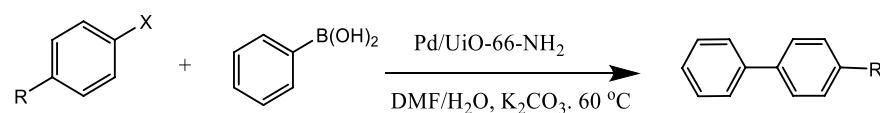
<sup>c</sup>For Pd(PPh<sub>3</sub>)<sub>2</sub>Cl<sub>2</sub> catalyst

<sup>d</sup>For Pd<sub>2</sub>(dba)<sub>3</sub>

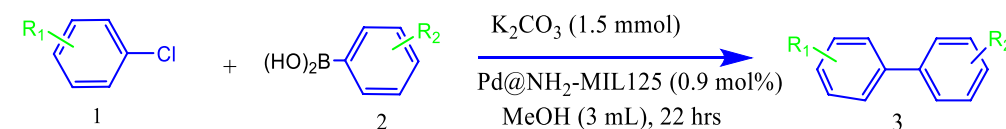
<sup>e</sup>For Pd/C (5%)

<sup>f</sup>After exposure of the catalyst to air for 2.5 h

<sup>g</sup>5 repeats with a standard deviation for both Pd NP@3a and Pd/C (5%). Where @3a is organic molecular cage

**Table 2** Suzuki–Miyaura coupling reaction of different aryl halides with phenylboronic acid catalyzed by Pd/UiO-66-NH<sub>2</sub> (reaction conditions: aryl halide (1 mmol), phenylboronic acid (1.1 mmol),K<sub>2</sub>CO<sub>3</sub> (1.5 mmol), Pd/UiO-66-NH<sub>2</sub> (0.01 g, 0.25 mol% Pd), H<sub>2</sub>O/DMF (1 mL/2 mL) at 60 °C) (Kardanpour et al. 2014) © Elsevier, reproduced with permission

Entry	R	X	Time (min)	Yield (%) <sup>a</sup>	TOF (h <sup>-1</sup> )
1	H	I	10	92	2190.5
2	4-OMe	I	10	95	2261.9
3	4-Me	I	10	93	2214.3
4	4-Ac	I	13	90	1666.7
5	H <sup>b</sup>	Cl	41	80	467.8
6	4-CHO <sup>b</sup>	Cl	60	85	340
7	H	Br	30	90	697.7
8	4-Ac	Br	32	93	699.2
9	4-CHO	Br	35	91	623.3

<sup>a</sup>GC yield<sup>b</sup>The reaction was performed at 80 °C**Table 3** Pd@NH<sub>2</sub>-MIL-125 promoted Suzuki coupling reaction with different substituents (reaction conditions: chlorobenzene (1 mmol), phenylboronic acid (1.3 mmol), K<sub>2</sub>CO<sub>3</sub> (1.5 mmol), MeOH (3 mL),Pd@NH<sub>2</sub>-MIL-125 (0.9 mol% of Pd), 22 h) (Puthiaraj and Ahn 2015) © Elsevier, reproduced with permission

Entry	R <sub>1</sub>	R <sub>2</sub>	Yield (%) <sup>a</sup>	TOF (h <sup>-1</sup> )
1	H	H	86	4.3
2	4-CH <sub>3</sub>	H	83	4.3
3	H	4-CH <sub>3</sub>	80	4.0
4	3-NO <sub>2</sub>	H	79	3.9
5	4-OCH <sub>3</sub>	4-OCH <sub>3</sub>	80	4.0

<sup>a</sup>GC analysis, conversion based on aryl chlorides

run, the leaching of Pd was detected by a hot filtration test (HFT). Furthermore, the Field Emission Scanning Electron Microscope (FESEM) image confirms the intact morphology of nanocatalyst Pd@Bipy-PMO nanocatalyst used in the 6th run (Fig. 6a–c).

Strongly cross-linked Pd-based NPs have been synthesized for Suzuki–Miyaura and Mizoroki–Heck cross-coupling reactions. The heterogeneous nanocatalyst was developed by immobilizing the Pd NPs with a polymer containing a ligand of 4'-(4-hydroxyphenyl)-2,2':6',2''-terpyridine (HPTPy) ligand. The cross-linkage of the polymer with trimethylolpropane triacrylate (TMPTA) units was synthesized by polymerization of itaconic acid-HPTPy (ITC-HPTPy)

monomer [so-called cross-linked poly (ITC-HPTPy)]. The stabilized Pd-based nanocatalyst offers excellent efficiency of up to 98% and 213 h<sup>-1</sup> TOF. The catalyst was separated by centrifugation to be used consecutively. The Scanning Electron Microscope (SEM) image of the sixth time reused nanocatalyst proved the stability without any change (Fig. 7a–d), while the energy-dispersive X-ray spectroscopy (EDX) spectrum of the recovered nanocatalyst showed little leaching of Pd into the solution over the multiple runs (Fig. 7e, f) (Targhan et al. 2020). In another recent study, Ahmadi et al. (2020) synthesized magnetic mesoporous silica nanocomposite (Fe<sub>3</sub>O<sub>4</sub>-MCM-41) functioned with palladium Schiff base complex which has been applied as

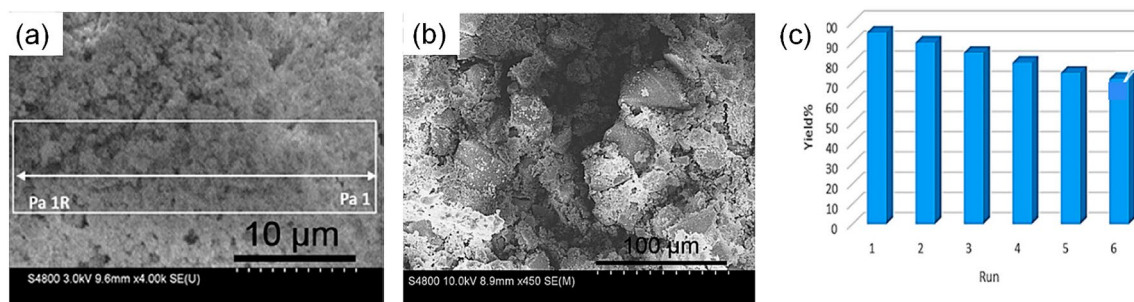


**Fig. 6** FESEM images of **a** Pd@Bipy-PMO **b** the corresponding FESEM image after 6th run **c** recyclability study of Pd@Bipy-PMO catalyst in Suzuki reaction (Ahadi et al. 2019) © MDPI, reproduced with permission

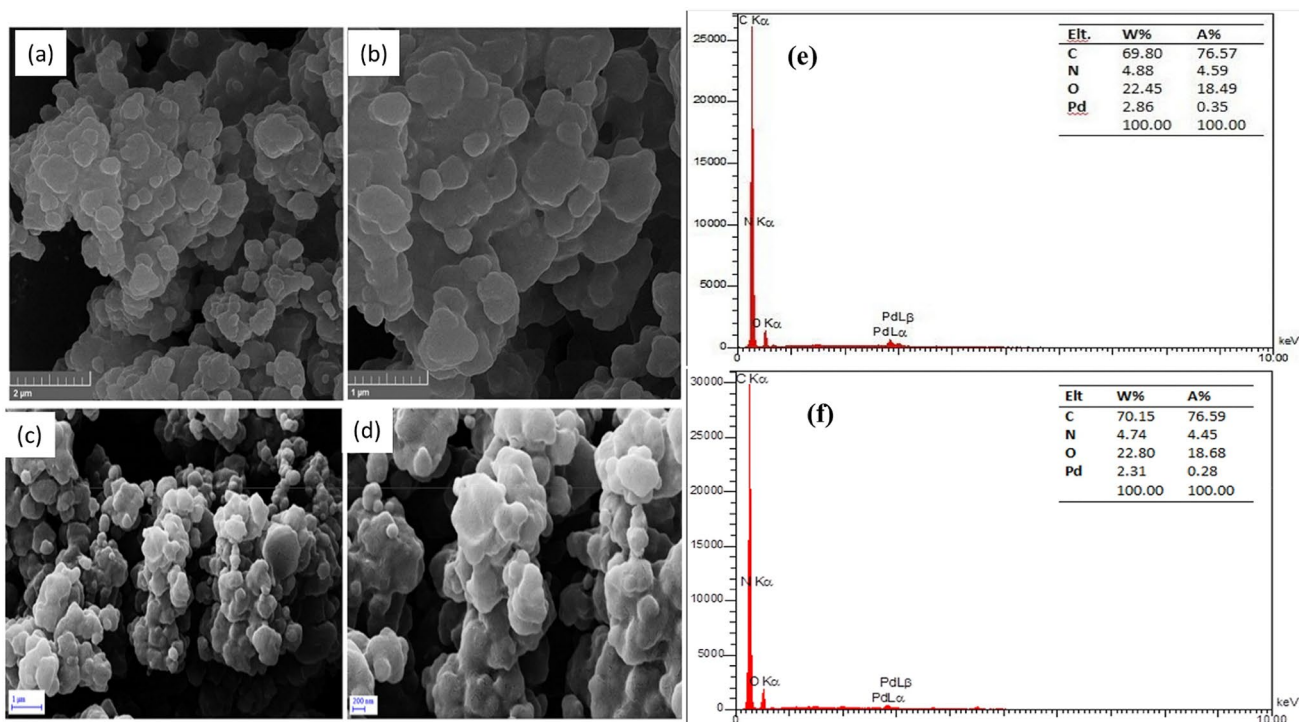


**Fig. 7** SEM images of **a** and **b** fresh, **c** and **d** recovered after 6th run, EDX pattern of **e** fresh and **f** recovered after 6th run of cross-linked poly (ITC-HPTPy)-Pd (Targhan et al. 2020) © Springer, reproduced with permission

an efficient catalyst for Suzuki–Miyaura. The  $\text{Fe}_3\text{O}_4$ @MCM-41-SB-Pd nanocomposite was able to produce a 98% yield of the substituted biphenyl derivatives in a short reaction time (0.16 h) using DMF as a solvent. The catalyst was recovered using an external magnet and reused five times without a noticeable change in its activity; FTIR analysis of the nanocomposite confirmed that the structure of the nanocomposite was not changed after five runs.

A magnetically recovered and stable Pd@ $\text{Fe}_3\text{O}_4$  nanocatalyst has been checked for the hydrogenation of nitroarenes and Suzuki–Miyaura reactions by taking 2 mmol of the substrates, 5 mL of ethanol, 50 mg load of the catalyst under 1 atm of hydrogen pressure, and the reaction progress was

controlled by TLC and conversion was checked by Gas Chromatography (GC). On the other hand, 5 mL ethanol, 0.5 mmol of aryl chloride, 0.6 mmol of phenyl boric acid, and 1.5 mmol of  $\text{K}_3\text{PO}_4$  were used for the Suzuki–Miyaura reactions. Over 99% conversion of hydrogenation of various substrates using Pd@ $\text{Fe}_3\text{O}_4$  as a catalyst has been confirmed. Suzuki–Miyaura coupling reactions involving aryl chlorides, bromides, and iodides with phenyl boric acid have also shown > 90% yield of biphenyl when electron-withdrawing substituents are attached to the aryl halides than electron-releasing groups (Amali and Rana 2009).

Sawoo et al. (2009) studied the catalytic activity of Pd NPs for C–C coupling reactions. The NPs was synthesized



**Table 4** Pd nanoparticles-catalyzed Sonogashira coupling reaction with aryl halide and alkyne (aryl bromide (1 mmol), alkyne (1.2 mmol),  $K_2CO_3$  (2 mmol), water (4 mL), Pd nanoparticle in water (0.01 equiv with PEG 6000 1.0 equiv)) (Sawoo et al. 2009) © Elsevier, reproduced with permission

$$\text{Ar-X} + \text{C}\equiv\text{C-R}^1 \xrightarrow[\text{K}_2\text{CO}_3]{\text{Pd NP, H}_2\text{O}} \text{Ar-C}\equiv\text{C-R}^1$$

Entry	Aryl halide	Alkyne	Product	Time (h)	Yield% <sup>b</sup>
1				2 <sup>c</sup>	95
2				3.5 <sup>c</sup>	95
3				2 <sup>c</sup>	92
4				5 <sup>d</sup>	94
5				5 <sup>d</sup>	88
6				3.5 <sup>d</sup>	90
7				3.5 <sup>d</sup>	90

<sup>b</sup>Isolated yield after purification by flash column chromatography (eluent: petroleum ether or ethyl acetate/petroleum ether)

<sup>c</sup>Reaction temperature is 55 °C

<sup>d</sup>Reaction temperature is 65 °C

**Fig. 8** CuO/AB-catalyzed Ullmann coupling reaction with various substrates (Woo et al. 2013) © Springer, reproduced with permission

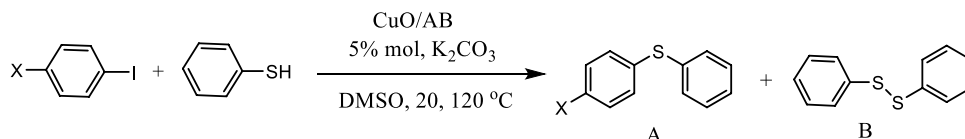
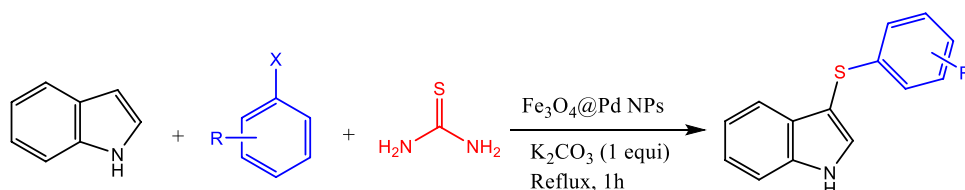


**Fig. 9** The formation of indole derivatives (Li et al. 2020) © Springer, reproduced with permission



in water and templated in a PEG stabilizer. Thus, the aqueous nano-sized Pd NPs were a highly efficient catalyst for Suzuki, Heck, Sonogashira, and Stille C–C coupling reactions where only water was used as a solvent in the reactions. A 95% yield of products was obtained from the Suzuki reaction after isolation and purification inside 3 h at room temperature. Similar activities of the NPs are observed in Heck, Sonogashira, and Stille C–C coupling reactions as summarized in Table 4.

Sulfur-containing (aryl sulfide) derivatives are important compounds in biological, pharmaceutical, and other materials. Thus, these compounds are synthesized using nanostructure catalysts such as CuO hollow nanostructures through Ullmann reactions. The reaction of iodobenzene

with thiophenol using the charcoal (CuO/C) in DMF and 120 °C provided a low conversion rate and not selective to diphenyl thioether or diphenyl disulfide products (Fig. 8). Acetylene black (CuO/AB) was used to overcome the problems but till the low conversion of the reaction was observed but high selectivity among the products has been observed (Woo et al. 2013).

Similarly, Sengupta et al. (2017) used nickel NPs supported on reduced graphene oxide (Ni/RGO-40) for C–S cross-coupling reaction between an aryl halide and thiol using DMF solvent,  $K_2CO_3$  as a base at 100 °C. The C–S coupling reactions between the iodoarene and aryl thiols with different groups such as OMe, F,  $COCH_3$ , and  $NO_2$  were equally efficient in the coupling reaction to produce

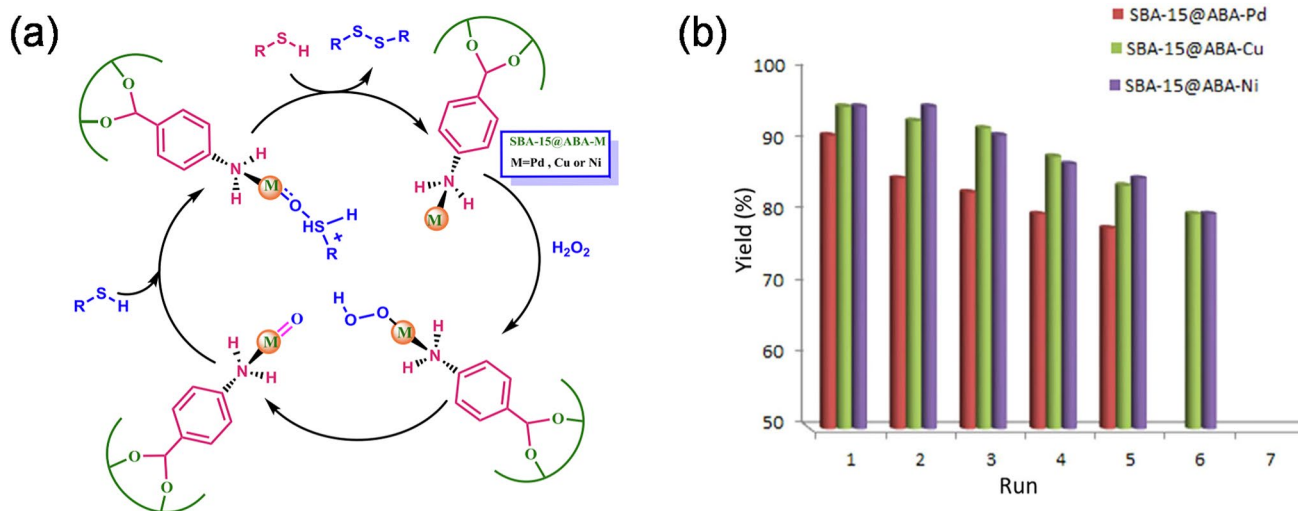


**Fig. 10** **a** Proposed mechanism for oxidative coupling of thiols in the presence of SBA-15@ABA-M (M=Ni, Cu and Pd) **b** Recycling test of the prepared catalysts for the oxidation of 4-methylthiophen under

optimized conditions in the presence of SBA-15@ABA-Cu, SBA-15@ABA-Ni, and SBA-15@ABA-Pd (Tamoradi et al. 2019) © Elsevier, reproduced with permission

the unsymmetrical diary sulfides in the range of 88–93% yield products. Aliphatic thiols were also resulted in the coupling reaction in the formation of unsymmetrical aryl alkyl thioether with a relatively lower yield of 75–80%, indicating the aliphatic thiols are less reactive in the C–S coupling than the aromatic thiols. Finally, the Ni/RGO-40 nanocatalyst was recovered using a magnet, washed using excess ethanol, dried in a vacuum oven, and reused six times and a 91% yield of products was obtained in the sixth run. Selective sulfenylation of indole derivatives has been carried out via C–S formation using cellulose-derived  $\text{Fe}_3\text{O}_4$ @Pd NPs (Fig. 9). The magnetically separable NP employed a 98% yield of the product using 1 mol% of the  $\text{Fe}_3\text{O}_4$ @Pd NPs. The catalyst was reused five times to give a 90% yield of the products (Li et al. 2020).

Santa Barbara Amorphous (SBA-15) is known as a hybrid catalyst due to the combination of organic and organometallic supporters. Thus, mesoporous silica/silicate-aluminosilicates have unique properties (uniform pore size (4.6–30 nm), well-defined pore structure, and size distribution, high surface area, high thermal stability) mostly used as advanced support in metathesis catalyst (Balcar and Cejka 2019; Crucianelli et al. 2019). The mesoporous silica is applied as a support to immobilize the metal nanocatalyst in the heterogeneous catalysts for protecting them from sintering and leaching out as well as for mass transports of reactants, intermediates, and products (Wang et al. 2020). A recent study by Tamoradi et al. (2019) on BA-15@ABA-M (M=Cu, Ni, and Pd) reported an efficient, novel, and green catalyst oxidative under mild conditions. The immobilized Cu, Ni, and Pd complexes on SBA-15 mesostructured were carried out for

coupling of thiols for the synthesis of disulfide compounds using  $\text{H}_2\text{O}_2$  as an oxidant. The catalyst was stable, used for a wide range of thiols with excellent yield and shorter reaction time. At the end of the operation, the SBA-15@ABA-M catalyst was separated from the reaction mixture by simple filtration, washed with ethyl acetate to remove the residual products, and the catalyst has been reused for several runs and performed without any metal leaching or significant decrease in its activity. Finally, the proposed reaction mechanism has been deduced (Fig. 10a, b).

A magnetically recycled heterogeneous nanocatalyst has been fabricated via functionalization of SBA-15 with Schiff base ligand, and then immobilization of Pd NPs ( $\text{Fe}_3\text{O}_4$ -Pd@SF-SBA-15) for C–C Heck coupling reaction. The catalytic activity of  $\text{Fe}_3\text{O}_4$ -Pd@SF-SBA-15 was investigated on the synthesis of stilbene from aryl halides with styrene derivatives as a model reaction as shown in the reaction mechanism and 97% yield of stilbene has been obtained after 40-min reaction time (Fig. 11). The  $\text{Fe}_3\text{O}_4$ -Pd@SF-SBA-15 nanocatalyst can be reused eight times without a significant loss of its catalytic activity. Stability evaluation of the nanocatalyst via Inductively Coupled Plasma Optical Emission Spectrometry (ICP-OES) and X-ray diffraction (XRD) confirmed that only 0.093 wt% of Pd was leached after the eighth cycle (Khodaei and Dehghan 2018).

Palladium NPs supported on magnesium ferrite catalyst ( $\text{Pd}/\text{MgFe}_2\text{O}_4$ ) was applied for the synthesis of a marketed anticancer drug PCI-32765 under the name IMBRUVICAVR (Ibrutinib-BTK inhibitor) following the C–C coupling (Suzuki) and C–N coupling reactions. The nanocatalyst showed outstanding activity with 99%

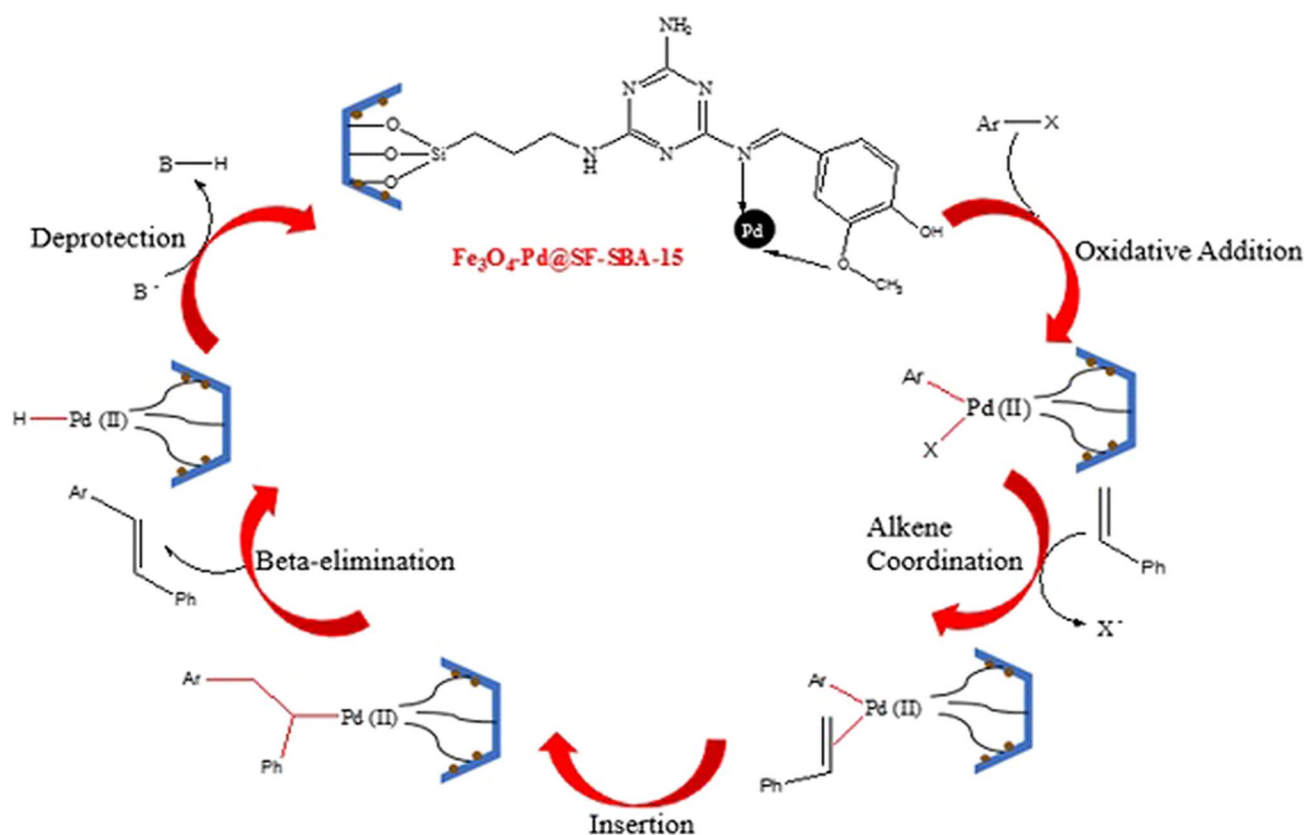


**Fig. 11** Mechanism of  $\text{Fe}_3\text{O}_4\text{-Pd@SF-SBA-15}$ -catalyzed Heck reaction (Khodaei and Dehghan 2018) © John Wiley and Sons, reproduced with permission

yield using 0.2 mol% of  $\text{Pd/MgFe}_2\text{O}_4$  loading with 495 and  $247.7 \text{ h}^{-1}$  turnover number (TON) and TOF, respectively, towards ligand-less Suzuki coupling reaction using greener solvent mixture water: ethanol to synthesize the 5-(4-phenoxyphenyl)-7H-pyrrolo[2,3-d]pyrimidin-4-ylamine intermediate for the marketing drug PCI-32765 (Dasari et al. 2020).

Works reported by researchers on the C–C coupling reactions using different nanocatalyst under a certain reaction conditions are summarized in Table 5 below.

### Reduction reactions

The reduction reaction is a central and vital reaction type used to manufacture different important industrial products such as biologically active compounds, pharmaceutical ingredients, dyes, rubbers, and other chemicals in different chemical industries. Traditionally, the hydrogenation and reduction reactions are performed under the transition metal catalysts (Pt, Pd, Ni, Cu, Ru) applying toxic reducing agents like  $\text{NaBH}_4$ ,  $\text{LiAlH}_4$ , hydrazine, etc. which are not safe (Gawande et al. 2016). Various structures of aniline, major building blocks, and drug and dye intermediates are

obtained from the nitroaryl compounds via nanocatalysts in a reasonable yield and conversion (Huang et al. 2018). Consequently, several approaches have been designed to produce stable, reusable, and durable heterogeneous nanocatalysts (Shokouhimehr 2015). Gold NPs (Au NPs) are among the promising catalyst with excellent activity, plasmonic property, and separations from organic reactions. Supported Au NPs are stable and recyclable compared with the other NPs (Table 6). Immobilization or functionalization of Au NPs with supporting materials, particularly with iron-based materials, is beneficial in terms of ease of separation and stability (Sharma et al. 2016a; Moon et al. 2018; Kazemi 2020a). The nanocatalysts in the form of  $\text{Au/AlO}_3$ ,  $\text{Au/Fe}_2\text{O}_3$ ,  $\text{Au/TiO}_2$ ,  $\text{Au/ZnO}$ , and  $\text{Au/SiO}_2$  are studied for organic reactions (Ballarin et al. 2017; Martins et al. 2017). Bhaduri et al. (2019) used recyclable  $\text{Au/SiO}_2\text{-shell/Fe}_3\text{O}_4\text{-core}$  for the reduction of nitroaromatic compounds. The Au nanocomposites have been tested for the reduction of 4-nitrophenol (4-NP) and 2-nitroaniline (2-NA) under an aqueous solution with  $\text{NaBH}_4$ . The magnetically recyclable nanocomposite was highly stable ( $\sim 3$  months), reused up to 10 runs, and high activity of 100% conversion within 225 s, 700 ppm of 4-NP or 2-NA was observed.

**Table 5** Summary of C–C cross-coupling reactions

Reactant 1	Reactant 2	Product	Time (min)	Solvent	Temp (°C)	Nanocatalyst	Type of rxn	Yield (%)	Ref.
			-	H <sub>2</sub> O, TBAOH	90	Pd-NPs/ZrO <sub>2</sub>	Heck	81	Monopoli et al. (2010)
			-	H <sub>2</sub> O, TBAOH	90	Pd-NPs/ZrO <sub>2</sub>	Suzuki	90	Monopoli et al. (2010)
			180	MeOH	80	Pd/MOF-5	Sonogashira	98	Gao et al. (2010)
			180	EtOH	80	Pd@ZPGly	Suzuki	97	Kozell et al. (2017)
			180	EtOH	80	Pd@ZPGly	Suzuki	98	Kozell et al. (2017)
			180	EtOH	80	Pd@ZPGly	Suzuki	98	Kozell et al. (2017)
			180	CH <sub>3</sub> CN	120	Pd@ZPGly	Heck	97	Kozell et al. (2017)
			30	H <sub>2</sub> O/EtOH	40	Pd/MIL-53(Al)-NH <sub>2</sub>	Suzuki	97	Huang et al. (2011)
			30	H <sub>2</sub> O/EtOH	40	Pd/MIL-53(Al)-NH <sub>2</sub>	Suzuki	95	Huang et al. (2011)
			90	DMF/H <sub>2</sub> O	80	OXDH-Pd	Suzuki	92	Panchal et al. (2018)
			60	1,4-dioxane, Water	80	OXDH-Pd	Suzuki	98	Panchal et al. (2018)
			45	TBAA, TBAB	120	Co	Heck	90	Islam and Mia (2020)
			45	TBAA, TBAB	120	Co	Heck	85	Islam and Mia (2020)
			45	TBAA, TBAB	120	Co	Heck	90	Islam and Mia (2020)
	Ph <sub>3</sub> SnCl		100	PEG-400		Fe <sub>3</sub> O <sub>4</sub> @PT A-Pd	Stille	94	Ghorbani-choghamarani and Norouzi (2016)
	Ph <sub>3</sub> SnCl		45	PEG-400		Fe <sub>3</sub> O <sub>4</sub> @PT A-Pd	Stille	78	Ghorbani-choghamarani and Norouzi (2016)
	Ph <sub>3</sub> SnCl		45	PEG-400		Fe <sub>3</sub> O <sub>4</sub> @PT A-Pd	Stille	97	Ghorbani-choghamarani and Norouzi (2016)
	Ph <sub>3</sub> SnCl		190	PEG-400		Fe <sub>3</sub> O <sub>4</sub> @PT A-Pd	Stille	97	Ghorbani-choghamarani and Norouzi (2016)
			3	TBAC	80	PS-PdO	Hiyama	88	Sakon et al. (2017)
			2	H <sub>2</sub> O	90	Pd	Hiyama	98	Srimani et al. (2007)
	-		20	H <sub>2</sub> O	90	Pd@CSP	Ullmann	55	Kamal et al. (2012)
	-		20	H <sub>2</sub> O	90	Pd@CSP	Ullmann	50	Kamal et al. (2012)
	-		-	H <sub>2</sub> O, EtOH	25	Pd	Ullmann	96	Rasouli and Ranjbar (2013)
	-		-	H <sub>2</sub> O, EtOH	70	Pd	Ullmann	79	Rasouli and Ranjbar (2013)
			1.5	THF	70	Pd	Hiyama	90	Akubo et al. (2019)
			2	THF	70	Pd	Hiyama	82	Akubo et al. (2019)
			3	THF	70	Pd	Hiyama	85	Akubo et al. (2019)
			3.5	THF	70	Pd	Hiyama	85	Akubo et al. (2019)

TBAOH tetra(*n*-butyl)ammonium hydroxide, OXDH oxacalix[4]arene dihydrazide, TBAA tetrabutylammonium acetate, TBAB tetrabutylammonium bromide, THF tetrahydrofura

**Table 6** Comparison of Au with other nanocatalysts in the reduction reaction of nitroaromatics

Nanocatalysts	Reactant	Reaction conditions	Product	No of runs	Conversion (%)	References
Au NS	4-NP	5 min, 21.1 $\mu\text{mol}$ Au NS, 5 $\mu\text{mol}$ 4-NP	4-AP	15	100	Jin et al. (2020)
CA–Au NP	4-NP	0.4 mM Au NP, 1 mL 4-NP, water (1.8 mL), $\text{NaBH}_4$ (200 Mm, 85 °C, 12 h)	4-AP	–	99.8	Seo et al. (2017)
Cu NWs	4-NP	5 mL 4-NP = 1 mM and 0.5 mL $\text{NaBH}_4$ = 50 mM, 60 s	4-AP	10	99	Hashimi et al. (2019)
Pd/ $\text{Fe}_3\text{O}_4$ /PEI/RGO	4-NP	2 mg/mL catalyst, 1 mM, 100 mL 4-NP	4-AP	10	92	Su et al. (2016)
ZVIN (zero-valent iron NP)	4-NP	0.2 M $\text{NaBH}_4$ , 10 mg/L, 0.2 mM 4-NP, 20 min	4-AP	5	96.8	Sravanthi et al. (2019)
Ag/mCFT	4-NA	–	DAB	10	98	Emadi et al. (2020)
Ag@ $\text{SiO}_2$	NB	6 h, 413 K, 2.0 MPa	Aniline	10	99.9%	Zhao et al. (2020a)

Au NS Au nanosphere, mCTF mesoporous Carbon Triazine Framework, DAB 1,4-diaminobenzene

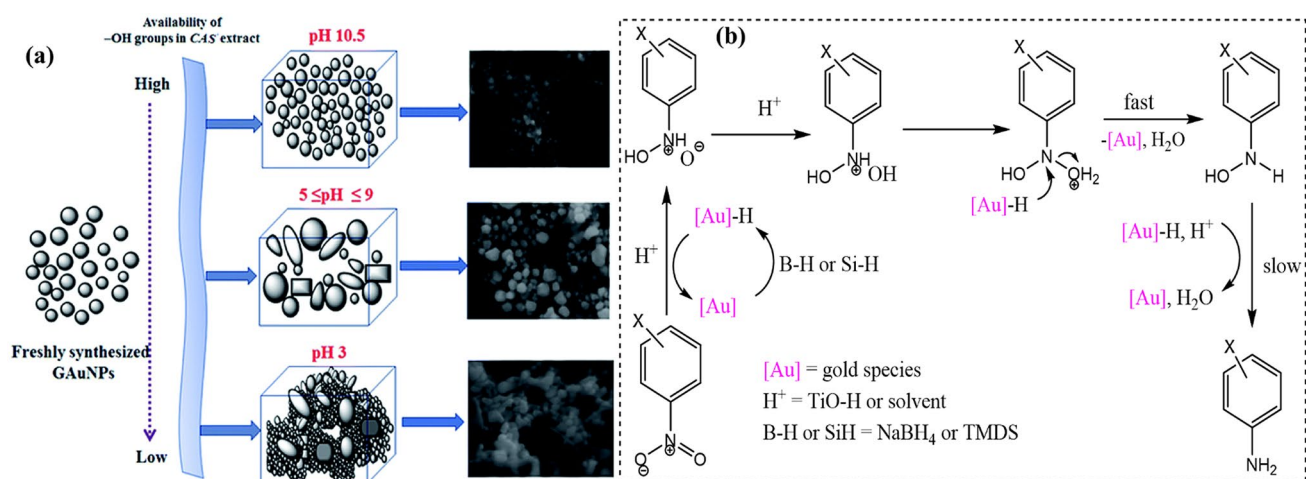


**Fig. 12** **a** A schematic representation of the shape and size control of Au NPs in CAS extract-mediated synthesis process through pH variation. The SEM images presented in the right column correspond to the samples prepared at corresponding pH values of the reaction mixtures (Bogireddy et al. 2018) © Royal Society of Chemistry, reproduced with permission

Plant-mediated Au NPs of different size have been fabricated using sun-dried *Coffea arabica* seed (CAS) extracts for the reduction of 4-NP. The synthesis strategy of size and shape control was implemented by adjusting the pH concentration of the plant extract (Fig. 12a) (Bogireddy et al. 2018). The bioinspired NPs showed a 100% reduction of the nitrophenol to aminophenol. Fountoulaki et al. (2014) studied the reduction of nitroaromatics using mesoporous titania-supported gold NP assemblies (Au/MTA) nanocatalyst in the presence of  $\text{NaBH}_4$  or 1,3,3-tetramethyl disiloxane (TMDS). Electron-withdrawing-containing nitroaromatic compounds was reduced faster than the electron-donating-containing one. The nanocatalyst showed an excellent yield (> 99%) of products using ethanol as a solvent and TMDS as a hydrogen

source. Depending on the proposed reaction mechanism, the B–H or Si–H bond cleavage occurs at the rate-determining step to give [Au]–H which facilitates the rapid reduction of nitroarenes (Fig. 12b).

It has been found that Au nanocatalyst has demonstrated excellent performance in many organic reactions such as selective reduction and oxidation. However, the high cost of Au should be considered in future developments (Albero and García 2019). Though, Au NP showed excellent and selective reduction for nitroaromatic reduction, the origins of its catalytic performances are not properly deduced (Zhao et al. 2019a).

Ag NPs have been fabricated stabilizing on the combination of porous igneous rock volcanic pumice (VP) and Chitosan (CTS) polymeric network for the reduction of

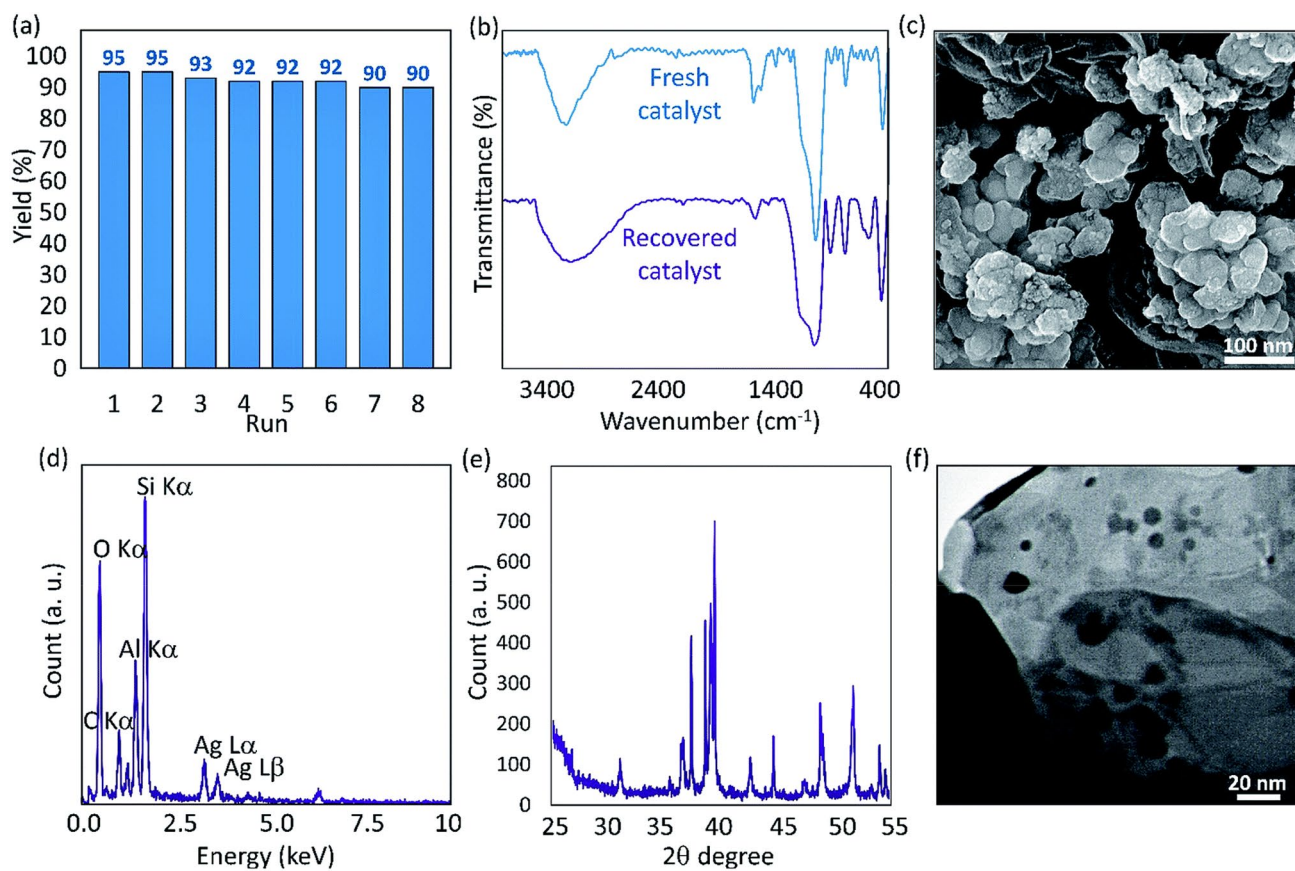


**Fig. 13** **a** Recyclability diagram **b** the FTIR spectra of fresh and recovered catalyst **c** SEM image **d** EDX spectrum **e** XRD pattern and **f** TEM image of the recovered Ag@VP/CTS nanocatalyst (Taheri-ledari et al. 2020) © Royal Society of Chemistry, reproduced with permission

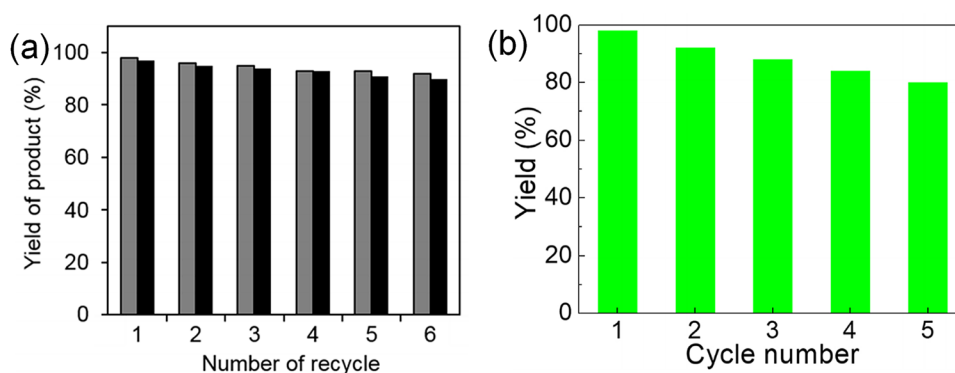
**Table 7** Reuse of the MRN–Pd catalysts in heterogeneous reduction of nitrobenzene (Shokouhimehr et al. 2018) © Royal Society of Chemistry, reproduced with permission

**Magnetic recycling of robust magnetic nanocomposite catalyst**

Cycle number	1	2	3	4	5	6	7
Yield of product (%)	99	98	99	99	97	97	95

Reaction conditions: nitrobenzene (1 mmol), NaBH<sub>4</sub> (1.2 mmol), MRN–Pd catalysts (1 mol% Pd), H<sub>2</sub>O (15 mL), room temperature, 45 min. The yields were determined by GC–MS

**Fig. 14** **a** Reusability of HAP-Pd catalyst in heterogeneous reduction of nitrobenzene (gray columns) and oxidation of cycloheptanol (black columns (Shokouhimehr et al. 2019) © MDPI, reproduced with permission **b** Repeated cycling studies for the reduction of nitrophenol to aminophenol using the FeHCFe@Pd catalyst (Zhang et al. 2020) © Elsevier, reproduced with permission



nitrobenzene to aniline. The Ag@VP/CTS composite has been able to reduce the nitrobenzene in a very short period of time through an electron transfer system. The catalyst was magnetically collected from the reaction mixtures, washed with water, oven-dried, and further reused for eight successive cycles without significant loss. Only 5% of its catalytic activity has been reduced in the eighth series since the first run (Fig. 13a). Furthermore, SEM, Transmission Electron Microscope (TEM), EDX images, FTIR, and XRD spectrum of the nanocatalyst confirmed that no changes have been observed in its morphology, size distribution, and characteristic spectra compared with the fresh sample (Fig. 13b–f) (Taheri-ledari et al. 2020).

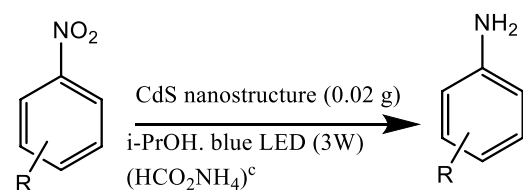
Jacinto et al. (2009a) studied the catalytic application of amino acid-modified silica-coated magnetic Pt(0) NPs for the hydrogenation of alkenes and ketones. A series of hydrogenation reactions was carried out against benzene, toluene, styrene, *p*-xylene, and prop-1-en-2-ylbenzene and the catalyst showed 98.9% of the conversion of styrene to ethylbenzene, 100% selectivity for the conversion of prop-1-en-2-ylbenzene to cumene. Similarly, over 99% conversion of ketones to alcohols was achieved by the catalyst (e.g.; 3-pentanone to 3-pentanol) at 1200 h<sup>-1</sup> TON. Finally, the catalyst was recovered using an external magnet and reused several times (14 successive reductions) without losing its activity. Activated palladium sucrose NP (APdS NP) was used for the reduction of nitrobenzene derivatives into aniline derivatives. A 100% yield of the products was obtained and the NPs was effective, green, recyclable, and non-hazardous catalyst (Samsonu et al. 2018). Stable, effective Pd NPs stabilized by Pd/PEG was used for the reduction of styrene to ethylbenzene, the reduction reaction carried out at higher styrene concentration to exhibit 100% conversion in 90 min at room temperature; however, the conversion decreases to 80% upon decreasing the styrene concentration. Similarly, the catalyst Pd/PEG was used to reduce nitrobenzene with 93% conversion and 100% selectivity (Harraz et al. 2012). Zeynizadeh et al. (2017) fabricate magnetically recoverable NiFe<sub>2</sub>O<sub>4</sub>@Cu nanocatalyst for the reduction of nitroarenes

to arylamines in the presence of NaBH<sub>4</sub>. The reduction reaction of the nitroamines was taking place in 1 min, 0.15 g of NPs load, and 1:2.5 molar ratio of the substrate to NBH<sub>4</sub> to yield > 95% of arylamines. The NP was recovered using an external magnet, washed with ethanol, dried in the atmosphere, and reused further seven times without losing its catalytic activity. Similar studies have been conducted by Shokouhimehr et al. (2018) to synthesize magnetically retrievable nanocomposite embedded with Pd nanocatalyst (MRN–Pd) for the reduction of nitroaromatics in aqueous solution. The heterogeneous nanocatalyst was recycled with an external magnet and reused several times without noticeable loss of its activity to retain 95% yield in the seventh run. Thus, the supported Pd nanocatalyst was stable, durable, and easily separated by a small magnet (Table 7).

In another study, the above authors synthesized hydroxyapatite (HAP)-supported Pd nanocatalyst for the reduction of nitroaromatics and oxidation of alcohols under aqueous solution using NaBH<sub>4</sub> and H<sub>2</sub>O<sub>2</sub>, respectively. The catalyst afforded excellent performance and stability in a continuous work-up for six runs without significant loss in both the reduction and oxidation reactions (Fig. 14a) (Shokouhimehr et al. 2019). Zhang et al. (2020) reported the synthesis of Prussian blue analogs (PBAs) modified Pd nanocatalyst for the reduction of nitroaromatics to amino aromatic. The composite exhibited excellent activity due to the multiple electron transfer that was improved the poor electronic conductivity of the PBAs. Out of the six types of hexacyanoferrate(III)-based PBAs, MHCFe (M = Mn, Fe, Co, Ni, Cu, and Zn), the FeHCFe nanocatalyst was noticeably performed better activity in the reduction of the nitroaromatics. The Pd-loaded nanocatalyst (FeHCFe@Pd) showed excellent yields in both the electron-withdrawing and -donating group containing nitroaromatics to give 90–99% yield in 5 min. The FeHCFe@Pd nanocatalyst promises an advantage such as a small amount of the catalyst (5 mg) was enough for the complete conversion, it was selective only for the reduction of nitro groups to their corresponding amino groups, it exhibited a TOF value of

**Table 8** The reduction of nitrobenzene derivatives to corresponding amines via CdS nanostructure (photocatalyst, 20 mg; nitro compound alcoholic solution ( $1 \times 10^{-2}$  M), 5 mL; irradiation with blue LED

(3 W), 80 mL; irradiation time, 20 h in CdS catalyst), Ni-PVAm/SBA-15, Cu, and N-TiO<sub>2</sub> nanoparticles (Wang et al. 2009; Kalbasi et al. 2011; Duan et al. 2012; Eskandari et al. 2014)



Entry	R	Yield (%) <sup>a,b</sup>				Time (min)	Conversion (%) <sup>a,b</sup>	Selectivity (%) <sup>b</sup>
		CdS	Ni-PVAm/ SBA-15	Cu	N-TiO <sub>2</sub>			
1	4-NC	90	–	–	–	–	100	90
2	4-NO <sub>2</sub>	97	–	–	–	–	100	97
3	3-Cl	90	–	95	–	–	100	90
4	4-Cl	–	–	95	99.47 ± 0.15	6	–	–
5	2-OH	–	–	–	99.27 ± 0.21	10	–	–
6	3-OH	–	98	–	97.57 ± 0.40	3, 12.5	–	–
7	4-OH	–	98	66	99.37 ± 0.35	7, 85	–	–
8	CH <sub>3</sub> CO-	98	–	–	–	–	100	98
9	H	55 (97)	98	–	–	20	77 (100)	71 (97)
10	2-CHO	–	–	–	92.06 ± 0.36	7.5	–	–
11	3-CHO	–	–	–	95.48 ± 0.42	7.5	–	–
12	4-CHO	–	–	90	97.96 ± 0.27	7.5	–	–
13	2-NO <sub>2</sub>	50 (100)	–	–	–	–	50 (100)	100 (100)
14	2-CH <sub>3</sub>	–	98	87	96.50 ± 0.46	4, 10	–	–
15	3-CH <sub>3</sub>	47 (100)	–	91	97.33 ± 0.47	9.5	64 (100)	73 (100)
16	4-CH <sub>3</sub>	40 (100)	–	91	98.07 ± 0.27	7.5	86 (100)	46 (100)
17 <sup>c</sup>	H	19 (23)	–	–	–	–	21 (25)	90 (92)

<sup>a</sup>Determined by gas chromatography

<sup>b</sup>Numbers in parentheses represent results in the presence of 50 mg of the HCO<sub>2</sub>NH<sub>4</sub>

<sup>c</sup>In the presence of commercial CdS

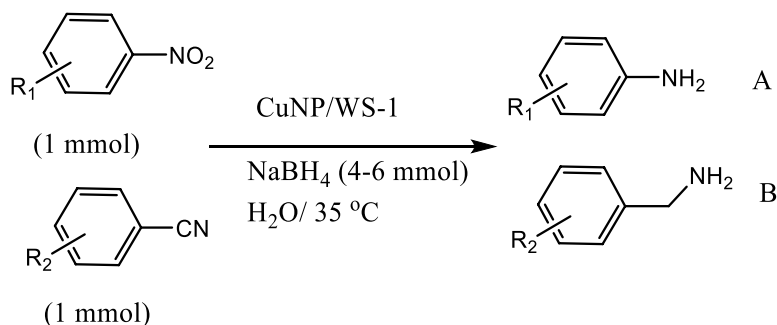
$1.43 \text{ s}^{-1}$ , the composite was recycled and reused 5 times without significant loss (Fig. 14b).

Photocatalytic reduction of aromatic nitro compounds to aromatic amines using CdS NPs was carried out by Eskandari et al. (2014) under light-emitting diode (LED) irradiation. The CdS photocatalyst showed excellent activity and yield in the reduction reaction with aromatic nitro compounds having electron-withdrawing substituents (CN, COR, NO<sub>2</sub>, Cl) to give a higher yield than electron-donating groups (Me, OMe, OH). Furthermore, the photocatalyst (CdS) shows highly selective, performed in mild conditions, and can be reused six times. Other NPs like Ni nanoparticles-polyvinyl amine/SBA-15 (Ni-PVAm/SBA-15), Cu, and N-TiO<sub>2</sub> were also showed good activity as summarized in Table 8.

Magnetic graphene oxide-supported Pd NP (C-Fe<sub>3</sub>O<sub>4</sub>-Pd) catalyst is prepared for the reduction of nitrobenzene to

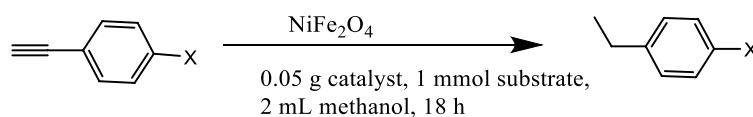
aniline under room temperature and 30 min reaction to exhibit 100% conversion, 99% selectivity, 99% yield using NaBH<sub>4</sub> as a hydrogen donor. Similarly, substituted nitrobenzene derivatives also reduced in the same condition to exhibit good yields and conversions. Finally, the catalyst (C-Fe<sub>3</sub>O<sub>4</sub>-Pd) was recovered and reused several times by washing with water, ethanol, and drying under an oven to perform its catalytic activity without an apparent loss (Zhou et al. 2016). Zamani et al. (2018) synthesized Walnut shell-stabilized copper NPs (Cu NP/WS) for the reduction of nitroarenes and benzonitriles and the C–C coupling reaction using water as a solvent. The Cu NP/WS showed remarkable catalytic activity and stability to reuse several times without significantly losing its initial activity. The small size of the NPs (15–22 nm) plays a crucial role in the reduction of nitroarenes and benzonitriles in water up to 100% yield products (Table 9).



**Table 9** Reduction of nitroarenes and benzonitriles in water (Zamani et al. 2018; Ansari et al. 2020)

Entry	Yield				
	Cu NP/WS		Fe <sub>3</sub> O <sub>4</sub> -MWCNTs@PEI-Ag	Cu NP/WS	
	R <sub>1</sub>		R <sub>2</sub>		
1	H	93	H	98	100
2	2-OH	99	2-Cl	92	85
3	3-OH	90	2-CN	88	–
4	4-OH	91	4-Cl		97
5	4-Me	100	3-Cl		98
6	4-CN	95	2-CH <sub>2</sub> BR	94	–
7	2,3 di-Me	98	2,4-Di-Cl		96
8	4-CO <sub>2</sub> H	93	–		–

GC yield, NaBH<sub>4</sub> (mmol) was used in both catalysts

**Table 10** Hydrogenation of alkynes with nano-ferrite–Ru and nano-ferrite–Ni catalysts (Baruwati et al. 2009; Polshettiwar et al. 2009)

Entry	X	Product	Yield%	
			Ferrite-Ru <sup>b</sup>	Ferrite-Ni <sup>a</sup>
1	H		95	97
2	F		96	92
3	Cl		96	91
4	OMe		95	90
5	CH <sub>3</sub> (CH <sub>2</sub> ) <sub>7</sub> ≡	CH <sub>3</sub> (CH <sub>2</sub> ) <sub>7</sub> CH <sub>2</sub> CH <sub>3</sub>	98	98

<sup>a</sup>Reactions were carried out with 1 mmol of alkyne, 50 mg of nano-ferrite–Ni, and 2 mL of methanol at room temperature, in an autoclave at 100 psi hydrogen pressure for 24 h

<sup>b</sup>Reactions performed at room temperature, catalyst 0.05 g, MeOH 2.0 mL, substrate 1 mmol, time 18 h

A study by Baruwati et al. (2009) on a magnetically recoverable supported ruthenium catalyst supported on magnetic NPs (NiFe<sub>2</sub>O<sub>4</sub>) has successfully used for the hydrogenation of alkynes to alkane and the reduction of carbonyl compounds to alcohols. High yield products (>95%) were achieved even after the fifth reaction cycle at room temperature. Similar studies by Polshettiwar et al. (2009) were

conducted using the nano-ferrite catalyst for the hydrogenation reactions (Table 10).

Veisi et al. (2021) used *Fritillaria imperialis* flower extract-mediated Pd NPs-fabricated magnetic Fe<sub>3</sub>O<sub>4</sub> (Fe<sub>3</sub>O<sub>4</sub>@Fritillaria/Pd) nanocomposite for the reduction of nitroarenes. Excellent results (98%) yield of aniline derivatives was obtained. The green, bioinspired, and magnetically

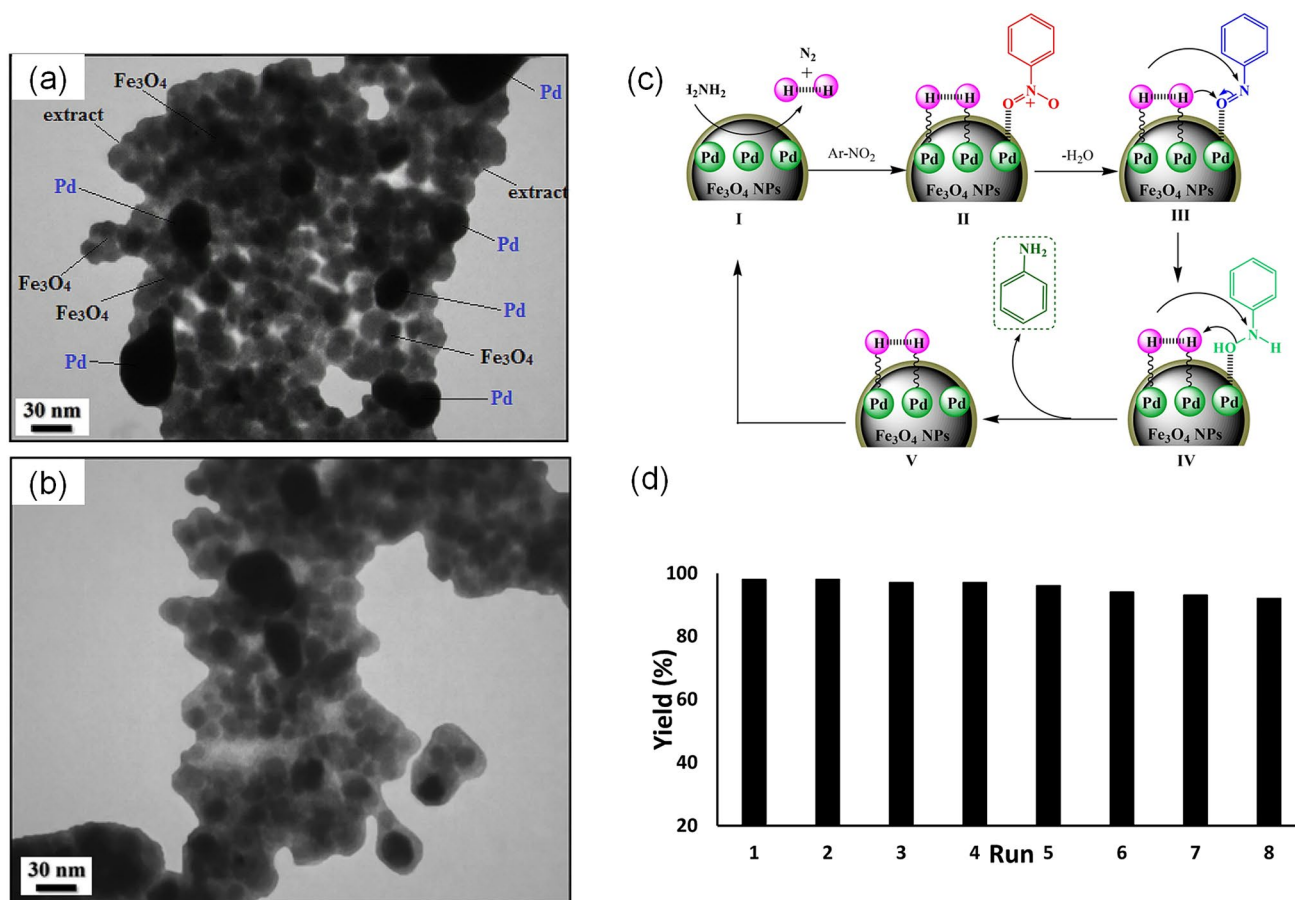


**Fig. 15** TEM images of **a** fresh, **b** 7 times reused Fe<sub>3</sub>O<sub>4</sub>@Fritillaria/Pd NPs **c** Reaction mechanism for the reduction of nitrobenzene over Fe<sub>3</sub>O<sub>4</sub>@Fritillaria/Pd catalyst **d** Reusability of Fe<sub>3</sub>O<sub>4</sub>@Fritillaria/Pd

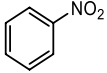
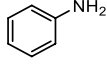
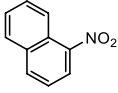
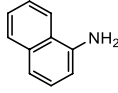
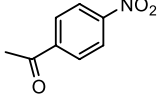
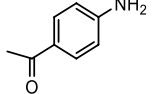
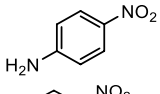
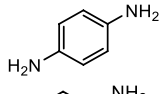
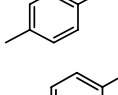
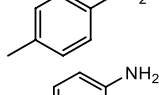
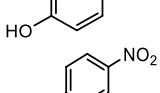
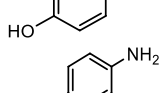
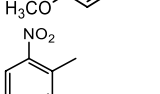
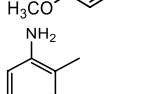
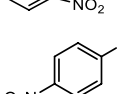
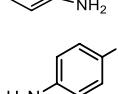
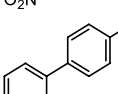
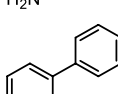
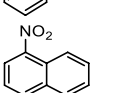
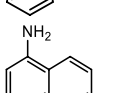
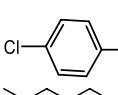
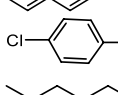
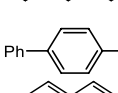
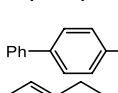
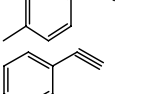
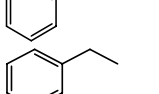
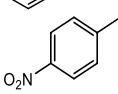
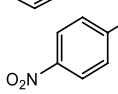
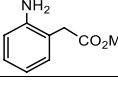
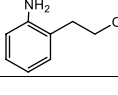
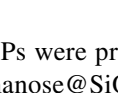
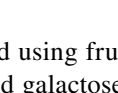
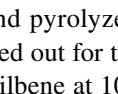
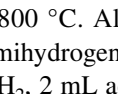


catalyst for reduction of nitrobenzene (Veisi et al. 2021) © Springer nature, reproduced with permission

separable nanocomposite catalyst was stable and performed for seven consecutive runs. TEM and EDX analysis of the 7 reused nanocomposites do not show any structural, morphological, or any sign of agglomeration (Fig. 15a, b, d). Finally, the proposed reaction mechanism was forwarded. The hydrazine first adsorbs on the surface of Pd NPs followed by N<sub>2</sub> formation and subsequent nitroarenes adsorption on the catalyst surface results in the formation of aniline (Fig. 15c).

Abu-reziq et al. (2007) synthesized Pt NPs supported on magnetite NPs for the purpose of hydrogenation of alkynes and reduction of  $\alpha$ - $\beta$ -unsaturated aldehydes into alcohols. The NPs were stable, readily recoverable by an external magnet, suitable in ILs, and selective to isomers (*cis* products) for alkyne hydrogenation and allyl alcohols were mainly produced. For example, the product of diphenylacetylene hydrogenation yields *cis*-stilbene (95%) and *trans*-stilbene (5%), 1-ethynyl-4-methylbenzene to 1-methyl-4-vinylbenzene (88%) and 1-ethyl-4-methylbenzene (12%), cinnamaldehyde to 3-phenylprop-2-en-1-ol (99%), and

2-methyl-3-phenylacrylaldehyde to 2-methyl-3-phenylprop-2-en-1-ol (90%) was achieved using the catalyst. Stein et al. (2011) synthesized iron nanoparticles (Fe-NPs) supported on chemically derived graphene (CDG) for the reduction of alkene and alkyne to their corresponding alkane under THF, room temperature, and 30 bars. The hydrogenation of styrene, cyclooctene, 1-hexene, 1-octene, norbornene, and 1-phenyl-1-propyne results in 99, 99, 100, 100, 100, and 100% product yields (alkane); however, cyclopentene, cyclohexene, and *trans*-stilbene yield 73, 79, and 7% of the products only. The Fe NP-CDG exhibited good catalytic activity in most of the alkene including cyclic alkene, but unsuitable for the hydrogenation of internal double bonds of a cyclic system; on the other hand, no product was achieved in the hydrogenation of tri- and tetrasubstituted olefins. Disubstituted alkynes were catalyzed better than the terminal once. The catalyst was stable and reused in several runs without significantly altering the catalytic activity. A monodisperse Ni NPs was reported for stereo- and chemoselective semihydrogenation of alkynes to alkenes. The

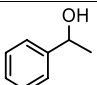
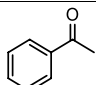
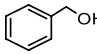
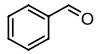
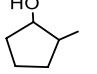
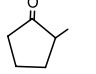


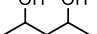

**Table 11** Summary of reduction and hydrogenation reaction yields using nanocatalyst

Reactant	Product	Time (min)	Solvent	Temp (°C)	Nanocatalyst	Yield (%)	Ref.
		45	H <sub>2</sub> O	50	Pd@C	100	Sadjadi et al. (2020)
		155	H <sub>2</sub> O	50	Pd@C	85	Sadjadi et al. (2020)
		100	H <sub>2</sub> O	50	Pd@C	90	Sadjadi et al. (2020)
		180	H <sub>2</sub> O	50	Pd@C	55	Sadjadi et al. (2020)
		5	H <sub>2</sub> O:EtOH	25	Pd(OAc) <sub>2</sub>	98	Yan et al. (2020)
		5	H <sub>2</sub> O:EtOH	25	Pd(OAc) <sub>2</sub>	90	Yan et al. (2020)
		7	H <sub>2</sub> O:EtOH	25	Pd(OAc) <sub>2</sub>	96	Yan et al. (2020)
		60	EtOH	80	Fe <sub>3</sub> O <sub>4</sub>	99	Kim et al. (2011b)
		1:5 h	EtOH	80	Fe <sub>3</sub> O <sub>4</sub>	99	Kim et al. (2011b)
		1:5 h	EtOH	80	Fe <sub>3</sub> O <sub>4</sub>	99	Kim et al. (2011b)
		20 min	H <sub>2</sub> O:MeOH	-	Pd	>99	Eghbali et al. (2018)
		20 min	H <sub>2</sub> O:MeOH	-	Pd	81	Eghbali et al. (2018)
		20 h	EtOH	25	Pd	85	Lu et al. (2017)
		20 h	EtOH	25	Pd	85	Lu et al. (2017)
		24 h	CDCl <sub>3</sub>	25	Pd	>99	Mahdaly et al. (2019)
		24 h	CDCl <sub>3</sub>	25	Pd	>99	Mahdaly et al. (2019)
		24 h	CDCl <sub>3</sub>	25	Pd	>99	Mahdaly et al. (2019)
		3 h	THF/H <sub>2</sub> O	100	Ag	55.6	Feng et al. (2018)

NPs were prepared using fructose@SiO<sub>2</sub>, glucose@SiO<sub>2</sub>, manose@SiO<sub>2</sub>, and galactose@SiO<sub>2</sub> supporting materials and pyrolyzed at 800 °C. All the Ni-base NPs were carried out for the semihydrogenation of diphenylacetylene to stilbene at 10 bar H<sub>2</sub>, 2 mL acetonitrile, 110 °C, 15 h, and

10 mg of catalyst (1.6 mol% Ni) to exhibited >99% conversion, 94% yield, 99:1% selectivity of Z:E isomers of stilbene and 5% yield of alkane. Diphenylacetylene derivatives (with different electron-withdrawing and -donating groups) were also tested using the catalyst and high-yield products with

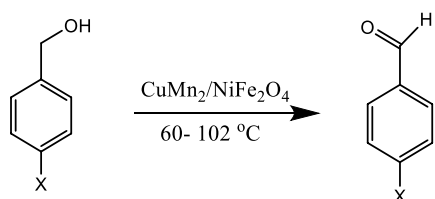
**Table 12** Oxidation of alcohols (reaction conditions: alcohol (0.18 mmol), Fe<sub>3</sub>O<sub>4</sub>/SiO<sub>2</sub>/Ru<sup>3+</sup> (Ru: 4 mol%), toluene (1 mL), 3 h, 100 °C, 3 atm O<sub>2</sub>) by Ru(III) magnetically recoverable catalyst (Jacinto et al. 2009b) © Elsevier, reproduced with permission

No:	Substrate	Product	Conversion (%)	Selectivity (%)
1			>99	>99
2			>99	>99
3			>99	>99
4			82	>99
5			>99	>99

<sup>a</sup>Measured by GC–MS<sup>b</sup>7 h

stereo- (98–100% *Z*-alkene formation) and chemo-selectivity were observed. Finally, the NPs were recycled and reused for seven consecutive runs to give > 90% yield and similar selectivity (Murugesan et al. 2019). Fan et al. (2017) fabricated TiO<sub>2</sub>-supported Pd catalysts (Pd/TiO<sub>2</sub>) for phenylacetylene semihydrogenation to styrene. Three samples of the NPs were prepared using photodeposition (PD) and deposition–precipitation method (DP) both supported on the anatase TiO<sub>2</sub>, and further thermally dried PD at 300 °C (PD-300). The DP catalyst showed higher initial performance in the conversion of phenylacetylene to styrene reaches 100% at 40 min but after 60 min, the selectivity of styrene is failed to 0%. In contrast, the PD catalyst retains high selectivity of forming styrene even after a 100-min reaction time with a 95% selectivity. The PD-300 catalyst was also performed

similarly to the PD but declined rapidly when the conversion reaches 100%. This is due to the reason that quasi-spherical Pd ensembles (regular) arrangement was observed on the DP catalyst while thermal treatment of Pd disorganized the structure to have various boundaries in PD and PD-300. The reduction of nitroaromatic to aromatic amines extensively studied using NPs as a catalyst. Since the nitroamines are toxic and environmentally unfriendly, reduction to their corresponding nontoxic amines is important. For example, nitrophenol can be transformed into harmless aminophenol that is an important intermediate for dyes and pharmaceuticals in advanced yield (Table 11) (Zhang et al. 2019a). Water-soluble Pd NPs have been used for selective hydrogenation of phenol to cyclohexanone. The water-soluble Pd NPs were stabilized over PVP and > 99% conversions have

**Table 13** Selective oxidation of benzyl alcohols into corresponding aldehydes over CuMn<sub>2</sub> and NiFe<sub>2</sub>O<sub>4</sub> catalysts using molecular oxygen as oxidant (Ali et al. 2015; Iraqi et al. 2020)

Entry	X	Time (min)	Conversion (%)		Selectivity (%) CuMn <sub>2</sub>	Specific activity (mmol g <sup>-1</sup> h <sup>-1</sup> )
			CuMn <sub>2</sub>	NiFe <sub>2</sub> O <sub>4</sub>		
1	H	20	100	85	> 99	30, 28.3 <sup>a</sup>
2	CH <sub>3</sub>	20	100		> 99	30
3	NO <sub>2</sub>	25	100	88	> 99	24, 29.3 <sup>a</sup>
4	Cl	50	100	81	> 99	12, 27.0 <sup>a</sup>
5	CF <sub>3</sub>	60	100		> 99	10
6	C(CH <sub>3</sub> ) <sub>3</sub>	30	100		> 99	20

Reaction condition: 200 mg CuMn<sub>2</sub> mixed catalyst, 2 mmol substrates, 10 mL toluene solvent, 100–102 °C, NiFe<sub>2</sub>O<sub>4</sub>: 10 mg; solvent: CH<sub>3</sub>CN, *t* = 3 h

<sup>a</sup>For NiFe<sub>2</sub>O<sub>4</sub> catalyst

been achieved in 16 h, 1 atm H<sub>2</sub>, and 90 °C to cyclohexanone with > 99% selectivity; however, the use of Ru NPs showed 99% dominantly to cyclohexanol (99.8% selectivity). Another nanocatalyst such as Pt NPs has been also checked for the hydrogenation of phenol and the conversion of phenol to cyclohexanone decreased to 19.2% with 77.2% selectivity (Zhu et al. 2014).

## Oxidation reaction

The oxidation reaction is the most important chemical process in organic chemistry and is central to the design and development of new and novel value-added products. Aldehydes, ketones, epoxides, and organic acids are the most important sources of drugs, vitamins, fragrances, and selective oxidation of these products from alcohols, unsaturated hydrocarbons, and other sources are required. Conventionally, oxidation reactions are performed at high temperature and pressure using stoichiometric amounts of oxidants, such as chromates, oxalyl chloride, or hypervalent iodides, permanganate, or *N*-chlorosuccinimide, and volatile organic solvents which are not environmentally benign due to the release of a large amount of hazardous waste byproducts. As well, it is difficult to recycle and separate catalysts from the products (Guo et al. 2011; Imamura et al. 2013; Gawande et al. 2016). Therefore, the oxidation reaction carried out under mild conditions having a high yield and recovery with minimum waste byproducts is vital. Nowadays, nano-level catalysts are applied in oxidation reactions to produce reasonable results with remarkable selection, conversions, and separation (Liu et al. 2015).

Jacinto et al. (2009b) have reported Ru(0) and Ru(III) catalysts functionalized on silica-coated magnetic support that possess great catalytic performance and recovery properties. Thus, the magnetically separable Ru(III) catalyst (Fe<sub>3</sub>O<sub>4</sub>/SiO<sub>2</sub>/Ru<sup>3+</sup>) was used for the oxidation of primary and secondary alcohols to their corresponding aldehydes and ketones with remarkable conversion and selectivity as shown in Table 12 below. In addition, the magnetically separate Ru(0) form was active for the hydrogenation of cyclohexene with a conversion of > 99% and 420 h<sup>-1</sup> TOF.

Ali et al. (2015) also studied the oxidation of benzylic alcohols using copper-manganese mixed oxide NPs (CuMn<sub>2</sub>) as a catalyst. Thus, the CuMn<sub>2</sub> nanocatalyst showed excellent catalytic performance for the oxidation of benzylic alcohols to their corresponding aldehydes with > 99% selectivity and 100% conversion in a very short period of time and 100 °C. However, NiFeO<sub>4</sub> MNCs performed below a 90% conversion and had a longer reaction time. The reaction is highly dependent on the electronic, steric effects of the substituents, and electron-withdrawing groups attached to the

benzylic alcohols which demand a long time to complete the reaction (Table 13).

Alcohol oxidation was carried out by the copper(II) phthalocyanine nanocatalyst, using water as a solvent and tetra-*n*-butyl-ammonium-peroxo-monosulfate (*n*-Bu<sub>4</sub>NHSO<sub>5</sub>) as an oxidant at 85 °C. Both aliphatic and aromatic alcohol derivatives were employed in the oxidation reaction by the nanocatalysts and 80–95% yield of products has been achieved by varying the substituents on the cyclic alkane and aromatic alcohol derivatives; however, only 64% yield of propanone was obtained from 2-propanol. Finally, the catalyst has been separated from the product by simple extraction with ether and reused several times without any change in its activity (Kheirjou et al. 2016). A novel DNA–Montmorillonite (MMT hybrid)-supported Pt, Pd, and Au NPs were successfully prepared for the conversion of alcohols to aldehydes, acids, and esters selectivity and effectively using water as a solvent. Thus, the natural DNA–MMT-supported NPs showed remarkable selection oxidation of the primary alcohols. Yields of up to 98, 94, and 98% of carboxylic acid, esters, and aldehyde were obtained corresponding to Pd/DNA–MMT, Au/DNA–MMT, and Pt/DNA–MMT catalysts, respectively. Catalysts have been separated by a simple phase separation process for subsequent reuse (Tang et al. 2013). Mn-graphene oxide nanocomposite (Mn<sup>2+</sup>/GO) was applied for alkene catalytic epoxidation typically, for styrene epoxidation in H<sub>2</sub>O<sub>2</sub> (30 wt%) in the presence of NaHCO<sub>3</sub>. The nanocomposite showed superior catalytic activity for the epoxidation of styrene with almost 95% of the yield of styrene epoxide obtained over the Mn<sup>2+</sup> ions loaded on the GO nanosheet and giving a high TOF value of 2000 h<sup>-1</sup>. Various alkenes were also undergoing epoxidation by the Mn<sup>2+</sup>/GO nanocomposite to yield 85–97% epoxide products and 96–99% conversions. Alkenes with a high electron density of the conjugated systems were highly effective due to the possibility of electrophilic cycloadditions (Zheng et al. 2014). A recyclable magnetic cobalt ferrite NP (CoFe<sub>2</sub>O<sub>4</sub>) was also applied for the oxidation of alkenes such as styrene, methyl styrene, 4-methoxystyrene, 4-nitrostyrene, cyclohexene, and 1-heptene to the corresponding carbonyl compounds. Oxidation of cyclohexene results in an allylic oxidation product, 2-cyclohexene-1-one with 75% yield and terminal olefins like 1-heptene was also transformed to epoxides with good yield and selectivity using *t*-BuOOH as an oxidant (Kooti and Afshari 2012). Oxidation of alcohols to aldehydes is very difficult in organic chemistry because over-oxidation occurs immediately to carboxylic acids and ester. Zhao et al. (2019b) studied the selective oxidation of alcohols to aldehydes using very small size (2 nm) Ru NPs. The non-supported Ru NPs were checked for the oxidation of aliphatic, aromatic, and unsaturated alcohols to aldehydes under a mild condition without the use of toxic solvents to exhibit > 90% selectivity. It shows an 85% selectivity for

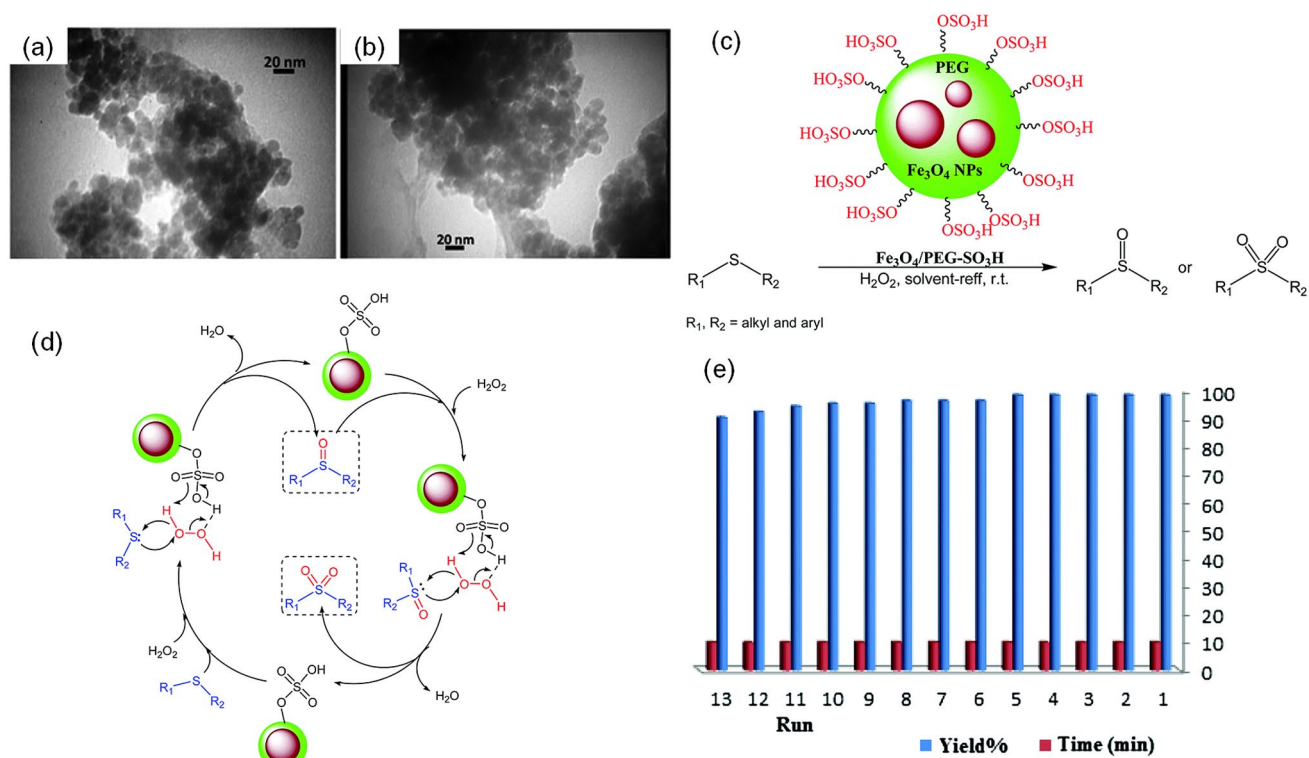


**Fig. 16** TEM images of fresh **a** and **b** reused catalyst Fe<sub>3</sub>O<sub>4</sub>/PEG-SO<sub>3</sub>H after the 12th run **c** Fe<sub>3</sub>O<sub>4</sub>/PEG-SO<sub>3</sub>H catalyzed the oxidation of using H<sub>2</sub>O<sub>2</sub> **d** Proposed mechanism for the oxidation of sulfide to the corresponding sulfoxide or sulfone with aqueous hydrogen perox-

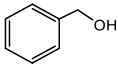
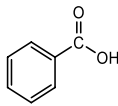
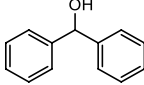
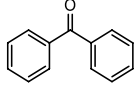
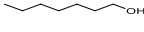
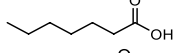
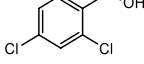
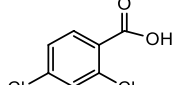
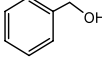
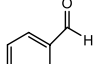
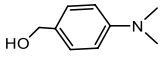
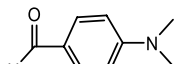
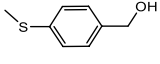
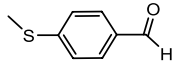
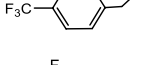
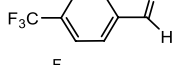
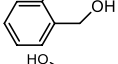
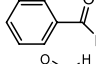
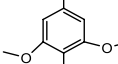
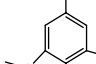
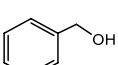
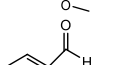
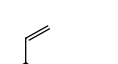
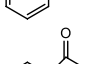
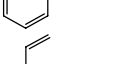
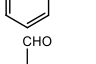
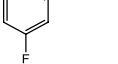
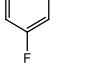
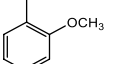
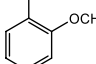
ide in the presence of Fe<sub>3</sub>O<sub>4</sub>/PEG-SO<sub>3</sub>H **e** Reusability of the nanocatalyst (Mirfakhraei et al. 2018) © Royal Society of Chemistry, reproduced with permission

**Table 14** Selective oxidation of sulfides to sulfoxides and to sulfones with 30% H<sub>2</sub>O<sub>2</sub> using MoO(O<sub>2</sub>)<sub>2</sub>@Bipy-PMO-IL (reaction condition: methyl phenyl sulfide (0.2 mmol), 30% aq. H<sub>2</sub>O<sub>2</sub> (0.4 mmol), MoO(O<sub>2</sub>)<sub>2</sub>@Bipy-PMO-IL (3 mol%) water (3 mL), r.t. 30 min) (Moaser et al. 2020) © Elsevier, reproduced with permission

Entry	Sulfide (S)	Sulfoxide (SO)	Yield [%] <sup>b</sup>	
			(SO)	(OSO)
1			90	10
2			91	9
3			90	90
4			88	8
5			80	15
6			57	<5

<sup>b</sup>Based on GC–Mass

**Table 15** Summary of oxidation of alcohols using nanocatalyst

Reactant	Product	Time	Solvent	Temp (°C)	Nanocatalyst	Yield (%)	TON	Ref.
		2 h	H <sub>2</sub> O	80	Pd@PPy/OMC	99	990	Ganji et al. (2020)
		18 h	H <sub>2</sub> O	80	Pd@PPy/OMC	98	98	Ganji et al. (2020)
		30 h	H <sub>2</sub> O	80	Pd@PPy/OMC	100	200	Ganji et al. (2020)
		16 h	H <sub>2</sub> O	80	Pd@PPy/OMC	87	435	Ganji et al. (2020)
		3 h	Toluene	80	Pt@cHs	99	-	Göksu et al. (2020a)
		3 h	Toluene	80	Pt@cHs	80	-	Göksu et al. (2020a)
		3 h	Toluene	80	Pt@cHs	55	-	Göksu et al. (2020a)
		3 h	Solvent free	40	Pd/AIO(OH)	99 ± 3	-	Goksu and Sen (2020)
		3 h	Solvent free	40	Pd/AIO(OH)	75 ± 2	-	Goksu and Sen (2020)
		3 h	Solvent free	40	Pd/AIO(OH)	99 ± 2	-	Goksu and Sen (2020)
		3 h	Solvent free	40	Pd/AIO(OH)	99 ± 2	-	Goksu and Sen (2020)
		2 h	Toluene	80	PtNi@SWCNT	>99 ± 1.0	-	Göksu et al. (2020b)
		4 h	Water	80	Fe-SNP	95	-	Rajabi et al. (2012)
		4 h	Water	80	Fe-SNP	92	-	Rajabi et al. (2012)
		4 h	Water	80	Fe-SNP	93	-	Rajabi et al. (2012)

Pt@cHs carbon hybrid-supported platinum nanoparticles, Pd/AIO(OH) aluminum oxy-hydroxide-supported palladium nanoparticles

**Fig. 17** Sonication of anthranilamide and aldehydes with Ag-CNTs as catalyst (Safari and Gandomi-Ravandi 2014)  
© Royal Society of Chemistry, reproduced with permission

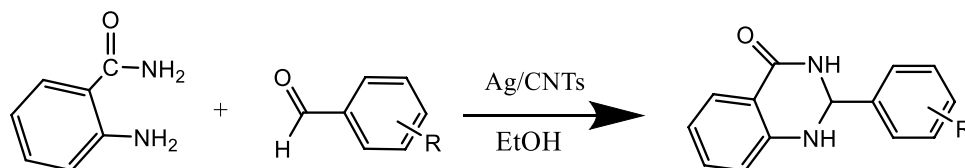
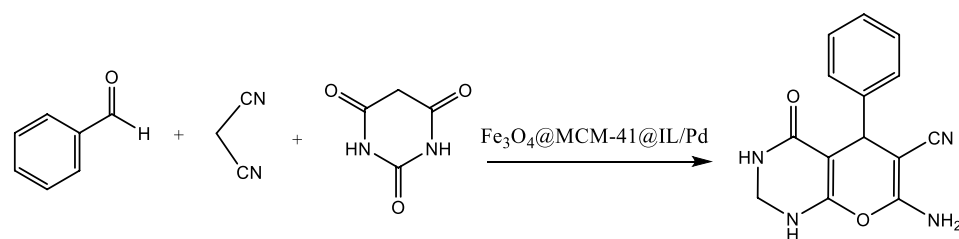


**Table 16** Recoverability and reusability of the Fe<sub>3</sub>O<sub>4</sub>@MCM-41@IL/Pd nanocatalyst under ultrasonic conditions (Abaezadeh et al. 2019) © John Wiley and Sons, reproduced with permission



Run	Time (min)	Yield (%)	Run	Time (min)	Yield (%)
1	10	96	7	12	90
2	10	94	8	14	92
3	10	95	9	14	90
4	10	95	10	14	90
5	10	94	11	18	88
6	12	92	12	18	86

<sup>a</sup>Reaction conditions: aldehyde (1 mmol), malononitrile (1 mmol), barbituric acid (1 mmol) and Fe<sub>3</sub>O<sub>4</sub>@MCM-41@IL/Pd (0.014 mol%) at 40 °C under ultrasonic waves

<sup>b</sup>Isolated yield

octanol-to-octanal conversion, which is 5–7 times higher than the other large-size Ru catalyst and the reference Ru/Al<sub>2</sub>O<sub>3</sub> catalyst. Similarly, Bhat et al. (2014) fabricated a nickel hydroxyl-coated nano-cobalt ferrite catalyst for the selective oxidation of alcohol into aldehydes. The magnetically recoverable nanocatalyst was active for the oxidation of primary and secondary alcohols with 87% conversion efficiency and 97% selectivity to their corresponding aldehydes in a reasonable yield (Table 15).

Mirfakhraei et al. (2018) designed sulfonated-polyethylene glycol-coated Fe<sub>3</sub>O<sub>4</sub> nanocomposite (Fe<sub>3</sub>O<sub>4</sub>/PEG–SO<sub>3</sub>H) as an effective and ecological nanocatalyst for the selective oxidation of sulfides to sulfoxides or sulfones. The immobilized MNC offered almost 100% yield of the products in 10 min. Further, the catalyst was recycled by a magnetic device and reused 13 times without loss. The leaching of the catalyst was controlled with HFT and the quality of the catalyst was preserved. The TEM images of the fresh nanocatalyst and the recycled catalyst after 12 cycles confirmed that the morphology and chemical structures of the nanocatalyst was retained (Fig. 16a, b, e). Elemental analysis of the 12th recycled catalyst demonstrated that the leaching of the active catalytic locations was less than 5% of the total quantity of the catalytic site. Finally, the proposed mechanism for the oxidation of sulfide to the corresponding sulfoxide or sulfone using the Fe<sub>3</sub>O<sub>4</sub>/PEG–SO<sub>3</sub>H was investigated (Fig. 16c, d).

In other studies, bipyridinium IL-bridged periodic mesoporous organosilica (Bipy-PMOs-IL) which was used as a support to immobilize oxygen-rich molybdenum

(VI)-based oxido-peroxido complex (MoO(O<sub>2</sub>)<sub>2</sub>@Bipy-PMO-IL) has been used for selective sulfide oxidation in the presence of H<sub>2</sub>O<sub>2</sub>. The hybrid catalyst showed excellent performance and easy work-up at ambient temperatures for the oxidation of sulfide derivatives. The MoO(O<sub>2</sub>)<sub>2</sub>@Bipy-PMO-IL catalyst was reused for five consecutive runs without significant loss; however, the MoO(O<sub>2</sub>)<sub>2</sub>@SBA-15 (without IL) significantly decreases its activity after the second run. The performance of the hybrid nanocomposite for the selective oxidation reaction of sulfides to sulfoxides under optimized conditions is summarized in Table 14 below (Moaser et al. 2020).

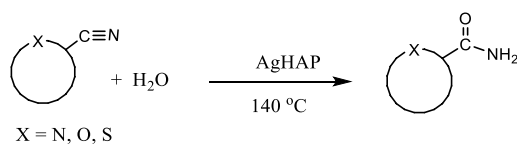
An early study by Yarmohammadi et al. (2021) also reported the oxidation of sulfide derivative into sulfoxides using copper-based on diamionaphthalene-coated magnetic NPs (CoFe<sub>2</sub>O<sub>4</sub>–DAN–Cu(II)). Under optimum conditions, 0.025 g of a load of catalyst, 1 mmol of sulfide, 30% H<sub>2</sub>O<sub>2</sub> (0.5 ml) at 25 °C, the synthesis yields of sulfoxides, symmetrical sulfides, and disulfides were about 99%, 95%, and 96%, respectively, with the highest selectivity. The catalyst was recycled nine times using a magnet and operated without significantly losing its catalytic activity as summarized in Table 15.

## Condensation and hydration reactions

Condensation and hydration reactions are very important in organic synthesis as well as in the chemical industries due to their wide range of intermediates for fragrance, medicine, agricultural chemicals, cosmetics, etc. In addition to this, the reactions are carried out biologically in protein formation



**Table 17** Hydration of various heteroaromatic nitriles using AgHA (reaction conditions: nitrile (1 mmol), AgHAP (0.1 g, Ag: 0.03 mmol), water (3 mL), 140 °C) (Mitsudome et al. 2009) © Royal Society of Chemistry, reproduced with permission



Entry	Nitrile	Amide	Tim (min)	Yield <sup>b</sup> (%)
1			15	99
2			60	99
3			10	99
4			30	99
5			20	98

<sup>a</sup>Reaction conditions: nitrile (1 mmol), AgHAP (0.1 g, Ag: 0.03 mmol), water (3 mL), 140 °C

<sup>b</sup>The values in parenthesis are isolated yields

via a peptide bond, carbohydrate (glycosidic), and other biochemical reactions and biomass hydrolysis like starch, lignin, hemicellulose for energy fuels in different chemical process (de Wild 2015; Höfer 2015). Therefore, the insolubility of the NPs in the hydration or condensation reaction makes them easily separated from the reaction products, solving one of the biggest problems associated with homogeneous catalysts (Downs and Tyler 2014).

Safari and Gandomi-Ravandi (2014) fabricated a carbon nanotube decorated Ag NP (Ag-CNT) as a heterogeneous nanocomposite catalyst for the synthesis of 2-aryl-2,3-dihydroquinazolin-4(1H)-ones as shown in Fig. 17. The synthesis of 2-aryl-2,3-dihydroquinazolin-4(1H)-one was carried out under ultrasonic irradiation since this method is convenient and gives good yields in a short period of time, high selectivity under mild condition. The effect of solvents on the yield of the product was also observed. The yield of the sonication of *o*-aminobezamide with benzaldehyde reaction was affected by a solvent and a 97% yield of the product was achieved using EtOH solvent in 5-min reaction time.

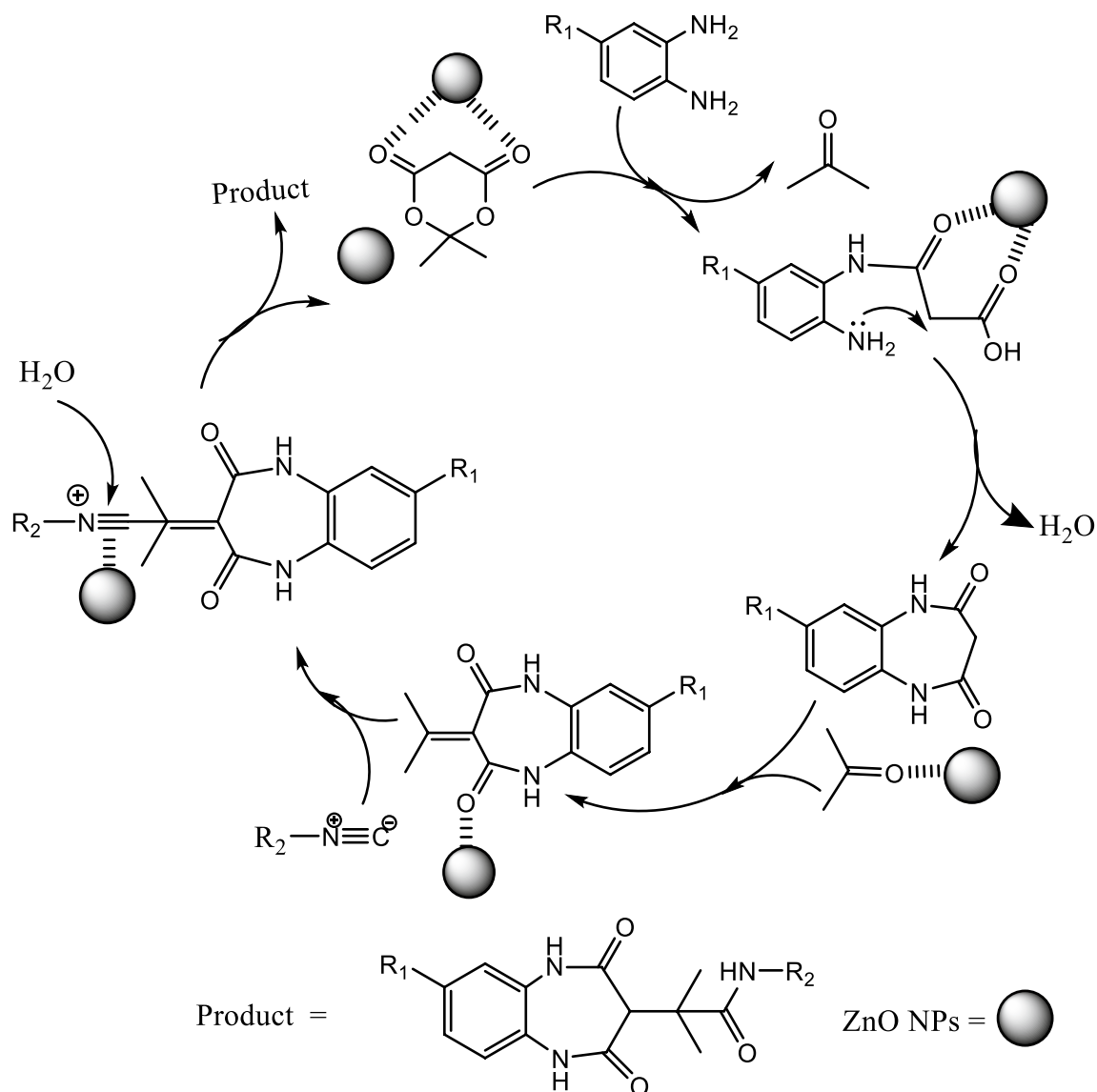
Abaezadeh et al. (2019) used magnetic mesoporous MCM-41 silica-supported ionic liquid/palladium complex (Fe<sub>3</sub>O<sub>4</sub>@MCM@IL/Pd) nanocatalyst for the synthesis of pyrano[2,3-d]pyrimidine derivatives. The core-structure nanocatalyst was recoverable and efficient for one-pot synthesis of the compounds under ultrasound and solvent-free conditions. A one-pot nucleophilic condensation between benzaldehyde, malononitrile, and barbituric acid under optimal conditions has taken place. The catalyst has been recovered and reused 12 times without noticeable loss of its initial performance (Table 16). Only 0.014 mol% of the catalyst was sufficient to

give 96% isolated yield of the product at 40 °C and 10 min reaction time. At the end of each run, the catalyst was recovered using an external magnet and washed with ethanol.

Mitsudome et al. (2009) studied the nanocatalyst hydroxyapatite-supported silver NPs (AgHAP) for the hydration of nitrile derivatives to their corresponding amines. Aromatic nitriles and their aliphatic nitrile derivatives have been hydrolyzed into amides. Hydration of heteroaromatic nitriles is usually difficult and the reaction rates are much lower than the other aromatic and aliphatic nitriles due to the strong coordination with metal centers. Thus, the AgHAP solves the problem of the difficulty of hydrating heteroaromatic nitriles, and 99% of yield products were obtained in less than 50 min reaction time (Table 17). Finally, the NP was highly efficient and reusable in the hydration reaction without any significant loss.

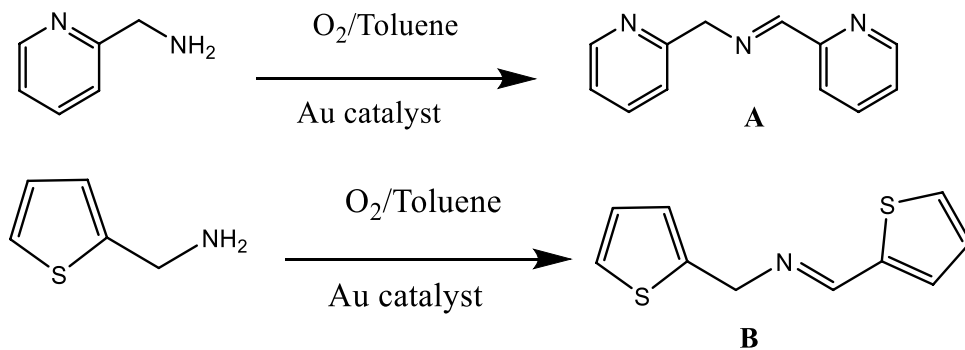
Ghasemzadeh and Safaei-ghomi (2015) use a ZnO NP to synthesize the biological and pharmaceutical compounds (benzo[b][1,5]diazepines) in a simple one-pot approach. The catalyst (ZnO) showed a superior catalytic activity and easily recyclable in a mild condition. A 93% yield of the product was obtained in 3.5 h; however, using another catalyst like Ni, CuO, MnO, and bulk ZnO only 45, 45, 52, and 62% yields products have been obtained, respectively. They also proposed the reaction mechanism of forming 1,5-benzodiazepin-2-ones using the ZnO NPs catalyst as shown in Fig. 18 below. The catalyst was separated from the reaction medium by dissolving the mixture with methanol and followed by centrifugation.

Grirrane et al. (2009) use supported gold NP catalysts (Au/C, Au/TiO<sub>2</sub>) for the oxidation of benzylamines (primary



**Fig. 18** Proposed reaction pathway for the synthesis of 1,5-benzodiazepin-2-ones by ZnO NPs (Ghasemzadeh and Safaei-gohmi 2015) © Taylor & Francis, reproduced with permission

**Fig. 19** Oxidation of heteroaryl amines to the corresponding *N*-arylidene arylmethanamines (Griirane et al. 2009) © Elsevier, reproduced with permission



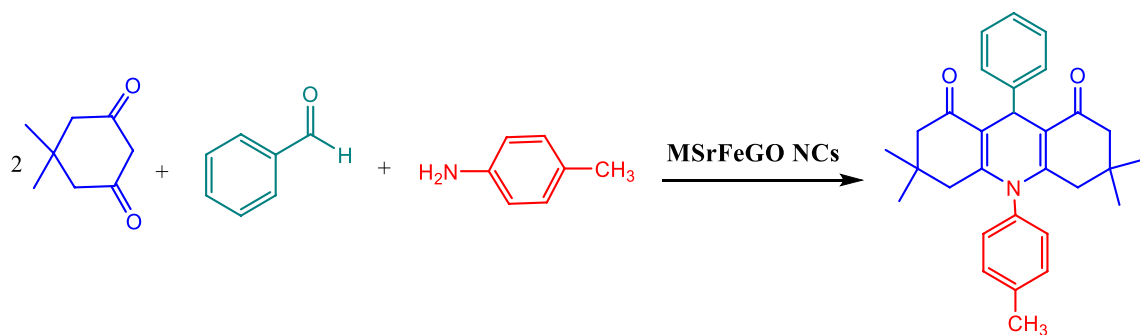


**Fig. 20** Synthesis of acridine derivatives

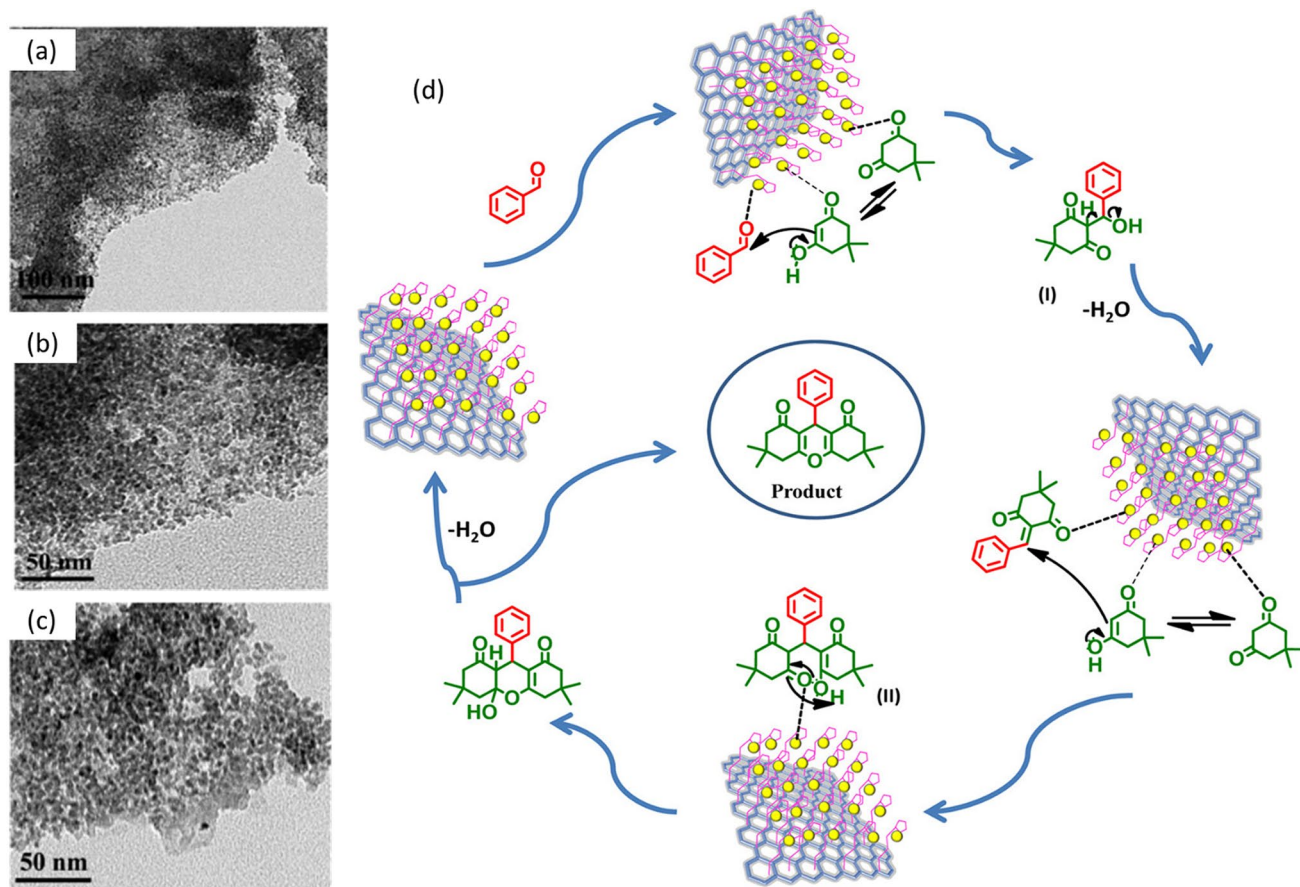


**Fig. 21** HRTEM micrographs of **a**, **b** fresh Cu(II)-Fur-APTES/GO nanocatalyst, and **c** recovered Cu(II)-Fur-APTES/GO nanocatalyst **d** Plausible mechanism for synthesis of xanthenes using the Cu(II)-Fur-

APTES/GO nanocatalyst (Subodh et al. 2018) © American Chemical Society, reproduced with permission

amines) to *N*-benzylidene benzylamines with molecular oxygen in toluene. The nanocatalyst was highly active, selective with extraordinary performance in the *N*–*N* coupling reaction. They have also studied that the catalyst can be used for other heterocyclic amines having sulfur in their ring. 96% conversion with 98% selectivity has been obtained using

Au/C for the production of **A** in 8 min and 99% conversion and selectivity has been obtained to produce product **B** using the same catalyst in 120 min. However, a 91% conversion and 86% selectivity have been observed for product **B** using Au/TiO<sub>2</sub> in 1800 min (Fig. 19).

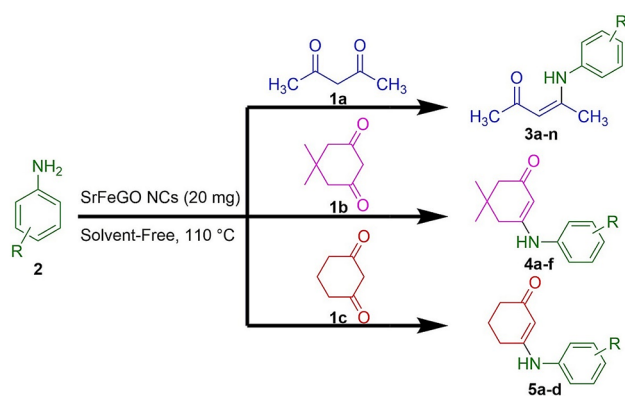


**Fig. 22** SrFeGO NC-catalyzed synthesis of  $\beta$ -enamino ketones (Mousavi et al. 2019b) © John Wiley and Sons, reproduced with permission

Recoverable graphene-based strontium MNC (MSr-FerGO NCs) has been synthesized under solvent-free conditions for the synthesis of acridine derivatives from dimedone, aromatic amines/ammonium acetate, and various aromatic aldehydes (Fig. 20). The nanocatalyst was novel and green for the synthesis of the biologically active compounds in a simple procedure, 97% yield, magnetic separable, and reusable several times without significant loss of its catalytic behavior (Mousavi et al. 2019a). Bimetallic Pd–Ni alloy NPs supported on graphite oxide (GO) have been reported to catalyze the Knoevenagel condensation reaction between aldehydes and malononitrile. The nanocatalyst was stable and reused several runs without decreasing its catalytic activity, the reaction was taking place in a short time with straightforward work-up procedures under mild conditions (Lolak et al. 2019).

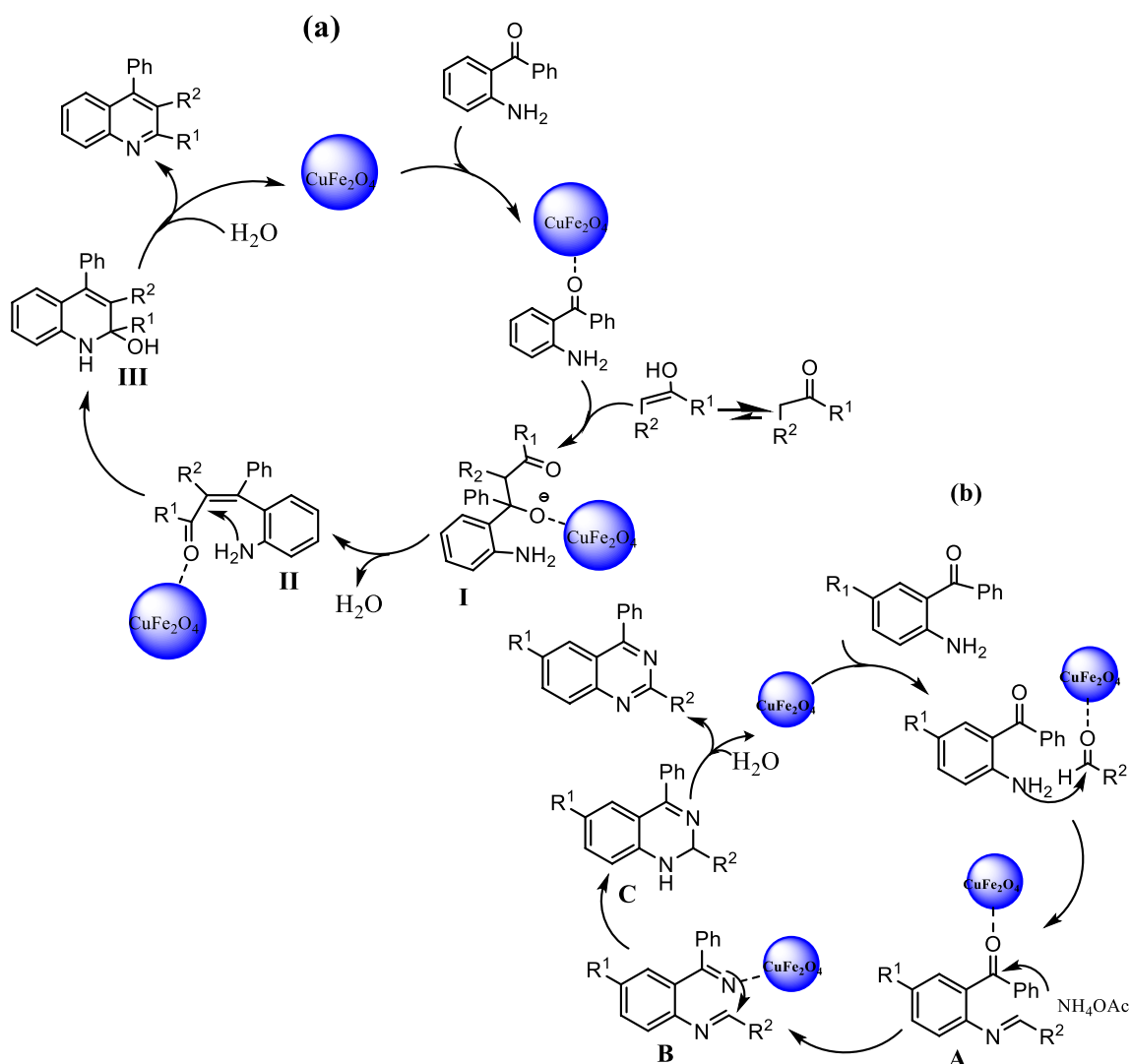


**Fig. 23** The proposed mechanism for the synthesis **a** quinazolines and **b** quinolines using  $\text{CuFe}_2\text{O}_4$  NPs (Baghbanian and Farhang 2014) © Royal Society of Chemistry, reproduced with permission

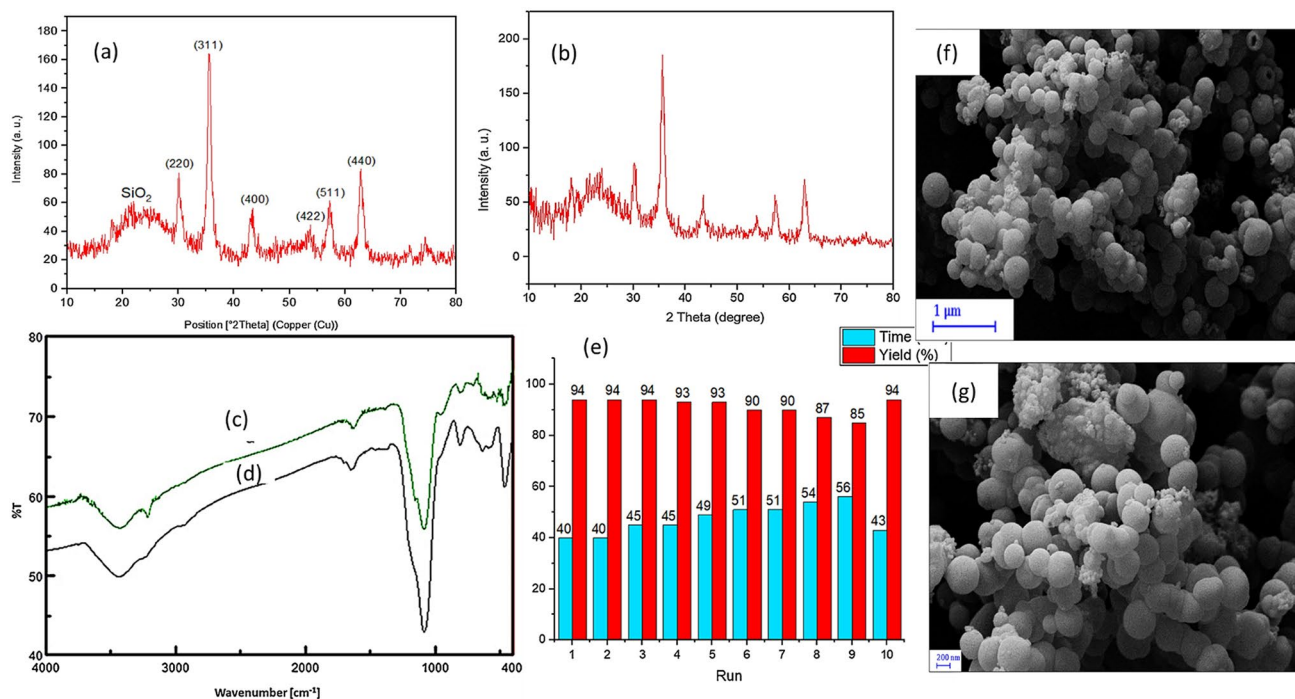


**Fig. 24** **a** WA-PXRD pattern of the fresh Mag@Ti-NOS nanocomposite **b** WA-PXRD pattern of the recovered Mag@Ti-NOS nanocatalyst after eight times of recovery and reuse **c** FTIR spectrum of fresh Mag@Ti-NOS **d** FTIR of recovered Mag@Ti-NOS nanocatalyst **e** Reusability of the Mag@Ti-NOS nanocatalyst in the synthe-

sis of tetrahydrobenzo[b]pyrans **f** SEM image of the Mag@Ti-NOS nanocomposite **g** The SEM image of the recovered Mag@Ti NOS nanocatalyst (Shaker and Elhamifar 2021) © Elsevier, reproduced with permission

In another study, fur-imine-functionalized graphene oxide-immobilized copper oxide nanoparticle (Cu(II)-Fur-APTES/GO) was synthesized for the synthesis of xanthen compounds. The nanocatalyst exhibited excellent yields (95%) of products in 25–50-min reaction time, easy work-up, simple product separations without byproducts. The (Cu(II)-Fur-APTES/GO) has been separated from the reaction mixtures via centrifugation, washing with ethyl acetate and ethanol, dried under vacuum, and reused for five runs without noticeable effect. Further, high-resolution transmission electron microscopy (HRTEM) images of the five times reused Cu(II)-Fur-APTES/GO nanocatalyst showed in Fig. 21c confirm no significant morphology change was observed compared to the fresh HRTEM images (Fig. 21a, b) indicating no agglomeration of CuO NPs occur. Finally, Cu(II)-Fur-APTES/GO activates the carbonyl group of benzaldehyde to make it more susceptible to nucleophilic attack by 5,5-dimethyl-1,3-cyclohexanedione to form intermediate (I); the addition of another molecule of 5,5-dimethyl-1,3-cyclohexanedione via Michael addition results in the formation of intermediate (II). Intramolecular cyclization occurs after the successful elimination of H<sub>2</sub>O which regenerates the nanocatalyst (Fig. 21d) (Subodh et al. 2018).

A novel and reusable SrFeGO magnetic nanocatalyst for a potential synthesis of  $\beta$ -enamino ketones in a highly pure form without the need for chromatographic purifications has been investigated (Fig. 22). The nanocatalyst was recovered using an external magnet and reused several times without a significant decrease in the synthesis efficiency. It also found that the synthesis protocol shows an excellent yield of up to 98% in a very short period of time. As a result, the nanocatalyst has been effective in solvent-free, easy work-up procedures and environmentally sound analytical procedures (Mousavi et al. 2019b).

Baghbanian and Farhang (2014) synthesized a magnetically recoverable and reusable CuFe<sub>2</sub>O<sub>4</sub> nanocatalyst for the synthesis of quinoline and quinazoline derivatives. As shown in Fig. 23a, b a plausible mechanism for the formation of quinazolines and quinolines using CuFe<sub>2</sub>O<sub>4</sub> NPs, methylene ketones are expected activated by the catalyst leads to aldol condensation to forms intermediate **I** and dehydration (**II**) and protonation between the carbonyl and amine results in ring closure and intermediate **III** is formed and eventually the removal of H<sub>2</sub>O gives the quinoline derivatives. Finally, the CuFe<sub>2</sub>O<sub>4</sub> NPs was recovered by an external magnet, washed with distilled water and ethanol, dried in an oven, and reused five times to give 95, 94, 92, 92, and 88% yield of the products consequently. Mazloumi and Shirini (2020)

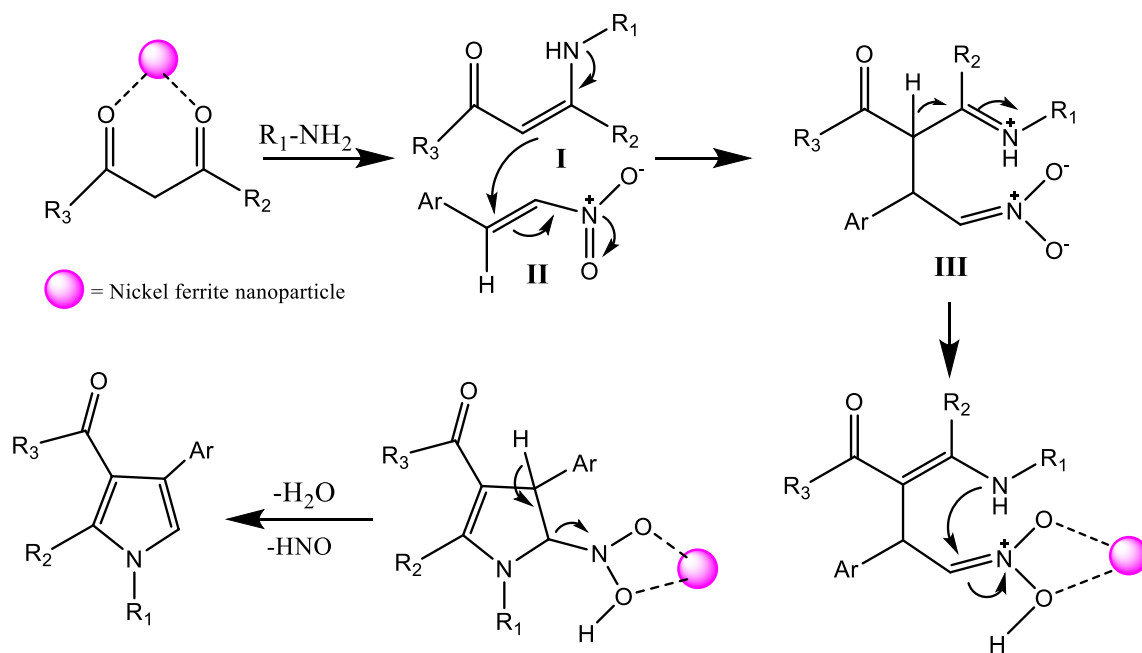


**Fig. 25** Proposed reaction mechanism of synthesizing pyrroles (Moghaddam et al. 2015) © Royal Society of Chemistry, reproduced with permission

use nanoporous  $\text{TiO}_2$  ( $\text{TiO}_2$ -[*bip*]- $\text{NH}_2^+\text{HSO}_4^-$ ) supported on IL bridges to synthesize quinoline, quinazoline, and *spiro*-quinazoline derivatives under solvent-free conditions. Electron-withdrawing and -donating groups containing aromatic aldehydes in their para position of the benzene ring were converted in a shorter time than the Cl and Br containing in the meta position. The aromatic aldehydes that contain  $\text{NO}_2$ ,  $\text{OH}^-$ , and Cl in the para position also converted with a lower yield to their corresponding quinoline, quinazoline, and *spiro*-quinazoline derivatives due to the steric hindrance. The nanoporous catalyst was recovered by filtration using ethanol, dried at room temperature, and reused several times to provide 94%, 93%, 90%, and 90% yields in the first, second, third, and fourth cycles in 5-, 6-, 6-, and 8-min reaction time, respectively.

A very recent study by Shaker and Elhamifar (2021) on magnetic Ti-loaded phenylene-based nanoporous organosilica (Mag@Ti-NOS) nanocomposite has been carried out for the synthesis of tetrahydrobenzo[*b*]pyrans using multicomponent synthesis pathway, condensation of 1 mol of each malononitrile, aldehyde, dimedone, 0.23 mol% Mag@Ti-NOS catalyst, and 5 ml  $\text{H}_2\text{O}$  took place. The supported MNCs was performed in water at 50 °C under ultrasonic conditions. The nanocomposite was recovered using a magnet and reused up to ten passes with no perceptible effect. The recovered nanocatalyst was washed using a Soxhlet apparatus by ethanol to characterize using XRD, FTIR, and SEM after 8 runs, confirming the retaining of the catalyst as

a uniform spherical structure providing the same as the fresh nanocatalyst (Fig. 24a–f).

## Heterocyclic scaffolds

Designing and synthesizing of diverse functionalized complex heterocyclic compounds are challenging. The formation of multi-bonds in one operation becomes one of the major challenges in chemistry (Ahoovie et al. 2018). The rapid growth of catalyst chemistry provides a robust and efficient catalyst that can be realized in a multicomponent reaction (MCR). In the MCR three or more substrates are combined in a single reaction vessel to form the product. Biologically important compounds such as substituted pyridine, tetrazole, and imidazoles are synthesized in such a way using MNCs (Kidwai et al. 2012; Forouzanahdel et al. 2020; Pawar and Chikate 2021). MCRs offered rapid and convergent construction of compounds from their starting reactants without isolation and purification of the intermediates, it saves time, cost, and energy than classical methods (Wang and Astruc 2014). These days, biologically active heterocyclic compounds are synthesized using a one-pot MCR (Ezzatzadeh et al. 2017). The synthesis of heterocyclic compounds such as triazoles, tetrazoles, pyrroles, etc. through multicomponent coupling reactions showed remarkable advantages of efficiency, waste minimization, and cost over the traditional synthetic approaches. Biologically active compounds and pharmaceutical intermediate route compounds are synthesized

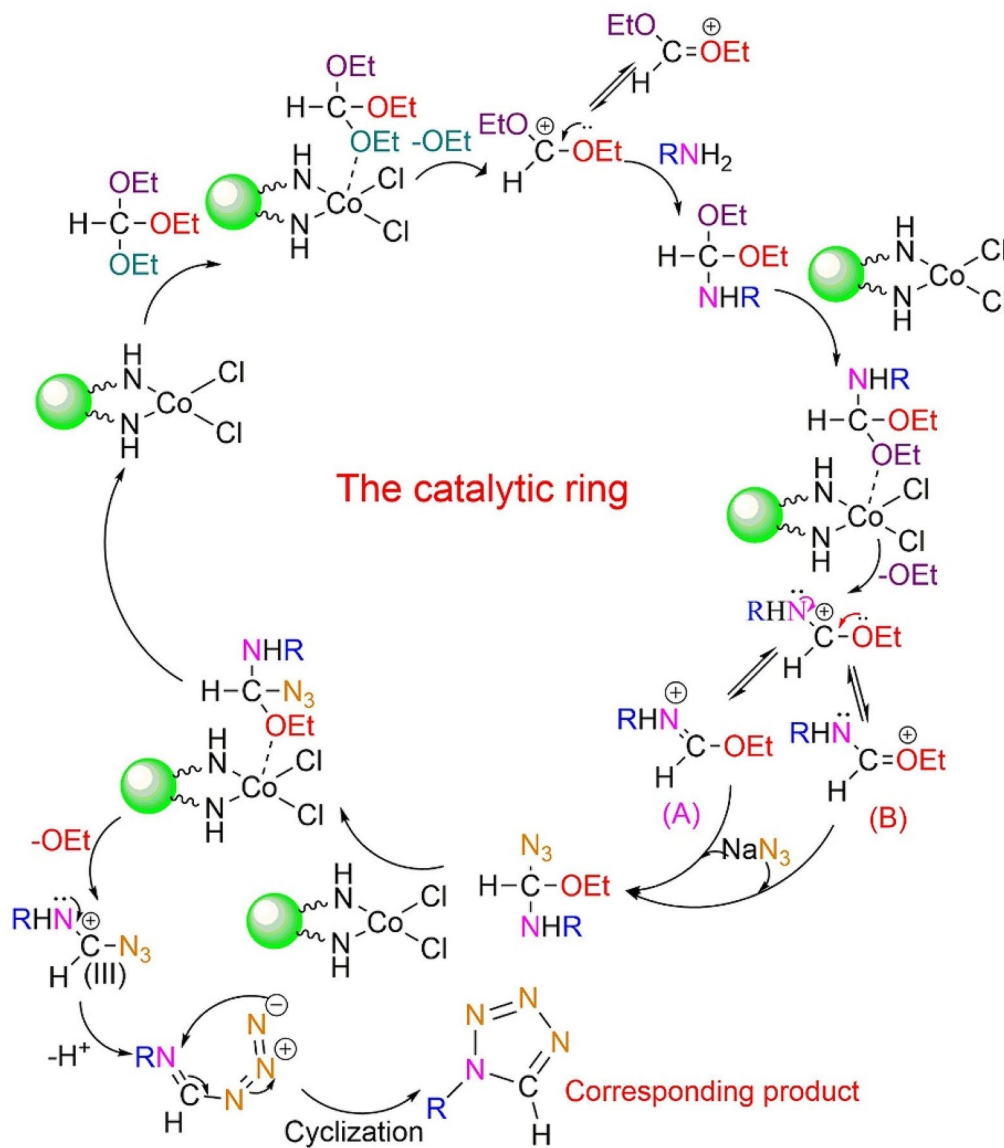
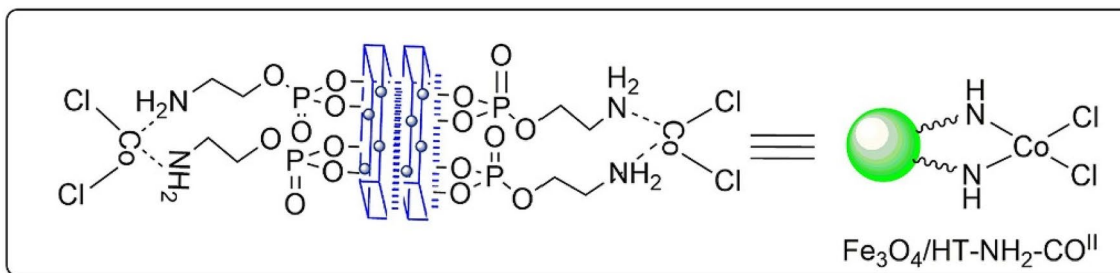


**Fig. 26** The suggested mechanism for the synthesis of tetrazoles with  $\text{Fe}_3\text{O}_4/\text{HT@AEPH}_2\text{-Co}^{\text{II}}$  (Salimi et al. 2020) © Elsevier, reproduced with permission

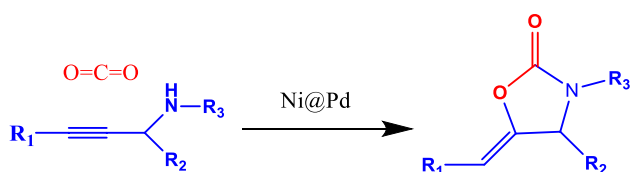


**Fig. 27** Synthesis of 2-oxazolidinone using Ni@Pd catalyst

using the 1, 3-dipolar cycloaddition (Gawande et al. 2014; Motahharifar et al. 2020).

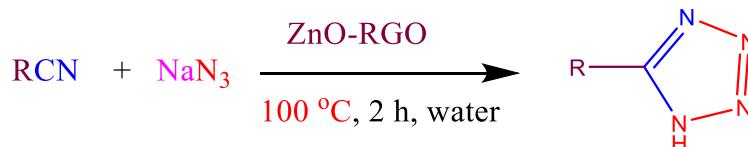
Moghaddam et al. (2015) applied nickel ferrite NPs for the synthesis of pyrroles. The catalyst was used effectively to synthesize the product in an average yield of 70–96% in different amounts of catalyst concentration, at 100 °C, 3–4 h. The catalyst was reused nine times without significant loss. After each run, the catalyst was separated by an external magnetic field and washed with distilled water. They proposed a facile, efficient, eco-friendly, and one-pot process for

the four-component synthesis of pyrroles with nickel ferrite NPs as a recyclable catalyst as shown in Fig. 25.

Khorrarnabadi et al. (2020) used a facile method to synthesize Cu NPs coated with Fe<sub>3</sub>O<sub>4</sub> magnetic NPs. The nanocatalyst was able to perform at 100 °C, without the use of a solvent to synthesize various tetrazole compounds with the highest product yield > 90%. The catalyst has been separated from the product via filtration, washed with ethanol, and dried in a vacuum, and reused five times without losing its activity to yield 94%, 90%, 86%, 83%, and 81% corresponding to the first, second, third, fourth, and fifth cycles, respectively. In another study, Fe<sub>3</sub>O<sub>4</sub>@HT@AEPH<sub>2</sub>-Co<sup>II</sup>, a bifunctional heterogeneous nanocomposite has been synthesized via amino-functionalized (Fe<sub>3</sub>O<sub>4</sub>@ hydrotalcite (HT)) with 2-aminoethyl dihydrogen phosphate (AEPH<sub>2</sub>) and then Co<sup>II</sup> immobilized onto an aminated ferrite NPs results in the formation of, Fe<sub>3</sub>O<sub>4</sub>@HT@AEPH<sub>2</sub>-Co<sup>II</sup>. The catalyst was used for the preparation of substituted 1H-tetrazoles from a sodium azide, triethyl orthoformate, and amine. The

**Table 18** Synthesis of 5-substituted-1H-tetrazoles catalyzed by ZnO-RGO (Benzonitrile (1 mmol), sodium azide (1.1 mmol), catalyst (20

wt%), water (2 mL), 100 °C) (Clarina and Rama 2018; Tahmasbi et al. 2020)



Entry	R	Time (h)	Yield (%) <sup>a</sup>		TON (h <sup>-1</sup> ) <sup>b</sup>
			ZnO-RGO	Pd-adenine@boehmite	
1	C <sub>6</sub> H <sub>5</sub> -	2, 1:30 <sup>d</sup>	94, 96 <sup>c</sup>	90	39, 21.1 <sup>d</sup>
2	<i>p</i> -ClC <sub>6</sub> H <sub>4</sub> -	2, 1:40 <sup>d</sup>	96	89	37, 19.8 <sup>d</sup>
3	<i>p</i> -NO <sub>2</sub> C <sub>6</sub> H <sub>4</sub> -	2, 21 <sup>d</sup>	96	88	40, 20.2 <sup>d</sup>
4	<i>p</i> -NH <sub>2</sub> C <sub>6</sub> H <sub>4</sub> -	5	86	–	35–
5	C <sub>6</sub> H <sub>5</sub> CH <sub>2</sub> -	8, 6:10 <sup>d</sup>	84	88	31, 19.6 <sup>d</sup>
6	CH <sub>3</sub> -	8	80	–	29
7	CNCH <sub>2</sub> -	8	86	–	35

<sup>a</sup>Isolated yield

<sup>b</sup>The moles of tetrazoles formed per mole of catalyst

<sup>c</sup>Yield of gram-scale reactions with benzonitrile (10 mmol), sodium azide (11 mmol)

<sup>d</sup>Under Pd-adenine@boehmite

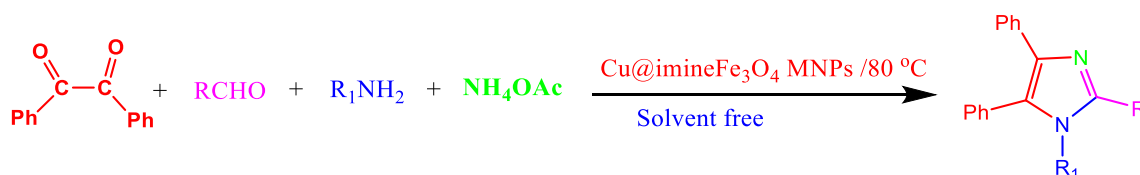


**Fig. 28** Preparation of 1,2,4,5-tetrasubstituted imidazoles derivatives using Cu@imine/Fe<sub>3</sub>O<sub>4</sub> MNPs as a catalyst (Thwin et al. 2019) © Royal Society of Chemistry, reproduced with permission



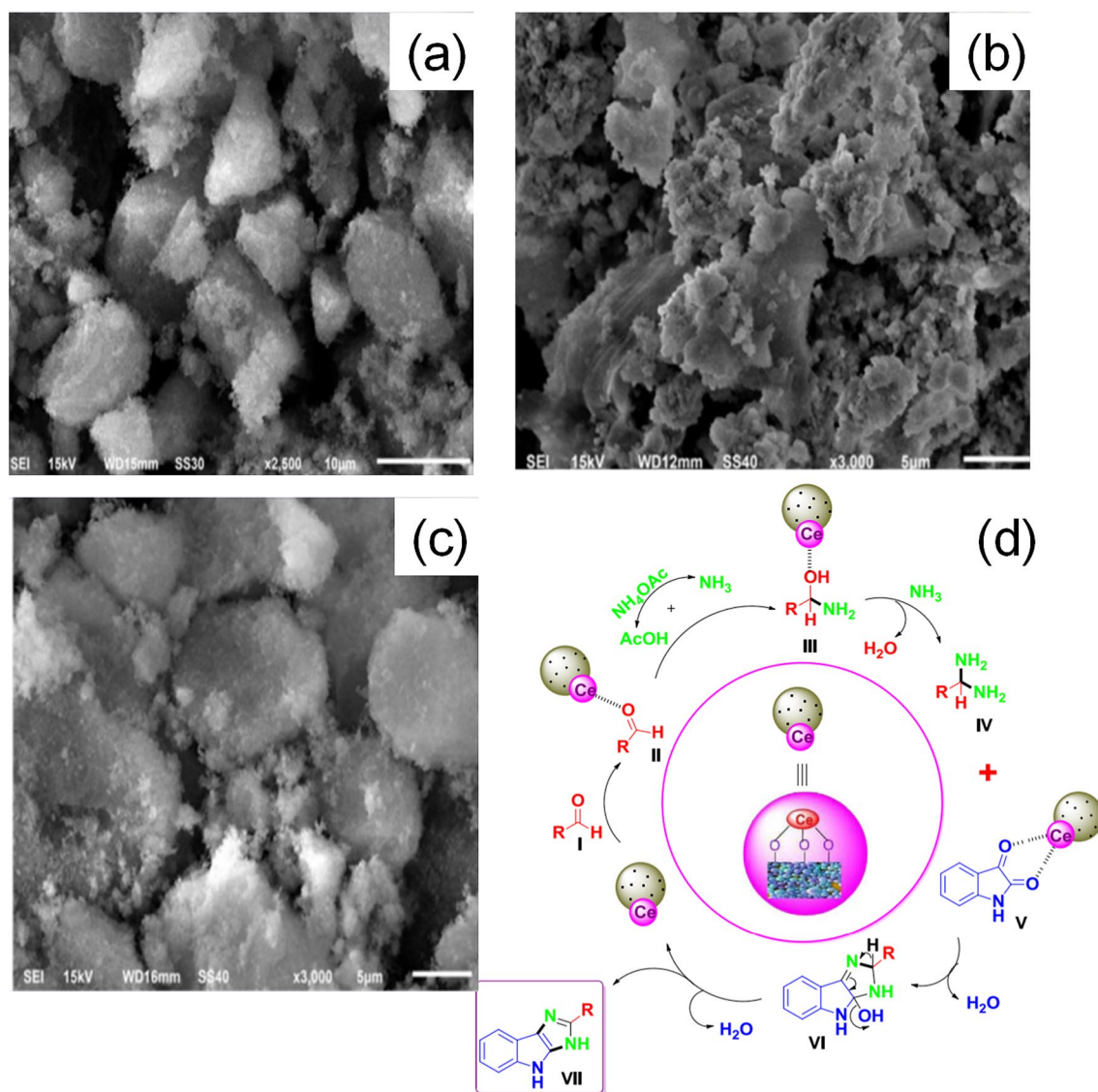


**Fig. 29** SEM image of **a** fresh catalyst (Ce@STANPs/ZrO<sub>2</sub>) **b** recycled catalyst after the seventh run **c** zirconia **d** plausible mechanism for the synthesis of imidazoles derivatives (Khan and Siddiqui 2018) © American Chemical Society, reproduced with permission

nanocatalyst promotes the cyclization reaction via facilitating the elimination reaction (Fig. 26). Finally, the catalyst exhibited a 95% pure yield of tetrazole. The catalyst has been recovered using an external magnet, washed with ethyl acetate, and dried and used for five runs without deterioration (Salimi et al. 2020).

Zhi-tao (2020) used bimetallic Ni@Pd confined in a metal–organic framework cavity for the cycloaddition of amine (propargylic amines) with carbon dioxide in an aqueous solution to produce 2-oxazolidinones (Fig. 27) in a one-pot synthesis. The catalyst was stable even in moisture and thermal conditions, highly selective, and recovered up to ten times to be reused. Excellent yields (95%) of the product

have been obtained and it was found that very little leaching (0.4%) of the catalyst was observed in each run.

Novel  $\gamma$ -Fe<sub>2</sub>O<sub>3</sub> supported on hydroxyapatite (HAP) NPs was synthesized by Kale et al. (2013) for the fabrication of disubstituted 1,2,3-triazoles from terminal alkynes and in situ-generated organic azide in aqueous media without the addition of any reagent or base. The  $\gamma$ -Fe<sub>2</sub>O<sub>3</sub>–HAP NPs showed 100% regioselectivity for the cycloaddition reaction with five times recovering using an external magnet and reusing without trailing its initial activity. Other various aromatic or aliphatic halides and alkynes are synthesized using this NP and offered a good yield (up to 94%) using only water as a solvent making it a green method. Clarina and Rama (2018) reported the [3 + 2] cycloaddition of nitriles

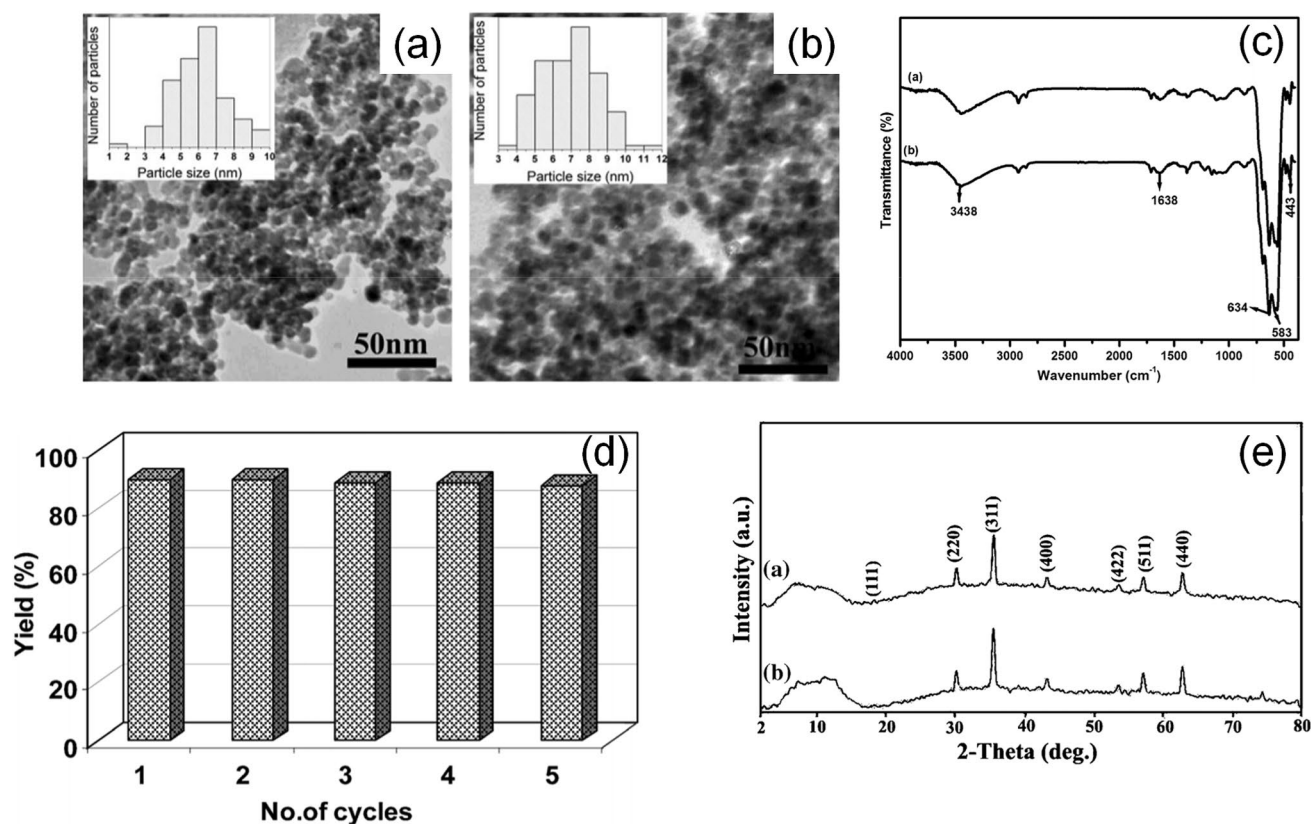


**Fig. 30** TEM images of **a** fresh, **b** used MRIONC **c** FTIR spectra of fresh and used MRIONC **d** recyclability of the catalyst for the synthesis of 2-phenylquinazolines **e** XRD patterns of fresh and used MRI-

ONC (Anand et al. 2012) © Royal Society of Chemistry, reproduced with permission

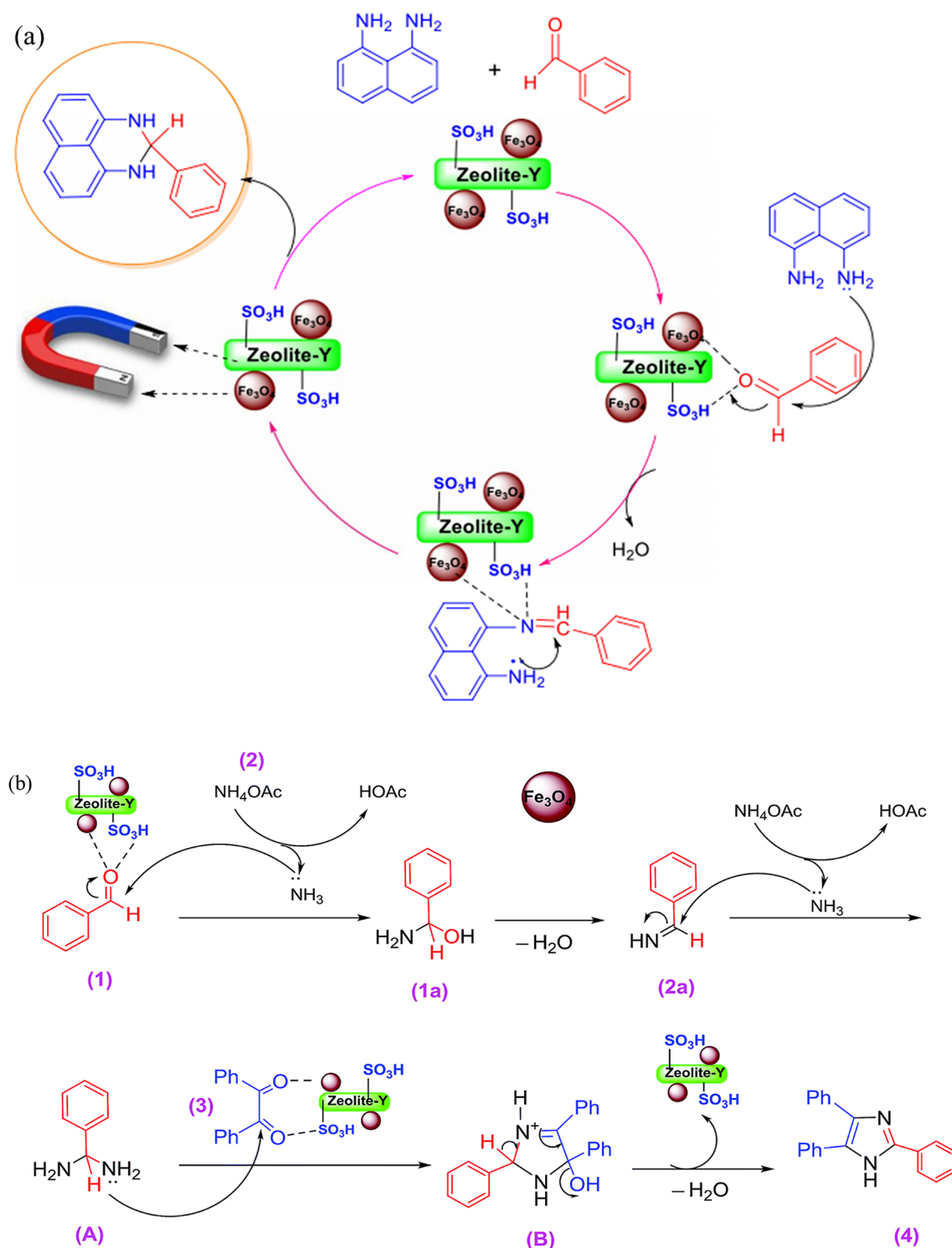
with sodium azide using ZnO NPs anchored on reduced graphene oxide (ZnO–RGO) and green solvent (water). The study was extended to various aromatic, heteroaromatic, aliphatic nitriles, and aromatic nitriles with electron-withdrawing groups at the para position convert in a very short period of time than the electron-donating groups to give the highest yield of > 86% (Table 18). The catalyst was removed by simple filtration from the reaction and washed with distilled water and ethanol to remove organic products, dried at 100 °C for 1 h.

An effective and recyclable Cu@imine/Fe<sub>3</sub>O<sub>4</sub> MNCs catalyst was applied for the synthesis of biologically important polysubstituted pyrroles and 1,2,4,5-tetrasubstituted imidazole derivatives under normal reaction conditions and one-pot MCRs synthesis (Fig. 28). Promising yields up to 95% of the products are formed using 0.36 mol% of the catalyst at 80 °C and early at 35 min when the R1 and R groups are aniline and benzaldehyde, respectively. Similarly, the benzil and RCHO were also replaced by ethyl acetoacetate and nitromethane, respectively, and gives up to 98% in 20-min reaction time using the nanocatalyst. The product was dissolved using hot mixtures of ethyl acetate and ethanol (4:1); then nanocatalyst was recovered using an external magnet,

washed with chloroform, dried, and reused for a minimum of six turns (Thwin et al. 2019).

A recent study by Khan and Siddiqui (2018) reported the synthesis of cerium-immobilized silicotungstic acid nanoparticle-impregnated zirconia (Ce@STANPs/ZrO<sub>2</sub>), for the multicomponent synthesis of imidazole derivatives under MW in water. The reaction has been taken using isatin, benzaldehyde, and ammonium acetate to produce a 94% isolated yield of 2-phenyl-3,4-dihydroimidazo[4,5-b] indole. The catalyst has been recycled by extraction with ethyl acetate and filtration up to seven times and offered 88% conversion. SEM, XRD, and FTIR characterizations of the fresh and seven times reused Ce@STANPs/ZrO<sub>2</sub> confirmed that the surface morphology and spectrum patterns of the recovered catalyst do not show any structural changes (Fig. 29a–c). The reaction mechanism applying the catalyst was also deduced as shown in Fig. 29d.

2-Phenylquinazoline derivatives were synthesized using a magnetically recoverable iron oxide ( $\gamma$ -Fe<sub>2</sub>O<sub>3</sub>) nanocatalyst (MRIONC) under solvent-free conditions. The catalyst was separated and reused five times without losing using an external magnet and the presence of electron-withdrawing substituents on the aniline increases the yield of the product.

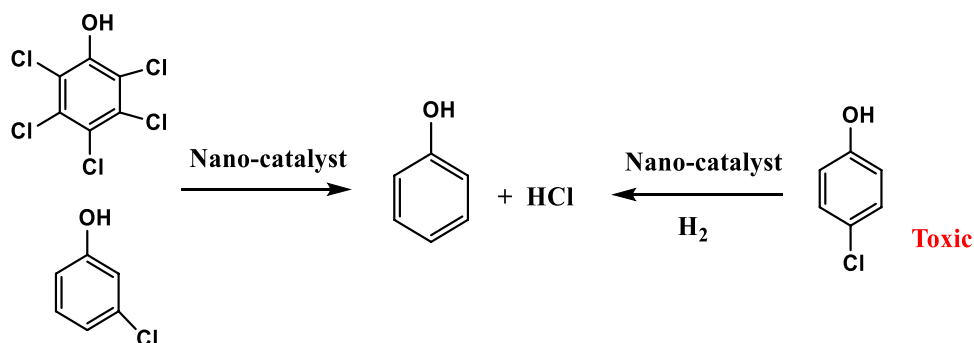
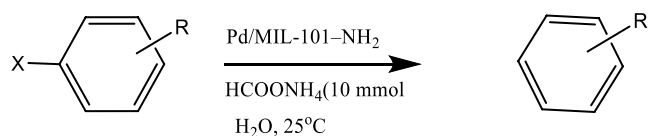


**Fig. 31 a** Proposed mechanism for the synthesis of perimidine derivatives using  $\text{Fe}_3\text{O}_4/\text{zeolite-SO}_3\text{H}$  (Kalhor et al. 2019) © Springer, reproduced with permission **b** The suggested mechanism of trisubsti-

tuted imidazoles synthesis using  $\text{Fe}_3\text{O}_4/\text{SO}_3\text{H@zeolite-Y}$  (Kalhor and Zarnegar 2019) © Royal Society of Chemistry, reproduced with permission

Characterization of the MRIONC using XRD, TEM, and FTIR revealed that no substantial changes of the fresh and reused catalyst have been observed, spherical structure and

spectrum characteristic patterns of the original structures of the maghemite catalyst have retained (Fig. 30a–e) (Anand et al. 2012).

**Fig. 32** Dechlorination of chlorinated compounds**Table 19** Dehalogenation of aryl chlorides in water with HCOONH<sub>4</sub> (Huang et al. 2012) (reaction conditions: aryl chloride (1 mmol), HCOONH<sub>4</sub> (10 mmol), Pd/MIL-101–NH<sub>2</sub> (1 mol% Pd), H<sub>2</sub>O (5 ml), room temperature) © Elsevier, reproduced with permission

Entry	X	R	Time (h)	Yield (%) <sup>a</sup>
1	Cl	4-OH	3	98
2	Cl	H	6	92
3	Br	H	6	97
4	I	H	6	81
5	Cl	2-OH	3	93
6	Cl	3-OH	3	97
7	Cl	4-NH <sub>2</sub>	3	96
8	Cl	4-NO <sub>2</sub>	6	91
9	Cl	4-OMe	6	96
10	Cl	4-COOMe	6	92
11	Cl	4-COOH	6	93
12	1,3,5-Cl	4-OH	8	94
13	1,2,4-Cl	H	8	95

<sup>a</sup>GC yield (*n*-dodecane as internal standard)<sup>b</sup>5 wt% Pd/C (1 mol% Pd)<sup>c</sup>Pd/MIL-53(Al)–NH<sub>2</sub> (1 mol% Pd)<sup>d</sup>Tetrabutylammonium bromide (0.1 mmol) as phase-transfer agent

Kalhor et al. (2019) synthesized pyrimidine derivatives under solvent-free conditions using the multifunctional Fe<sub>3</sub>O<sub>4</sub>@zeolite–SO<sub>3</sub>H MNCs. The MNCs activate the reactant and intermediate during the nucleophilic attack of 1,8-diaminonaphthalene following the imine formation with subsequent elimination of water. Intramolecular nucleophilic attack with the second amine leads to the formation of pyrimidine by cyclization (Fig. 31a). Excellent isolated yields (97%) have been obtained. The nanocatalyst has been separated using a magnet, washed with hot ethanol and dried at room temperature, and reused six times without deterioration. In another study, the above authors used

Fe<sub>3</sub>O<sub>4</sub>/SO<sub>3</sub>H@zeolite-Y to synthesize pyrimidine and trisubstituted imidazoles. They have synthesized the pyrimidine derivatives similar to their previous reaction mechanism to obtain an isolated 98% yield of the product. The trisubstituted imidazole derivatives were synthesized using one-pot MCRs (aldehyde, benzil, and ammonium acetate) considering as a model of reaction. The multifunctional Fe<sub>3</sub>O<sub>4</sub>/SO<sub>3</sub>H@zeolite-Y nanocatalyst activates the cycloaddition due to its Lewis (Fe<sub>3</sub>O<sub>4</sub>) and Brønsted acid (SO<sub>3</sub>H) sites. The polarized aldehyde group (1) results in the formation of hydroxyl-amine intermediate (1a) and further dehydrated to imine (2a), the addition of ammonium acetate produces

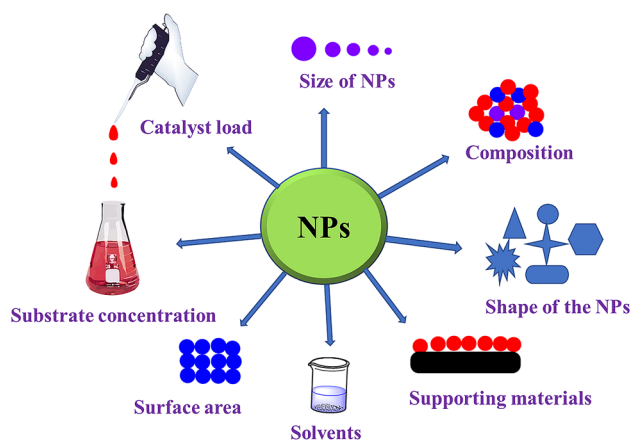


**Fig. 33** Factors affecting the catalytic performance of nanocatalyst in organic reactions

diamine intermediate (A) and the condensation with benzil (3), cyclization, and dehydration with rearrangement via imino intermediate (B) results in the formation of the trisubstituted imidazole (4) (Fig. 31b). The nanocatalyst was recovered using an external magnet, washed with ethyl acetate and dried at 50 °C, and reused for five consecutive runs without noticeable loss of its initial activity (Kalhor and Zarnegar 2019).

Similarly, an early study by Arora et al. (2021) used sulfamic acid-functionalized hollow magnetically separable solid-acid (HMS-SA) nanocatalyst for the synthesis of 2,4,5-trisubstituted imidazoles under ultrasonic irradiation. A one-pot three-component reaction of benzil (1 mmol), benzaldehyde (1 mmol), ammonium acetate (5 mmol), and 30 mg load of the catalyst have been employed to give 99% yield of the product in 25-min reaction time.

## Dehalogenation

Halogenated hydrocarbons, mostly chlorinated aromatic hydrocarbons, chlorinated alkanes, olefins, organochlorine pesticides, and other bromine and chlorine-containing organic compounds are important chemical raw materials and organic solvents, which are widely used in medicine, leather, electronics, pesticide, and herbicide industries. The effluent of these chemical byproducts in the production and use spreading of the products in agricultural activities pose a threat to the environment and human health (Li et al. 2019). The dehalogenation reaction is mostly practiced in the water treatment to remove the toxic halogens such as Cl from the polychlorinated, organochlorine, chlorophenols, and others frequently used in insecticide, sanitizer compounds (Fig. 32) (Li et al. 2018). Most of the chlorophenols (CPs) are persistent and difficult to degrade and bioaccumulate an extended period of time. Therefore, a catalyst that can be tolerated in

organic and inorganic compounds in wastewater or other chemical industries is required (Hildebrand et al. 2009).

Dechlorinations of persistent pesticides such as dichlorodiphenyltrichloroethane (DDT) have been carried out by bimetallic Fe/Pd NPs to offer up to 93% removal efficiency and till it has a minimum concentration below the carcinogenesis limit (Ulucan-altuntas and Debik 2020). Similar studies by Corte et al. (2011) was reported for the dechlorination of diclofenac and trichloroethylene (TCE) via biologically mediated Pd, Au, and Pd/Au NPs. The bio-Pd/Fe shows better activity in the dechlorination reaction to achieve 78% efficiency than the monometallic NPs in the diclofenac dechlorination and the TCE was also transformed to ethane via the bio-Pd/Au. Huang et al. (2012) prepared Pd NPs encapsulated in the mesoporous cages of amine-functionalized metal–organic frameworks (MOFs) MIL-101(Cr)–NH<sub>2</sub> catalyst for the dehalogenation of aryl chlorides in water under mild conditions. The nanocatalyst shows excellent catalytic performance in the dehalogenation reaction using water (Table 19). The catalytic activity of Pd/ MIL-101(Cr)–NH<sub>2</sub> decreases by only 6% in the fifth cycle to provide a 92% yield of the product. Finally, the catalyst was separated readily through centrifugation. Xu and Yang (2008) also studied the catalytic performance of water-soluble Pd NPs against the dehalogenation of aryl chloride, bromide, and iodide. Thus, the experiment was carried out for 3 h to give 98% yields as confirmed by the GC–MS data. The catalyst was used repeatedly several times without purification, but its catalytic performance decreased in the second and third runs.

Bimetallic Ni/Fe NP was applied for the catalytic dechlorination of *para*-nitrochlorobenzene (*p*-NCB). The bimetallic catalyst shows prominent activity in removing the chlorine from the aromatic compound with 100% efficiency for a particle with 2.0% Ni but reduces to 51% upon reducing the amount of Ni to 0.5%. As a result Ni plays a crucial role in reducing the activation energy of the reaction (Xu et al. 2009). The removal of the halogens from the organic compounds can also be carried out by the cross-coupling reaction such as Ullmann, Heck, Suzuki, Stille, Sonogashira, Kumada, Negishi, and Hiyama since the halogens are removed during the C–C coupling reaction (Navarro et al. 2004).

## Factors that affect the catalytic activities of the nanocatalysts in organic reactions

The catalytic performance of the nanocatalyst is affected by multiple factors when interacting in the reaction with the substrates. The NPs are synthesized and designed in different shapes, sizes, stoichiometric compositions (state art), surface area to volume ratio, and incorporate with

varieties of supporting, stabilizing, or capping agents. These factors are arising from the synthesis of the NPs and strongly affect the catalytic activity of the nanocatalyst in the reaction. On the other hand, factors such as the concentration of the substrate, load/concentration of the nanocatalyst, and the solvent are observed during the course of interaction between the nanocatalyst and the substrate (Fig. 33).

### Particle size

As particle sizes become smaller, further changes in the material properties are introduced. The structure of the electronic bands can change as in the gold that is inert in its bulk form, but catalytically active in different sectors when changed at the nano-level (Zhao et al. 2020b). The particle size of the nanocatalyst is very important in organic reaction, the small size of the NP enhances the surface area-to-volume ratio and improves the catalytic activity of the catalyst which allows interaction of more atoms on its surface and minimizes the load of the catalyst (Hussain et al. 2019). Decarolis et al. (2018) synthesized SiO<sub>2</sub> supported Pd NPs to investigate the effect of support materials in the hydrogenation of 1,3-butadiene at 1.5 h on stream. Three samples of different particle sizes were prepared to compare their conversion and selectivity of the reaction. The Pd/SiO<sub>2</sub> NPs (1.1 nm) exhibited 100% total conversion with the selectivity of 53.9% *n*-butane, 31.7% *trans*-2-butene, 2.5% 1-butene and 11.9% *cis*-2-butene, while the Pd/SiO<sub>2</sub> (1.9 nm) showed 19.1% total conversion to 0% *n*-butane, 31.6% *trans*-2-butene, 63.9% 1-butene and 4.4% *cis*-2-butene, and the last sample Pd/SiO<sub>2</sub> (2.7 nm) displayed 89.5% total conversion with 54.4% *n*-butane selectivity, 28.5% *trans*-2-butene, 7.0% 1-butene and 10.1% *cis*-2-butene. Kim et al. (2019) fabricated Pd NPs using SiO<sub>2</sub>, Al<sub>2</sub>O<sub>3</sub>, and silica–alumina supporters in three different particle sizes of each as Pd/SiO<sub>2</sub>-8, Pd/SiO<sub>2</sub>-13, Pd/SiO<sub>2</sub>-21, Pd/Al<sub>2</sub>O<sub>3</sub>-8, Pd/Al<sub>2</sub>O<sub>3</sub>-13, Pd/Al<sub>2</sub>O<sub>3</sub>-21 and Pd/SA-8, Pd/SA-13, Pd/SA-21 for the chemoselective hydrogenation of bio-oil chemicals; acetophenone (Aph), benzaldehyde (BA), and butyrophenone (Bph). The NPs in a small size exhibited higher conversion (100%) using Pd/SA-8 for BA in 3-h reaction time, while the Pd/SA-13 and Pd/SA-21 exhibited 65 and 50% conversions, respectively. In all the other reactions, the NPs which have 8 nm particle size showed a 100% conversion of Aph and Bph after 8 h reaction times, but the NPs with large size (21 nm) exhibited less than 50% conversion under the same condition. The Aph and Bph were less active than BA due to the strong electron density of the carbonyl oxygen. An Au NPs was prepared by Aromal et al. (2012) revealed that the small size Au NP (15) was complete the reduction of 4-nitrophenol to 4-aminophenol within 15 min, while the 20 nm Au NPs complete the reduction reaction in 20-min reaction

time. Similarly, a report by Jawale et al. (2014) confirmed that the small size Au NPs (3 nm) supported on CNT was 5.5 faster than the 20 nm Au NPs in the nitroarene reduction reactions. In some reactions, the trend of increasing catalytic performance along with the decreasing size of NPs is opposed by decreasing the catalytic activity of the NPs when the size of the NPs decreases. This is because when lower coordination number of the NPs readily dissociate chemical bonds such as O–O which allows a strong binding of the dissociate species resulting in poisoning the surface of the catalyst and enforces to slow down to couple with another reacting species in a catalytic cycle (Cao et al. 2016).

### Surface area

The surface area is considered as the main influential factor in determining the rate reaction of the heterogeneous catalyst (Gregor et al. 2010). The particle size of the nanocatalyst is inversely proportional to the surface area. Nanocatalyst with highly available surface area provides a broad range of catalytic activity, creating several pathways in the reaction which renders the selectivity, but having the advantage of excellent catalytic activity and recovery for several further reusability. However, the nanocatalysts that have limited active sites produce very selective, but low conversion and recovery (Zhu and Xu 2016). On this occasion, inert stabilizing or supporting materials are deposited to block some of the surface areas of the nanocatalyst when the selectivity of the reaction is required (selective poisoning of the catalyst surface) (Rioux et al. 2005; Kim and Lee 2018). The high surface area of the nanocatalyst increases the interaction with the reactant/substrate which provides an enhanced interaction system to achieve a good reaction rate that solves the problem of a homogeneous counterpart. A large surface area enhances the relative contribution of the surface energy so that thermodynamic stability decreases when the particle size decreases too (Thakore and Rathore 2015).

### Stabilizing and supporting materials

Synthesizing the nanocatalyst having both the heterogeneous and homogeneous catalysts property is challenging. Sometimes, the use of homogeneous catalysts in chemical synthesis is better because they are soluble in the reaction medium and increase the accessibility of the catalytic site to the incoming substrates. However, separating them from the reaction mixture is difficult and tedious. To alleviate such problems synthesizing the NPs by incorporating with different supporters such as silica, iron, organic ligands, polymers, and biological compounds are among the hot research issues of this era (Kazemi 2020b). Stabilizers are added to the nanocatalyst during the synthesis to prevent agglomeration and leaching. Polymer-stabilized metal NPs such as PVP-Pd

NPs of desired size and shape were designed for different organic reactions to improve catalytic stability, recovery, and reuse. Primarily, the support materials are added to improve the stability of the small size metal particle through anchoring. In addition to the stabilizing and supporting materials, capping agents are also used to modify the surface chemistry of the nanocatalyst for specific applications, especially for drug delivery to control their size and shape during chemical synthesis (Stankus et al. 2011; Pérez-Lorenzo 2012; Sankar et al. 2019). Traditionally, most of the heterogeneous catalysts have low catalytic activity because of their limited accessibility of the substrates at the active site of the catalyst. However, dispersing the catalyst active site over supporting materials such as carbon, which have high thermal stability, workable under acidic or basic conditions, tunable hydrophobicity and polarity, easily available and cheap compared with others, and easily recoverable from the reaction mixtures, is extensively used these days (Bahuguna et al. 2019). The strong interaction of the stabilizers with the NPs exhibited uniform and narrow particle size distribution; however, an excess amount of stabilizers can hinder the accessibility of the reactants to the NP active site (surface). Stabilizers that are poorly bound to the NPs on the other hand can easily remove or replace during the reaction conditions resulting in sintering and losing the stability of the NPs (Rossi et al. 2018). CNTs are well-known supporter catalysts in metal NPs such as Ru, Pt, Rh, Ni, Fe, and Pd to improve the catalytic activity and selectivity of the NPs in a variety of chemical reactions to attributed metal–support interaction and mass transfer (Hashemi et al. 2016). Maghemite-supported palladium NPs was prepared by Hajdu et al. (2020) for catalytic hydrogenation of nitrobenzene derivatives. The Pd NPs exhibited 99% conversion of aniline in all cases without forming byproducts and the nanocatalyst was recovered using a magnet for subsequent use without any post-treatment. Supporters strongly affect the size, composition, shape, and method of synthesizing the nanocatalyst. The additive supporters must physically and chemically stable during the chemical reaction, easily removed from the reaction media, and reusability without significant loss of catalytic activity (Monopoli et al. 2010). Fusini et al. (2020) synthesized Pd NPs supported on poly(4-vinylpyridine) 2% cross-linked with divinylbenzene (Pd/PVPy) for the Suzuki–Miyaura coupling reaction on both the activated and deactivated aromatic and bromide with boronic acids. Supported NPs showed remarkable conversion, selectivity, yield and reuse with very low Pd leaching. Decarolis et al. (2018) synthesized Pd NPs supported on SiO<sub>2</sub>, Si<sub>3</sub>N<sub>4</sub>, and Al<sub>2</sub>O<sub>3</sub> to study the effect of the supporting materials in the hydrogenation of 1,3-butadiene at 1.5-h time on stream. The sample Pd/Al<sub>2</sub>O<sub>3</sub>-30–8.5 exhibited 100% conversion to *n*-butane (100%) selectivity; however, the sample Pd/Si<sub>3</sub>N<sub>4</sub>-30–8.5 shows 100% conversion to 48.2% *n*-butane, 35.7%

*trans*-2-butene, 2.4% 1-butene and 13.6% *cis*-2-butene products. Finally, the Pd/SiO<sub>2</sub>-30–8.5 sample results in a low total conversion (20.1%) to 0% *n*-butane, 31.2% *trans*-2-butene, 64.3% 1-butene, and 4.3% *cis*-2-butene.

### Concentration (load of the NPs)

Regarding the loading of nanocatalyst into the reaction, the nobility, high cost, and scarcity of the metals in the earth reserve should be considered. The catalytic reaction carried out by a lower load (dose) of the nanocatalyst is a strong desire for a supported catalyst. The increase in atomic efficiency via higher dispersion of metal species gives a promising strategy (Sun et al. 2019). Initially, the rate of reaction may be increased linearly until all the active sites of the catalyst are occupied or deactivated (Sherborne et al. 2017). Cu NP was applied for the reduction of nitrobenzene derivatives to aniline derivatives using the combined MW and ultrasound irradiation techniques to promote the nano-Cu-catalyzed reduction of nitroarene compounds to its simultaneous enhancement of heat and mass transfer. An excellent yield of 89–99% of aniline derivatives was achieved chemoselectively with a lower dosage of the catalyst (20 mol%) at a short reaction time (3.5–4 min) (Feng et al. 2014). A report by Moghaddam et al. (2015) depicts the increase of the load of the catalyst increases efficiency in the synthesis of pyrroles using nickel ferrite NPs (NiFe<sub>2</sub>O<sub>4</sub>) catalyst to a certain degree and further increasing the load of the catalyst slow down the yield of the product. Using 1, 5, 10, and 20 mol% of the NiFe<sub>2</sub>O<sub>4</sub> at 100 °C results in 66, 95, 95 and 88% yields at 8-, 3-, 3-, and 3.5-h reaction time, respectively. This implies 5 mol% is the optimum amount of the catalyst concentration to achieve 95% yield in 3 h; however, increasing the catalyst amount to 20 mol% decreases the yield to 88% and the reaction time to 3.5 h since the active sites of the catalyst are already occupied. Mung bean starch-supported Au NPs (MBS-AuNPs) were synthesized by Chairam et al. (2017) for the reduction of 4-NP in the presence of NaBH<sub>4</sub>. The effect of the NPs concentration on the reduction rate of 4-NP reduction was investigated. Different amount of MBS-Au NPs catalyst corresponding to 20, 40, 60, 80, and 100 mg was applied and results in the variation of the reaction rate constant ( $k_{\text{obs}}$ ) to 0.0081, 0.0127, 0.0218, 0.0251 and 0.0326 min<sup>-1</sup>. Their result showed that increasing the dose of the NPs leads to an increase in the catalytic activity of the MBS-AuNPs nanocomposite. Jamatia et al. (2014) studied the synthesis of benzodiazepines and chemoselective 1,2-disubstituted benzimidazoles using magnetically recover Fe<sub>3</sub>O<sub>4</sub> nanocatalyst under solvent-free conditions. The condensation reaction of phenylenediamine (1, 1 mmol) and acetophenone (2, 2.2 mmol) without the catalyst showed less conversion (22%) but adding the nanocatalyst (2–10 mol%) increase the conversion of the benzodiazepines

and chemoselective 1,2-disubstituted benzimidazoles to a maximum yield of 95 and 92%, respectively, using 6 mol% of the  $\text{Fe}_3\text{O}_4$  nanocatalyst. Further increasing the amount of the catalyst to 8 and 10 does not improve the yield and conversion of the products and 6 mol% is an optimum catalyst concentration of the reaction.

### Substrates concentration

4-NP, the side products of pharmaceuticals, dyes, and pesticide industries has been reduced to 4-AP using water-soluble Pd NPs. Using a high concentration of 4-NP, the rate of the reaction was decrease since the surface area of the Pd NPs initially occupied by the 4-NP and fewer hydrogen species. However, decreasing the initial concentration of 4-NP and occupying the majority of the active site by hydrogen species allows increases the velocity of the reaction (Ayad et al. 2020). Wu and Chen (2012) used a bioinspired method to fabricate Au NPs using gum Arabic as a reducing agent and a stabilizing agent and conjugated on iron oxide NPs to enhance the recoverability of the nanocatalyst using an external magnet. The as-biosynthesized NPs was used for the reduction of 4-NP to 4-AP with  $\text{NaBH}_4$ . The reduction reaction followed pseudo-first-order kinetics and the rate constants have been increased upon increasing the dose of the Au nanocatalyst but the rate of the reaction was decreased when the initial 4-NP concentration is raised, suggesting that the reaction is diffusion controlled; hence, the rate constant is proportional to the diffusion co-efficient but inversely proportional to the concentration of the substrate (4-NP).

### Substrate structures

Substrate structures can impact the catalytic performance of the nanocatalyst in terms of conversion, yield, and selectivity. Substituent groups like electron-withdrawing and -donating species strongly influence in addition to the structures of being branched, linear, cyclic, saturated, unsaturated, etc. for example, the use of Ni, Pd, Pt, and Rh NPs in the hydrogenation of terminal olefins is much faster than the internal olefins due to the steric and accessibility effects (Delgado et al. 2017). Similarly, the reduction of 4-nitrophenol to 4-aminophenol which has short alkyl chains displayed better accessibility and activity than the other long chain-based alkyl groups using the  $\text{Au}_{25}(\text{SCH}_2\text{CH}_2\text{Ph})_{18}$  nanocluster (Zhao et al. 2019a). Silver NPs effectively catalyze the hydration of nitriles to their corresponding amides in water. The structure of the aromatic nitriles influences the rate and conversion of hydration. Aromatic nitriles, which have substituents at the ortho positions were less reactive than the meta and para positions due to the steric reason; on the other hand, electron-withdrawing substituents on the nitriles

decline the reaction than the electron-donating groups (Kim et al. 2011a).

### Composition effect

Most catalysts are deactivated because of surface changes, metal leaching, and poisoning. A lot of odd state art composites and structures are designed to improve the catalytic activity and to solve the problem of deactivating during the course of interaction by adding supporting materials, alloying, core-shell forming, etc. Multi-metallic NPs such as bimetallic, trimetallic, or even tetra-metallic NPs are fabricated as a catalyst for organic and electrochemistry to alleviate the problems such as poisoning by CO (Rucinska et al. 2020). For example, bimetallic nanomaterials have a different catalytic performance from their metal components due to the synergistic catalytic property of the bimetallic nanomaterials (Verma et al. 2019). A highly selective  $\text{Pd}_x\text{Au}_{1-x}$  ( $x = 0.02, 0.04, \text{ and } 0.09$ ) raspberry colloid-templated  $\text{SiO}_2$  ( $\text{Pd}_{0.04}\text{Au}_{0.96}$  RCT- $\text{SiO}_2$ ) was synthesized by Luneau et al. (2019) for the hydrogenation of 1-hexyne to 1-hexene. Thus, the bimetallic PdAu was highly selective, but almost similar in conversion with pure Pd. 97% of 1-hexene isomer was formed applying the bimetallic NPs catalyst whereas, hexane-dominated product was formed using the monometallic Pd NPs. On the other hand, the magnetic property or coercivity of multi-metallic/multicomponent MNCs is altered by the atomic ratio of the individual components. For example, the coercivity of  $\text{Fe}_x\text{Pt}_{1-x}$  and  $\text{Co}_x\text{Fe}_{3-x}\text{O}_4$  depends on the values of 'x'; for the former one, it ranges from 0.3 to 0.8 with maximum coercivity at  $x=0.55$ , and for the latter one, the coercivity raises with  $x$  ranges from 0 to 0.7 and decreases when  $x$  is beyond 0.7 (Wu et al. 2016). Rong et al. (2013) synthesizes bimetallic AgPd nanocatalysts for the hydrodechlorination of 4-chlorophenol purpose. The bimetallic NC was prepared in different forms as  $\text{AgPd}_x$  ( $x = 2, 4, 6, 9, 19$ ); thus, the atomic ratio of Ag/Pd shows a profound effect in the reaction with the  $\text{AgPd}_9$  nanocatalysts showed a maximum activity of TOF  $322 \text{ h}^{-1}$  than the other state arts of the nanocrystals.

### Solvents

Solvents play a vital role in the execution of procedures in chemical industries, most organic solvents (alcohols, ethers, hydrocarbon and more) are extensively used in large amounts to achieve high selectivity toward products. Solvents can influence the catalysis process by interacting directly interact with the nanocatalyst, the substrate, and the products and even in the synthesis of the NPs. As a result, interactions may slow down or increase the reaction rate, selectivity, and yield of the products. The selection of the solvents according to their properties is also crucial since some of them are non-polar, polar, hydrogen bond donors (acid), hydrogen bond-accepting (base)



solvent, etc. (Dyson and Jessop 2016). Their impact on safety, health, cost, and environmental pollutions are also the burning issue of the 21 centuries. Environmentally friendly and green solvents such as water, ILs, PEG, supercritical fluids, etc. are considered as green solvents in organic synthesis and chemical industries. However, the aforementioned liquids have also a limitation due to the low solubility of the organic compounds, especially in aqueous solutions make it hard for full utility and other techniques that increase the solubility of the compounds such as MW, and ultrasonic irradiation for rapid syntheses should be incorporated (Safari and Gandomi-Ravandi 2014; Qamar et al. 2015; Dubey and Kumar 2020). Water is considered as a green solvent in the chemical transformations because of its readily available, safe, non-flammable, non-carcinogenic, and environmentally friendly. It is not only a solvent unless it is electrophile–nucleophile via the hydrogen and oxygen atoms and its ability to make hydrogen bonding are unique properties of water yet not present in other organic solvents that can enhance the rate of the reaction (Santra et al. 2013). The reaction which are poorly soluble in water or other solvents proceed lower yields and conversion by giving more byproducts. Therefore, reactions involving water-insoluble substrates/reagents may require more time and highest temperature for complete conversion (Beletskaya and Tyurin 2010). Krishnakumar et al. (2012) reported the effect of solvents (toluene and benzene) for the synthesis of bis-isoquinolinone derivatives from isocoumarins and 1,7-heptadiazine using ZnO NPs (10 mol%). It was found that 70, 75, 89, 84, 80% and 72, 76, 90, 85, 83% yield of the products were obtained corresponding to toluene and benzene solvents, respectively, making H, CH<sub>3</sub>, F, Cl, Br at the 3-substituted isocoumarins. A Suzuki–Miyaura (SM) cross-coupling reaction between (4-(methoxycarbonyl)phenyl)boronic acid and 2-bromothiophene was carried out using Pd-derived catalyst under 10% of acetone, 10% of THF, 10% toluene and without any co-solvents. 53, 81, 78, and 46% yield of the 2-methyl-4-(thiophen-2-yl)benzoate was produced corresponding to acetone, THF, toluene, and without co-solvent, respectively (Gabriel et al. 2016). Glutathione-protected Pd, PdAu, and PdPt NPs were applied for the conversion of allyl alcohol into 1-propanol (hydrogenation) and propanal (isomerization) in a biphasic organic/aqueous solvent mixture. All the NPs exhibited > 80% selectivity for the isomer propanal product under different organic solvents. The (75:25) Pd:Au-Glu under the dichloromethane showed 12% hydrogenation and 88% isomerization in inert gas, 8 and 92%, 16 and 84% hydrogenation and isomerization were observed using chloromethane and ethyl acetate solvents, respectively. No significant change was observed applying oxygen gas in the reaction. The ethyl acetate solvent was better in terms of TOF (507 mole of product/mole metal/hour at 20 mL/min H<sub>2</sub> flow) and recyclability than the dichloromethane (388) and chloromethane (327) (Bhama et al. 2020).

## Conclusion and future prospects

The use of nanocatalysts in organic, pharmaceutical, and biological applications is a recent focus of the research community. The nanocatalysts are synthesized in very small particle size, larger surface area, and different morphological features which make them highly active in organic synthesis and reactions such as C–C coupling, oxidation, reduction, condensation, and more. Moreover, the nanocatalysts are stable and can be recovered for further use without losing their original catalytic activity. Nanocatalysts such as Au, Pd, Cu, Ru, iron-based NPs, and mixed NPs with organic and inorganic stabilizers showed promising performance in the organic reactions. The nanocatalysts displayed remarkable performance and high yields, conversion, and selectivity than the conventional catalysts. The use of toxic reagents, solvents, harsh, and rigorous conditions are minimized by the use of NPs as a catalyst. More focus should be given to NPs that are templated in organic or supported with iron as they show better stability and magnetic recovery of the nanocatalyst. The MNCs are cheaper, robust, and prepared from the base metal Fe can be used several times without significantly losing of its catalytic activity.

To date, extensive studies have been conducted on the fabrication of the nanocatalyst through various strategic approaches for various applications and promising results are being achieved. On the other hand, there are also challenges that must be considered in the future developments and design of the nanocatalyst. Synthesized nanocatalysts that are environmentally friendly, economically visible and easy to use should be applied. Multi-metallic nanostructures like bi and TNPs should also be checked in organic synthesis due to their electronic transition and synergistic effect.

MNCs offered an excellent catalytic property and simply recycled from the reaction mixture using an external magnet several times without any remarkable changes in the initial catalytic operations. In addition, MNCs may operate in both in aqueous and non-aqueous solutions and even at ambient temperature. The MNCs are now used as a novel heterogeneous catalysts/nanocomposite to synthesize different heterocyclic scaffoldings. Despite the fabricating the nanocatalyst via various synthetic approaches of reduced particle size, their scale-up fabrication is still controversial.

On the other hand, loss of catalytic activity of the nanocatalyst has been observed due to sintering, leaching of soluble catalysts under harsh conditions. Some of the nanocatalysts like Au have high surface free energy and small size which lead them to the aggregation into larger particles or the loss of their supporters under harsh conditions. Therefore, the future development of the nanocatalyst should lie in synthesizing the nanocatalyst that resists sintering and leaching at multiple runs. The proper selection of modification,

functionalization and support should be investigated in the future to control the well-defined morphologies of the nanocatalyst during the scale-up operations. Synthesizing of small size and uniform nanocatalyst is challenging, the nanocatalyst tend to aggregate due to their high surface energies and van der Waals attraction that may reduce their catalytic performance and limited recyclability. Therefore, size and morphology-controlled synthesis of the nanocatalyst which have long-term stability, easily recycled, and with the additional goal of avoiding the employment of toxic capping agents and solvents in the reactions is required (Liu et al. 2020). The factors that affecting the catalytic performance of the nanocatalyst should be examined more.

#### Declaration

**Conflict of interest** The corresponding author states that there is no conflict of interest.

**Ethical approval** This article does not contain any studies with human participants or animals performed by the author.

**Informed consent** For this type of study formal consent is not required.

## References

- Abaezadeh S, Elhamifar D, Norouzi M, Shaker M (2019) Magnetic nanoporous MCM-41 supported ionic liquid/palladium complex: an efficient nanocatalyst with high recoverability. *Appl Organometal Chem* 33:e4862. <https://doi.org/10.1002/aoc.4862>
- Abu-dief AM, Abdel-fatah SM (2017) Development and functionalization of magnetic nanoparticles as powerful and green catalysts for organic synthesis. *Beni Suef Univ J Basic Appl Sci* 7:55–67. <https://doi.org/10.1016/j.bjbas.2017.05.008>
- Abu-reziq R, Wang D, Post M, Alper H (2007) Platinum nanoparticles supported on ionic liquid-modified magnetic nanoparticles: selective hydrogenation catalysts. *Adv Synth Catal* 347:2145–2150. <https://doi.org/10.1002/adsc.200700129>
- Ahadi A, Rostamnia S, Panahi P et al (2019) Palladium comprising dicationic bipyridinium supported periodic mesoporous organosilica (PMO): Pd@Bipy-PMO as an efficient hybrid catalyst for Suzuki–Miyaura cross-coupling reaction in water. *Catalysts* 9:140. <https://doi.org/10.3390/catal9020140>
- Ahmadi A, Sedaghat T, Azadi R, Motamedi H (2020) Magnetic mesoporous silica nanocomposite functionalized with palladium Schiff base complex: synthesis, characterization, catalytic efficacy in the Suzuki–Miyaura reaction and  $\alpha$ -amylase immobilization. *Catal Lett* 150:112–126. <https://doi.org/10.1007/s10562-019-02913-5>
- Ahooie ST, Azizi N, Yavari I, Hashemi MM (2018) Magnetically separable and recyclable g-C<sub>3</sub>N<sub>4</sub> nanocomposite catalyzed one-pot synthesis of substituted imidazoles. *J Iran Chem Soc* 15:855–862. <https://doi.org/10.1007/s13738-017-1284-9>
- Akubo K, Nahil MA, Williams PT (2019) Aromatic fuel oils produced from the pyrolysis-catalysis of polyethylene plastic with metal-impregnated zeolite catalysts. *J Energy Inst* 92:195–202. <https://doi.org/10.1016/j.joei.2017.10.009>
- Alamgholiloo H, Zhang S, Ahadi A et al (2019) Synthesis of bimetallic 4-PySI-Pd@Cu(BDC) via open metal site Cu-MOF: effect of metal and support of Pd@Cu-MOFs in H<sub>2</sub> generation from formic acid. *Mol Catal* 467:30–37. <https://doi.org/10.1016/j.mcat.2019.01.031>
- Alamgholiloo H, Rostamnia S, Hassankhani A et al (2020) Formation and stabilization of colloidal ultra-small palladium nanoparticles on diamine-modified Cr-MIL-101: synergic boost to hydrogen production from formic acid. *J Colloid Interface Sci* 567:126–135. <https://doi.org/10.1016/j.jcis.2020.01.087>
- Albero J, García H (2019) Catalysis by supported gold nanoparticles. In: Andrews DL, Lipson RH, Nann T (eds) *Comprehensive nanoscience and nanotechnology*. Elsevier, pp 91–108
- Ali R, Nour K, Al-warthan A, Siddiqui MRH (2015) Selective oxidation of benzylic alcohols using copper-manganese mixed oxide nanoparticles as catalyst. *Arab J Chem* 8:512–517. <https://doi.org/10.1016/j.arabjc.2013.05.012>
- Amali AJ, Rana RK (2009) Stabilisation of Pd(0) on surface functionalised Fe<sub>3</sub>O<sub>4</sub> nanoparticles: magnetically recoverable and stable recyclable catalyst for hydrogenation and Suzuki–Miyaura reactions. *Green Chem* 11:1781–1786. <https://doi.org/10.1039/b916261p>
- Amirmahani N, Mahmoodi NO, Bahramnejad M, Seyedi N (2020) Recent developments of metallic nanoparticles and their catalytic activity in organic reactions. *J Chin Chem Soc* 67:1326–1337. <https://doi.org/10.1002/jccs.201900534>
- Anand N, Prasad H, Satyanarayana T et al (2012) A magnetically recoverable  $\gamma$ -Fe<sub>2</sub>O<sub>3</sub> nanocatalyst for the synthesis of 2-phenylquinazolines under solvent-free conditions. *Catal Sci Technol* 2:570–574. <https://doi.org/10.1039/c1cy00341k>
- Ansari S, Khorshidi A, Shariati S (2020) Chemoselective reduction of nitro and nitrile compounds using an Fe<sub>3</sub>O<sub>4</sub>-MWCNTs@PEI-Ag nanocomposite as a reusable catalyst. *RSC Adv* 10:3554–3565. <https://doi.org/10.1039/c9ra09561f>
- Aromal SA, Babu KVD, Philip D (2012) Characterization and catalytic activity of gold nanoparticles synthesized using ayurvedic arishtams. *Spectrochim Acta Part A Mol Biomol Spectrosc* 96:1025–1030. <https://doi.org/10.1016/j.saa.2012.08.010>
- Arora G, Gupta R, Yadav P et al (2021) Ultrasonically-mediated one-pot synthesis of substituted imidazoles via sulfamic acid functionalized hollow magnetically retrievable solid-acid catalyst. *Curr Res Green Sustain Chem* 4:100050. <https://doi.org/10.1016/j.crgsc.2020.100050>
- Astruc D (2020) Introduction: nanoparticles in catalysis. *Chem Rev* 120:461–463. <https://doi.org/10.1021/acs.chemrev.8b00696>
- Ayad AI, Marín CB, Colaco E et al (2019) “Water soluble” palladium nanoparticle engineering for C–C coupling, reduction and cyclization catalysis. *Green Chem* 21:6646–6657. <https://doi.org/10.1039/c9gc02546d>
- Ayad AI, Luat D, Dris AO, Guénin E (2020) Kinetic analysis of 4-nitrophenol reduction by “Water-Soluble” palladium nanoparticles. *Nanomaterials* 10:1169. <https://doi.org/10.3390/nano10061169>
- Baghbanian SM, Farhang M (2014) CuFe<sub>2</sub>O<sub>4</sub> nanoparticles: a magnetically recoverable and reusable catalyst for the synthesis of quinoline and quinazoline derivatives in aqueous media. *RSC Adv* 4:11624–11633. <https://doi.org/10.1039/c3ra46119j>
- Bahuguna A, Kumar A, Krishnan V (2019) Carbon-Support-based heterogeneous nanocatalysts: synthesis and applications in organic reactions. *Asian J Org Chem* 8:1–44. <https://doi.org/10.1002/ajoc.201900259>
- Balcar H, Cejka J (2019) SBA-15 as a support for effective olefin metathesis catalysts. *Catalysts* 9:743. <https://doi.org/10.3390/catal9090743>
- Ballarin B, Barreca D, Boanini E et al (2017) Supported gold nanoparticles for alcohols oxidation in continuous-flow

- heterogeneous systems. *ACS Sustain Chem Eng* 5:4746–4756. <https://doi.org/10.1021/acssuschemeng.7b00133>
- Balou J, Khalilzadeh MA, Zareyee D (2019) An efficient and reusable nano catalyst for the synthesis of benzoxanthene and chromene derivatives. *Sci Rep* 9:3605. <https://doi.org/10.1038/s41598-019-40431-x>
- Baruwati B, Polshettiwar V, Varma RS (2009) Magnetically recoverable supported ruthenium catalyst for hydrogenation of alkynes and transfer hydrogenation of carbonyl compounds. *Tetrahedron Lett* 50:1215–1218. <https://doi.org/10.1016/j.tetlet.2009.01.014>
- Basavegowda N, Mishra K, Lee YR (2017) Synthesis, characterization, and catalytic applications of hematite ( $\alpha$ -Fe<sub>2</sub>O<sub>3</sub>) nanoparticles as reusable nanocatalyst. *Adv Nat Sci Nanosci Nanotechnol* 8:025017. <https://doi.org/10.1088/2043-6254/aa6885>
- Beletskaya I, Tyurin V (2010) Recyclable nanostructured catalytic systems in modern environmentally friendly organic synthesis. *Molecules* 15:4792–4814. <https://doi.org/10.3390/molecules15074792>
- Bhaduri K, Das BD, Kumar R et al (2019) Recyclable Au/SiO<sub>2</sub>-shell/Fe<sub>3</sub>O<sub>4</sub>-core catalyst for the reduction of nitro aromatic compounds in aqueous solution. *ACS Omega* 4:4071–4081. <https://doi.org/10.1021/acsomega.8b03655>
- Bhama S, Sibakoti TR, Jasinski JB, Zamborini FP (2020) Highly active, selective, and recyclable water-soluble glutathione-stabilized Pd and Pd-Alloy nanoparticle catalysts in biphasic solvent. *ChemCatChem* 12:2253–2261. <https://doi.org/10.1002/cctc.201901968>
- Bhaskaruni SVHS, Maddila S, Gangu KK, Jonnalagadda SB (2020) A review on multi-component green synthesis of N-containing heterocycles using mixed oxides as heterogeneous catalysts. *Arab J Chem* 13:1142–1178. <https://doi.org/10.1016/j.arabjc.2017.09.016>
- Bhat PB, Inam F, Bhat BR (2014) Nickel hydroxide/cobalt-ferrite magnetic nanocatalyst for alcohol oxidation. *ACS Comb Sci* 16:397–402
- Bogireddy NKR, Pal U, Gomez LM, Agarwal V (2018) Size controlled green synthesis of gold nanoparticles using *Coffea arabica* seed extract and their catalytic performance in 4-nitrophenol reduction. *RSC Adv* 8:24819–24826. <https://doi.org/10.1039/c8ra04332a>
- Cao S, Tao F, Tang Y et al (2016) Size- and shape-dependent catalytic performances of oxidation and reduction reactions on nanocatalysts. *Chem Soc Rev* 45:4747–4765. <https://doi.org/10.1039/c6cs00094k>
- Chairam S, Konkamdee W, Parakhun R (2017) Starch-supported gold nanoparticles and their use in 4-nitrophenol reduction. *J Saudi Chem Soc* 21:656–663. <https://doi.org/10.1016/j.jscs.2015.11.001>
- Chen L, Gao Z, Li Y (2015) Immobilization of Pd(II) on MOFs as a highly active heterogeneous catalyst for Suzuki–Miyaura and Ullmann-type coupling reactions. *Catal Today* 245:122–128. <https://doi.org/10.1016/j.cattod.2014.03.074>
- Chen B, He Y, Sung S et al (2020) Synthesis and characterization of magnetic nanoparticles coated with polystyrene sulfonic acid for biomedical applications. *Sci Technol Adv Mater* 21:471–481. <https://doi.org/10.1080/14686996.2020.1790032>
- Chng LL, Erathodiyil N, Ying JY (2013) Nanostructured catalysts for organic transformations. *Acc Chem Res* 46:1825–1837. <https://doi.org/10.1021/ar300197s>
- Clarina T, Rama V (2018) [3+2] Cycloaddition promoted by zinc oxide nanoparticles anchored on reduced graphene oxide using green solvent. *Synth Commun* 48:175–187. <https://doi.org/10.1080/00397911.2017.1393086>
- Crucianelli M, Bizzarri BM, Saladino R (2019) SBA-15 anchored metal containing catalysts in the oxidative desulfurization process. *Catalysts* 9:984. <https://doi.org/10.3390/catal9120984>
- Das D (2016) Multicomponent reactions in organic synthesis using copper-based nanocatalysts. *Chem Select* 1:1959–1980. <https://doi.org/10.1002/slct.201600414>
- Dasari GK, Sunkara S, Gadupudi RCP (2020) One-step synthesis of magnetically recyclable palladium loaded magnesium ferrite nanoparticles: application in synthesis of anticancer drug PCI-32765. *Inorg Nano Met Chem* 50:753–763. <https://doi.org/10.1080/24701556.2020.1724147>
- De Corte S, Hennebel T, Fitts P et al (2011) Biosupported bimetallic Pd-Au nanocatalysts for dechlorination of environmental contaminants. *Environ Sci Technol* 45:8506–8513. <https://doi.org/10.1021/es2019324>
- de Wild PJ (2015) Biomass pyrolysis for hybrid biorefineries. In: Larroche A, Rainer P, Mohammad H et al (eds) *Industrial biorefineries and white biotechnology*, 1st edn. Elsevier B.V., pp 341–368
- Decarolis D, Gonzalez IL, Gianolio D, Beale AM (2018) Effect of particle size and support type on Pd catalysts for 1,3-butadiene hydrogenation. *Top Catal* 61:162–174. <https://doi.org/10.1007/s11244-018-0887-4>
- Delgado JA, Benkirane O, Claver C et al (2017) Advances in the preparation of highly selective nanocatalysts for the semi-hydrogenation of alkynes using colloidal approaches. *Dalton Trans* 46:12381–12403. <https://doi.org/10.1039/c7dt01607g>
- Díaz-hernández A, Gracida J, García-almendárez BE et al (2018) Characterization of magnetic nanoparticles coated with chitosan: a potential approach for enzyme immobilization. *J Nanomater* 2018:1–11
- Dong Y, Xue F, Wei Y (2021) Magnetic nanoparticles supported N-heterocyclic palladium complex: synthesis and catalytic evaluations in Suzuki cross-coupling reaction. *J Phys Chem Solids* 153:110007. <https://doi.org/10.1016/j.jpcs.2021.110007>
- Downs EL, Tyler RD (2014) Nanoparticle catalysts for nitrile hydration. *Coord Chem Rev* 280:28–37. <https://doi.org/10.1016/j.ccr.2014.07.029>
- Duan Z, Ma G, Zhang W (2012) Preparation of copper nanoparticles and catalytic properties for the reduction of aromatic nitro compounds. *Bull Korean Chem Soc* 33:10–13. <https://doi.org/10.5012/bkcs.2012.33.12.4003>
- Dubey AV, Kumar AV (2020) A bio-inspired magnetically recoverable palladium nanocatalyst for the Ullmann coupling reaction of aryl halides and arylboronic acids in aqueous media. *Appl Organometal Chem* 34:e5570. <https://doi.org/10.1002/aoc.5570>
- Dyson PJ, Jessop PG (2016) Solvent effects in catalysis: rational improvements of catalysts via manipulation of solvent interactions. *Catal Sci Technol* 6:3302–3316. <https://doi.org/10.1039/c5cy02197a>
- Eghbali B, Nişancı B, Metin Ö (2018) Graphene hydrogel supported palladium nanoparticles as an efficient and reusable heterogeneous catalysts in the transfer hydrogenation of nitroarenes using ammonia borane as a hydrogen source. *Pure Appl Chem* 90:327–335. <https://doi.org/10.1515/pac-2017-0714>
- Emadi F, Nemati F, Elhampour A (2020) Silver nanoparticles supported on mesoporous triazine carbon material: a versatile catalyst for reduction of nitroaromatic compounds. *Chem Select* 5:4328–4336. <https://doi.org/10.1002/slct.202000645>
- Escoda-torroella M, Moya C, Rodríguez AF et al (2021) Selective control over the morphology and the oxidation state of iron oxide nanoparticles. *Langmuir* 37:35–45. <https://doi.org/10.1021/acs.langmuir.0c02221>
- Eskandari P, Kazemi F, Zand Z (2014) Photocatalytic reduction of aromatic nitro compounds using CdS nanostructure under blue LED irradiation. *J Photochem Photobiol A Chem* 274:7–12. <https://doi.org/10.1016/j.jphotochem.2013.09.011>

- Ezzatzadeh E, Hossaini Z, Rostamian R et al (2017) Fe<sub>3</sub>O<sub>4</sub> magnetic nanoparticles (MNPs) as reusable catalyst for the synthesis of chromene derivatives using multicomponent reaction of 4-hydroxycumarin basis on cheletropic reaction. *J Heterocycl Chem* 54:2906–2911. <https://doi.org/10.1002/jhet.2900>
- Fan Q, He S, Hao L et al (2017) Photodeposited Pd nanoparticles with disordered structure for phenylacetylene semihydrogenation. *Sci Rep* 7:42172. <https://doi.org/10.1038/srep42172>
- Feng H, Li Y, Lin S et al (2014) Nano Cu-catalyzed efficient and selective reduction of nitroarenes under combined microwave and ultrasound irradiation. *Sustain Chem Process* 2:14
- Feng W, Huang T, Gao L et al (2018) Textile-supported silver nanoparticles as a highly efficient and recyclable heterogeneous catalyst for nitroaromatic reduction at room temperature. *RSC Adv* 8:6288–6292. <https://doi.org/10.1039/c7ra13257c>
- Forouzandehdel S, Meskini M, Rami MR (2020) Design and application of (Fe<sub>3</sub>O<sub>4</sub>)-GO TfOH based AgNPs doped starch/PEG-poly (acrylic acid) nanocomposite as the magnetic nanocatalyst and the wound dress. *J Mol Struct* 1214:128142. <https://doi.org/10.1016/j.molstruc.2020.128142>
- Fountoulaki S, Daikopoulou V, Gkizis PL et al (2014) Mechanistic studies of the reduction of nitroarenes by NaBH<sub>4</sub> or hydrosilanes catalyzed by supported gold nanoparticles. *ACS Catal* 4:3504–3511. <https://doi.org/10.1021/cs500379u>
- Fusini G, Rizzo F, Angelici G et al (2020) Polyvinylpyridine-supported palladium nanoparticles: an efficient catalyst for Suzuki–Miyaura coupling reactions. *Catalysts* 10:330. <https://doi.org/10.3390/catal10030330>
- Gabriel CM, Lee NR, Bigorne F et al (2016) Effects of co-solvents on reactions run under micellar catalysis conditions. *Org Lett* 19:194–197. <https://doi.org/10.1021/acs.orglett.6b03468>
- Ganji N, Karimi B, Najafvand-derikvandi S, Vali H (2020) Palladium supported on a novel ordered mesoporous polypyrrole/carbon nanocomposite as a powerful heterogeneous catalyst for the aerobic oxidation of alcohols to carboxylic acids and ketones on water. *RSC Adv* 10:13616–13631. <https://doi.org/10.1039/c9ra10941b>
- Gao S, Zhao N, Shu M, Che S (2010) Palladium nanoparticles supported on MOF-5: a highly active catalyst for a ligand- and copper-free Sonogashira coupling reaction. *Appl Catal A Gen* 388:196–201. <https://doi.org/10.1016/j.apcata.2010.08.045>
- Gao C, Lyu F, Yin Y (2021) Encapsulated metal nanoparticles for catalysis. *Chem Rev* 121:834–881. <https://doi.org/10.1021/acs.chemrev.0c00237>
- Gawande MB, Rathil AK, Branco PS, Varma RS (2013) Sustainable utility of magnetically recyclable nano-catalysts in water: applications in organic synthesis. *Appl Sci* 3:656–674. <https://doi.org/10.3390/app3040656>
- Gawande MB, Shelke SN, Zboril R, Varma RS (2014) Microwave-assisted chemistry: synthetic applications for rapid assembly of nanomaterials and organics. *Acc Chem Res* 47:1338–1348. <https://doi.org/10.1021/ar400309b>
- Gawande MB, Goswami A, Asefa T et al (2016) Cu and Cu-based nanoparticles: synthesis and applications in catalysis. *Chem Rev* 116:3722–3811. <https://doi.org/10.1021/acs.chemrev.5b00482>
- Gebre SH (2021) Recent developments in the fabrication of magnetic nanoparticles for the synthesis of trisubstituted pyridines and imidazoles: a green approach. *Synth Commun* 51:1669–1699. <https://doi.org/10.1080/00397911.2021.1900257>
- Gebre SH, Sendeku MG (2019) New frontiers in the biosynthesis of metal oxide nanoparticles and their environmental applications: an overview. *SN Appl Sci* 1:928. <https://doi.org/10.1007/s42452-019-0931-4>
- Ghasemzadeh MA, Safaei-ghomi J (2015) Synthesis and characterization of ZnO nanoparticles: application to one-pot synthesis of benzo [b][1,5] diazepines. *Cogent Chem* 1:1095060. <https://doi.org/10.1080/23312009.2015.1095060>
- Ghobadi M, Razi MK, Javahershenas R, Kazemi M (2021) Nanomagnetic reusable catalysts in organic synthesis. *Synth Commun* 51:647–669. <https://doi.org/10.1080/00397911.2020.1819328>
- Ghorbani-choghamarani A, Norouzi M (2016) Suzuki, Stille and Heck cross-coupling reactions catalyzed by Fe<sub>3</sub>O<sub>4</sub>@PTA–Pd as a recyclable and efficient nanocatalyst in green solvents. *New J Chem* 40:6299–6307. <https://doi.org/10.1039/c6nj00088f>
- Göksu H, Burhan H, Mustafov SD, Şen F (2020a) Oxidation of benzyl alcohol compounds in the presence of carbon hybrid supported platinum nanoparticles (Pt@CHs) in oxygen atmosphere. *Sci Rep* 10:5439. <https://doi.org/10.1038/s41598-020-62400-5>
- Göksu H, Cellat K, Fatih Ş (2020b) Single-walled carbon nanotube supported PtNi nanoparticles (PtNi@SWCNT) catalyzed oxidation of benzyl alcohols to the benzaldehyde derivatives in oxygen atmosphere. *Sci Rep* 10:9656. <https://doi.org/10.1038/s41598-020-66492-x>
- Goksu H, Sen F (2020) Handy and highly efficient oxidation of benzylic alcohols to the benzaldehyde derivatives using heterogeneous Pd/AlO(OH) nanoparticles in solvent-free conditions. *Sci Rep* 10:5731. <https://doi.org/10.1038/s41598-020-62695-4>
- Goonasinghe C, Shaik M, Ratnaweera R et al (2020) A magnetically retrievable air and moisture stable gold and palladium nanocatalyst for efficient C–C coupling reactions. *R Soc Open Sci* 7:200916
- Govan J, Gun'ko YK (2014) Recent advances in the application of magnetic nanoparticles as a support for homogeneous catalysts. *Nanomaterials* 4:222–241. <https://doi.org/10.3390/nano4020222>
- Gregor C, Hermanek M, Jancik D et al (2010) The effect of surface area and crystal structure on the catalytic efficiency of iron(III) oxide nanoparticles in hydrogen peroxide decomposition. *Eur J Inorg Chem* 2010:2343–2351. <https://doi.org/10.1002/ejic.200901066>
- Grierrane A, Corma A, Garcia H (2009) Highly active and selective gold catalysts for the aerobic oxidative condensation of benzylamines to imines and one-pot, two-step synthesis of secondary benzylamines. *J Catal* 264:138–144. <https://doi.org/10.1016/j.jcat.2009.03.015>
- Gross E, Toste FD, Somorjai GA (2015) Polymer-encapsulated metallic nanoparticles as a bridge between homogeneous and heterogeneous catalysis. *Catal Lett* 145:126–138. <https://doi.org/10.1007/s10562-014-1436-9>
- Guo H, Kemell M, Al-hunaiti A et al (2011) Gold-palladium supported on porous steel fiber matrix: structured catalyst for benzyl alcohol oxidation and benzyl amine oxidation. *Catal Commun* 12:1260–1264. <https://doi.org/10.1016/j.catcom.2011.04.025>
- Hajdu V, Prekob Á, Muránszky G et al (2020) Catalytic activity of maghemite supported palladium catalyst in nitrobenzene hydrogenation. *React Kinet Mech Catal* 129:107–116. <https://doi.org/10.1007/s11144-019-01719-1>
- Harratz FA, El-hout SE, Killa HM, Ibrahim IA (2012) Palladium nanoparticles stabilized by polyethylene glycol: efficient, recyclable catalyst for hydrogenation of styrene and nitrobenzene. *J Catal* 286:184–192. <https://doi.org/10.1016/j.jcat.2011.11.001>
- Hashemi M, Khodaei MM, Teymouri M et al (2016) Preparation of NiO nanocatalyst supported on MWCNTs and its application in reduction of nitrobenzene to aniline in liquid phase. *Synth React Inorg Met Nanomet Chem* 46:959–967. <https://doi.org/10.1080/15533174.2013.862646>
- Hashimi AS, Amirul M, Mohd N et al (2019) Rapid catalytic reduction of 4-nitrophenol and clock reaction of methylene blue using copper nanowires. *Nanomaterials* 9:936
- Heuer-jungemann A, Feliu N, Bakaimi I et al (2019) The role of ligands in the chemical synthesis and applications of inorganic nanoparticles. *Chem Rev* 119:4819–4880. <https://doi.org/10.1021/acs.chemrev.8b00733>

- Hildebrand H, Mackenzie K, Kopinke F (2009) Pd/Fe<sub>3</sub>O<sub>4</sub> nanocatalysts for selective dehalogenation in wastewater treatment processes—influence of water constituents. *Appl Catal B Environ* 91:389–396. <https://doi.org/10.1016/j.apcatb.2009.06.006>
- Höfer R (2015) Sugar-and starch-based biorefineries. In: Larroche A, Rainer P, Mohammad H et al (eds) *Industrial biorefineries and white biotechnology*, 1st edn. Elsevier, pp 157–235
- Holade Y, Sahin NE, Servat K et al (2015) Recent advances in carbon supported metal nanoparticles preparation for oxygen reduction reaction in low temperature fuel cells. *Catalysts* 5:310–348. <https://doi.org/10.3390/catal5010310>
- Holz AJ, Pfeffer C, Zuo H et al (2019) In-situ generated gold nanoparticles on active carbon as reusable highly efficient catalysts for a Csp<sup>3</sup>–Csp<sup>3</sup> stille coupling. *Angew Chem Int Ed* 58:10330–10334. <https://doi.org/10.1002/anie.201902352>
- Hong K, Sajjadi M, Suh JM et al (2020) Palladium nanoparticles on assorted nanostructured supports: applications for Suzuki, Heck, and Sonogashira cross-coupling reactions. *ACS Appl Nano Mater* 3:2070–2103. <https://doi.org/10.1021/acsanm.9b02017>
- Huang Y, Zheng Z, Liu T et al (2011) Palladium nanoparticles supported on amino functionalized metal-organic frameworks as highly active catalysts for the Suzuki–Miyaura cross-coupling reaction. *Catal Commun* 14:27–31. <https://doi.org/10.1016/j.catcom.2011.07.004>
- Huang Y, Liu S, Lin Z et al (2012) Facile synthesis of palladium nanoparticles encapsulated in amine-functionalized mesoporous metal-organic frameworks and catalytic for dehalogenation of aryl chlorides. *J Catal* 292:111–117. <https://doi.org/10.1016/j.jcat.2012.05.003>
- Huang H, Wang X, Shang X et al (2018) Nitrogen-doped graphene-activated metallic nanoparticle-incorporated ordered mesoporous carbon nanocomposites for the hydrogenation of nitroarenes. *RSC Adv* 8:8898–8909. <https://doi.org/10.1039/c8ra00761f>
- Hussain SMS, Kamal MS, Hossain MK (2019) Recent developments in nanostructured palladium and other metal catalysts for organic transformation. *J Nanomater* 2019:1–17. <https://doi.org/10.1155/2019/1562130>
- Imamura K, Tsukahara H, Hamamichi K et al (2013) Simultaneous production of aromatic aldehydes and dihydrogen by photocatalytic dehydrogenation of liquid alcohols over metal-loaded titanium (IV) oxide under oxidant- and solvent-free conditions. *Appl Catal A Gen* 450:28–33. <https://doi.org/10.1016/j.apcata.2012.09.051>
- Iraqi S, Kashyap SS, Rashid H (2020) Nanoscale Advances catalyst for the selective oxidation of benzyl alcohol to benzaldehyde under mild conditions. *Nanoscale Adv* 2:5790–5802. <https://doi.org/10.1039/d0na00591f>
- Islam MS, Mia MAS (2020) Synthesis of dendrimer assisted cobalt nanoparticles and catalytic application in Heck coupling reactions in ionic liquid. *SN Appl Sci* 2:1–13. <https://doi.org/10.1007/s42452-020-2448-2>
- Jacinto MJ, Landers R, Rossi LM (2009a) Preparation of supported Pt(0) nanoparticles as efficient recyclable catalysts for hydrogenation of alkenes and ketones. *Catal Commun* 10:1971–1974. <https://doi.org/10.1016/j.catcom.2009.07.011>
- Jacinto MJ, Santos OHCF, Jardim RF et al (2009b) Preparation of recoverable Ru catalysts for liquid-phase oxidation and hydrogenation reactions. *Appl Catal A Gen* 360:177–182. <https://doi.org/10.1016/j.apcata.2009.03.018>
- Jamatia R, Saha M, Pal AK (2014) An efficient facile and one-pot synthesis of benzodiazepines and chemoselective 1,2-disubstituted benzimidazoles using a magnetically retrievable Fe<sub>3</sub>O<sub>4</sub> nanocatalyst under solvent free conditions. *RSC Adv* 4:12826–12833. <https://doi.org/10.1039/c3ra47860b>
- Jani MA, Bahrami K (2020) BNPs@Cur-Pd as a versatile and recyclable green nanocatalyst for Suzuki, Heck and Stille coupling reactions. *J Exp Nanosci* 15:182–201. <https://doi.org/10.1080/17458080.2020.1761959>
- Jawale DV, Gravel E, Geertsen V et al (2014) Size effect of gold nanoparticles supported on carbon nanotube as catalysts in selected organic reactions. *Tetrahedron* 70:6140–6145. <https://doi.org/10.1016/j.tet.2014.04.038>
- Jin L, Liu B, Duay SS, He J (2017) Engineering surface ligands of noble metal nanocatalysts in tuning the product selectivity. *Catalysts* 7:44. <https://doi.org/10.3390/catal7020044>
- Jin Q, Ma L, Zhou W et al (2020) Smart paper transformer: new insight for enhanced catalytic efficiency and reusability of noble metal nanocatalysts. *Chem Sci* 11:2915. <https://doi.org/10.1039/c9sc05287a>
- Kalbasi RJ, Nourbakhsh AA, Babaknezhad F (2011) Synthesis and characterization of Ni nanoparticles-polyvinylamine/SBA-15 catalyst for simple reduction of aromatic nitro compounds. *Catal Commun* 12:955–960. <https://doi.org/10.1016/j.catcom.2011.02.019>
- Kale SR, Kahandal SS, Gawande MB, Jayaram RV (2013) Magnetically recyclable  $\gamma$ -Fe<sub>2</sub>O<sub>3</sub>-HAP nanoparticles for the cycloaddition reaction of alkynes, halides and azides in aqueous media. *RSC Adv* 3:8184–8192. <https://doi.org/10.1039/c3ra00038a>
- Kalhor M, Zarnegar Z (2019) Fe<sub>3</sub>O<sub>4</sub>/SO<sub>3</sub>H@zeolite-Y as a novel multi-functional and magnetic nanocatalyst for clean and soft synthesis of imidazole and perimidine derivatives. *RSC Adv* 9:19333–19346. <https://doi.org/10.1039/c9ra02910a>
- Kalhor M, Zarnegar Z, Janghorban F, Mirshokraei SA (2019) Fe<sub>3</sub>O<sub>4</sub>@zeolite-SO<sub>3</sub>H as a magnetically bifunctional and retrievable nanocatalyst for green synthesis of perimidines. *Res Chem Intermed* 46:821–836. <https://doi.org/10.1007/s11164-019-03992-0>
- Kamal A, Srinivasulu V, Seshadri BN et al (2012) Water mediated Heck and Ullmann couplings by supported palladium nanoparticles: importance of surface polarity of the carbon spheres. *Green Chem* 14:2513–2522. <https://doi.org/10.1039/c2gc16430b>
- Kann N (2010) Recent applications of polymer supported organometallic catalysts in organic synthesis. *Molecules* 15:6306–6331. <https://doi.org/10.3390/molecules15096306>
- Kardanpour R, Tangestaninejad S, Mirkhani V et al (2014) Highly dispersed palladium nanoparticles supported on amino functionalized metal-organic frameworks as an efficient and reusable catalyst for Suzuki cross-coupling reaction. *J Organomet Chem* 761:127–133. <https://doi.org/10.1016/j.jorganchem.2014.03.012>
- Kazemi M (2020a) Based on magnetic nanoparticles: gold reusable nanomagnetic catalysts in organic synthesis. *Synth Commun* 50:2079–2094. <https://doi.org/10.1080/00397911.2020.1725058>
- Kazemi M (2020b) Based on CuFe<sub>2</sub>O<sub>4</sub> MNPs: magnetically recoverable nanocatalysts in coupling reactions. *Synth Commun* 50:2114–2131. <https://doi.org/10.1080/00397911.2020.1728335>
- Khan MU, Siddiqui ZN (2018) Ce@STANPs/ZrO<sub>2</sub> as nanocatalyst for multicomponent synthesis of isatin-derived imidazoles under green reaction conditions. *ACS Omega* 3:10357–10364. <https://doi.org/10.1021/acsomega.8b01043>
- Kheirjou S, Kheirjou R, Hossein A et al (2016) Selective aqueous oxidation of alcohols catalyzed by copper(II) phthalocyanine nanoparticles. *Comptes Rendus Chim* 19:314–319. <https://doi.org/10.1016/j.crci.2015.11.014>
- Khodaei MM, Dehghan M (2018) Palladium nanoparticles immobilized on Schiff base-functionalized mesoporous silica as a highly efficient and magnetically recoverable nanocatalyst for Heck coupling reaction. *Appl Organomet Chem* 33:e4618. <https://doi.org/10.1002/aoc.4618>
- Khorramabadi V, Habibi D, Heydari S (2020) Facile synthesis of tetrazoles catalyzed by the new copper nano-catalyst. *Green Chem Lett Rev* 13:50–59. <https://doi.org/10.1080/17518253.2020.1726505>

- Kidwai M, Jain A, Bhardwaj S (2012) Magnetic nanoparticles catalyzed synthesis of diverse N-heterocycles. *Mol Divers* 16:121–128. <https://doi.org/10.1007/s11030-011-9336-z>
- Kim C, Lee H (2018) Light-assisted surface reactions on metal nanoparticles. *Catal Sci Technol* 8:3718–3727. <https://doi.org/10.1039/C8CY00674A>
- Kim AY, Bae HS, Park S et al (2011a) Silver nanoparticle catalyzed selective hydration of nitriles to amides in water under neutral conditions. *Catal Lett* 141:685–690. <https://doi.org/10.1007/s10562-011-0561-y>
- Kim S, Kim E, Kim BM (2011b) Fe<sub>3</sub>O<sub>4</sub> nanoparticles: a conveniently reusable catalyst for the reduction of nitroarenes using hydrazine hydrate. *Chem Asian J* 6:1921–1925. <https://doi.org/10.1002/asia.201100311>
- Kim KD, Wang Z, Tao Y et al (2019) The comparative effect of particle size and support acidity on hydrogenation of aromatic ketones. *ChemCatChem* 11:1817–4810. <https://doi.org/10.1002/cctc.201900993>
- Kooti M, Afshari M (2012) Magnetic cobalt ferrite nanoparticles as an efficient catalyst for oxidation of alkenes. *Sci Iran* 19:1991–1995. <https://doi.org/10.1016/j.scient.2012.05.005>
- Kozell V, Giannoni T, Nocchetti M et al (2017) Immobilized palladium nanoparticles on zirconium carboxy-aminophosphonates nanosheets as an efficient recoverable heterogeneous catalyst for Suzuki–Miyaura and heck coupling. *Catalysts* 7:186. <https://doi.org/10.3390/catal7060186>
- Krishnakumar V, Kumar KM, Mandal BK, Khan FN (2012) Zinc oxide nanoparticles catalyzed condensation reaction of isocoumarins and 1,7-heptadiazine in the formation of bis-isoquinolinones. *Sci World J* 2012:1–7. <https://doi.org/10.1100/2012/619080>
- Li F, Liu Y, Wang L et al (2018) Application of heterogeneous catalysts in dechlorination of chlorophenols. In: Nuro A (ed) *Organochlorine*. IntechOpen, pp 47–63
- Li R, Zhou Z, Chen J et al (2019) The Improved hydrodechlorination catalytic reactions by concerted efforts of ionic liquid and activated carbon support. *New J Chem* 43:6659–6665. <https://doi.org/10.1039/C9NJ00273A>
- Li S, Wang J, Jin J et al (2020) Recyclable cellulose-derived—Fe<sub>3</sub>O<sub>4</sub>@Pd NPs for highly selective C–S formation by heterogeneously C–H sulfenylation of indoles. *Catal Lett* 150:2409–2414. <https://doi.org/10.1007/s10562-020-03144-9>
- Liu Y, Zhao G, Wang D, Li Y (2015) Heterogeneous catalysis for green chemistry based on nanocrystals. *Natl Sci Rev* 2:150–166. <https://doi.org/10.1093/nsr/nwv014>
- Liu M, Yu T, Huang R et al (2020) Fabrication of nanohybrids assisted by protein-based materials for catalytic applications. *Catal Sci Technol* 10:3515–3531. <https://doi.org/10.1039/c9cy02466b>
- Lolak N, Kuyuldar E, Burhan H et al (2019) Composites of palladium–nickel alloy nanoparticles and graphene oxide for the Knoevenagel condensation of aldehydes with malononitrile. *ACS Omega* 4:6848–6853. <https://doi.org/10.1021/acsomega.9b00485>
- Lu Y, Feng X, Takale BS et al (2017) Highly selective semihydrogenation of alkynes to alkenes by using an unsupported nanoporous palladium catalyst: no leaching of palladium into reaction mixture. *ACS Catal* 7:8296–8303. <https://doi.org/10.1021/acscatal.7b02915>
- Luneau M, Shirman T, Foucher AC et al (2019) Achieving high selectivity for alkyne hydrogenation at high conversions with compositionally optimized PdAu nanoparticle catalysts in raspberry colloid templated SiO<sub>2</sub>. *ACS Catal* 10:441–450. <https://doi.org/10.1021/acscatal.9b04243>
- Mahdaly MA, Zhu JS, Nguyen V, Shon Y (2019) Colloidal palladium nanoparticles for selective hydrogenation of styrene derivatives with reactive functional groups. *ACS Omega* 4:20819–20828. <https://doi.org/10.1021/acsomega.9b03335>
- Mallikarjuna K, Bathula C, Buruga K et al (2017) Green synthesis of palladium nanoparticles using fenugreek tea and their catalytic applications in organic reactions. *Mater Lett* 205:138–141. <https://doi.org/10.1016/j.matlet.2017.06.081>
- Martins LMDRS, Carabineiro SAC, Wang J et al (2017) Supported gold nanoparticles as reusable catalysts for oxidation reactions of industrial significance. *ChemCatChem* 9:1211–1221. <https://doi.org/10.1002/cctc.201601442>
- Mazloumi M, Shirini F (2020) Synthesis of quinolines, quinazolines and spiro-quinazolines using nanoporous TiO<sub>2</sub> containing an ionic liquid bridge as an efficient and reusable catalyst. *Polycycl Aromat Compd* 40:1–20. <https://doi.org/10.1080/10406638.2020.1827271>
- Mirfakhraei S, Hekmati M, Eshbala FH, Veisi H (2018) Fe<sub>3</sub>O<sub>4</sub>/PEG–SO<sub>3</sub>H as heterogeneous and magnetically recyclable nanocatalyst for oxidation of sulfides to sulfones or sulfoxides. *New J Chem* 42:1757–1761. <https://doi.org/10.1039/C7NJ02513K>
- Mitsudome T, Mikami Y, Mori H et al (2009) Supported silver nanoparticle catalyst for selective hydration of nitriles to amides in water. *Chem Commun* 14:3258–3260. <https://doi.org/10.1039/b902469g>
- Moaser GA, Ahadi A, Rouhani S et al (2020) Curbed of molybdenum oxido-diperoxido complex on ionic liquid body of mesoporous Bipy-PMO-IL as a promising catalyst for selective sulfide oxidation. *J Mol Liq* 312:113388. <https://doi.org/10.1016/j.molliq.2020.113388>
- Moghaddam FM, Foroughani BK, Rezvani HR (2015) Nickel ferrite nanoparticles: an efficient and reusable nanocatalyst for a neat, one-pot and four-component synthesis of pyrroles. *RSC Adv* 5:18092–18096. <https://doi.org/10.1039/C4RA09348H>
- Mohammadparast F, Dadgar AP, Tirumala RTA et al (2019) C–C coupling reactions catalyzed by gold nanoparticles: evidence for substrate-mediated leaching of surface atoms using localized surface plasmon resonance spectroscopy. *J Phys Chem C* 123:11539–11545. <https://doi.org/10.1021/acs.jpcc.8b12453>
- Monopoli A, Nacci A, Calò V et al (2010) Palladium/zirconium oxide nanocomposite as a highly recyclable catalyst for C–C coupling reactions in water. *Molecules* 15:4511–4525. <https://doi.org/10.3390/molecules15074511>
- Moon CW, Park J, Hong S et al (2018) Decoration of metal oxide surface with 111 form Au nanoparticles using PEGylation. *RSC Adv* 8:18442–18450. <https://doi.org/10.1039/c8ra03523g>
- Motahharifar N, Nasrollahzadeh M, Taheri-kafrani A et al (2020) Magnetic chitosan-copper nanocomposite: a plant assembled catalyst for the synthesis of amino and N-sulfonyl tetrazoles in eco-friendly media. *Carbohydr Polym* 232:115819. <https://doi.org/10.1016/j.carbpol.2019.115819>
- Mousavi SR, Nodeh HR, Foroumadi A (2019a) Magnetically recoverable graphene-based nanoparticles for the one-pot synthesis of acridine derivatives under solvent-free conditions. *Polycycl Aromat Compd* 39:1–15. <https://doi.org/10.1080/10406638.2019.1616305>
- Mousavi SR, Sereshti H, Nodeh HR, Foroumadi A (2019b) A novel and reusable magnetic nanocatalyst developed based on graphene oxide incorporated strontium nanoparticles for the facial synthesis of β-enamino ketones under solvent-free conditions. *Appl Organomet Chem* 33:e4644. <https://doi.org/10.1002/aoc.4644>
- Murugesan K, Alshammari AS, Sohail M et al (2019) Monodisperse nickel-nanoparticles for stereo- and chemoselective hydrogenation of alkynes to alkenes. *J Catal* 370:372–377. <https://doi.org/10.1016/j.jcat.2018.12.018>
- Nacci A, Cioffi N (2011) Special issue: nano-catalysts and nano-technologies for green organic synthesis. *Molecules* 16:1452–1453. <https://doi.org/10.3390/molecules16021452>

- Narayanan R (2010) Recent advances in noble metal nanocatalysts for Suzuki and Heck cross-coupling reactions. *Molecules* 15:2124–2138. <https://doi.org/10.3390/molecules15042124>
- Navarro O, Kaur H, Mahjoor P, Nolan SP (2004) Cross-coupling and dehalogenation reactions catalyzed by (N-heterocyclic carbene) Pd (allyl) Cl complexes. *J Org Chem* 69:3173–3180. <https://doi.org/10.1021/jo035834pCCC>
- Niakan M, Masteri-farahani M, Shekaari H, Karimi S (2021) Pd supported on clicked cellulose-modified magnetite-graphene oxide nanocomposite for C–C coupling reactions in deep eutectic solvent. *Carbohydr Polym* 251:117109. <https://doi.org/10.1016/j.carbpol.2020.117109>
- Panchal M, Kongor A, Mehta V et al (2018) Heck-type olefination and Suzuki coupling reactions using highly efficient oxacalix[4]arene wrapped nanopalladium catalyst. *J Saudi Chem Soc* 22:558–568. <https://doi.org/10.1016/j.jscs.2017.09.006>
- Pawar HR, Chikate RC (2021) One pot three component solvent free synthesis of N-substituted tetrazoles using RuO<sub>2</sub>/MMT catalyst. *J Mol Struct* 1225:24–26. <https://doi.org/10.1016/j.molstruc.2020.128985>
- Pérez-Lorenzo M (2012) Palladium nanoparticles as efficient catalysts for Suzuki cross-coupling reactions. *J Phys Chem Lett* 3:167–174. <https://doi.org/10.1021/jz2013984>
- Polshettiwar V, Baruwati B, Varma RS (2009) Nanoparticle-supported and magnetically recoverable nickel catalyst: a robust and economic hydrogenation and transfer hydrogenation protocol. *Green Chem* 11:127–131. <https://doi.org/10.1039/b815058c>
- Prechtl MHG, Scholten JD, Dupont J (2010) Carbon–carbon cross coupling reactions in ionic liquids catalysed by palladium metal nanoparticles. *Molecules* 15:3441–3461. <https://doi.org/10.3390/molecules15053441>
- Puthiaraj P, Ahn W (2015) Highly active palladium nanoparticles immobilized on NH<sub>2</sub>-MIL-125 as efficient and recyclable catalysts for Suzuki–Miyaura cross coupling reaction. *Catal Commun* 65:91–95. <https://doi.org/10.1016/j.catcom.2015.02.017>
- Qamar M, Elsayed RB, Alhooshani KR et al (2015) Highly efficient and selective oxidation of aromatic alcohols photocatalyzed by nanoporous hierarchical Pt/Bi<sub>2</sub>WO<sub>6</sub> in organic solvent-free environment. *ACS Appl Mater Interfaces* 7:1257–1269. <https://doi.org/10.1021/am507428r>
- Qin L, Zeng G, Lai C et al (2019) Synthetic strategies and application of gold-based nanocatalysts for nitroaromatics reduction. *Sci Total Environ* 652:93–116. <https://doi.org/10.1016/j.scitotenv.2018.10.215>
- Qiu L, Jin Y, Gong Y et al (2018) Cage-templated synthesis of highly stable palladium nanoparticles and their catalytic activities in Suzuki–Miyaura coupling. *Chem Sci* 9:676–680. <https://doi.org/10.1039/C7SC03148C>
- Rajabi F, Karimi N, Saidi R et al (2012) Unprecedented selective oxidation of styrene derivatives using a supported iron oxide nanocatalyst in aqueous medium. *Adv Synth Catal* 354:1707–1711. <https://doi.org/10.1002/adsc.201100630>
- Rasouli MA, Ranjbar PR (2013) Reductive ullmann coupling of aryl halides by palladium nanoparticles supported on cellulose, a recoverable heterogeneous catalyst. *Z Naturforsch* 68:946–950. <https://doi.org/10.5560/ZNB.2013-3048>
- Rioux RM, Song H, Hoefelmeyer JD et al (2005) High-surface-area catalyst design: synthesis, characterization, and reaction studies of platinum nanoparticles in mesoporous SBA-15 silica. *J Phys Chem B* 109:2192–2202. <https://doi.org/10.1021/jp048867x>
- Rong H, Cai S, Niu Z, Li Y (2013) Composition-dependent catalytic activity of bimetallic nanocrystals: AgPd-catalyzed hydrodechlorination of 4-chlorophenol. *ACS Catal* 3:1560–1563. <https://doi.org/10.1021/cs400282a>
- Rossi LM, Costa NJS, Silva FP, Wojcieszak R (2014) Magnetic nano-materials in catalysis: advanced catalysts for magnetic separation and beyond. *Green Chem* 16:2889–3380. <https://doi.org/10.1039/c4gc00164h>
- Rossi LM, Fiorio JL, Garcia MAS, Ferraz CP (2018) Role and fate of capping ligands in colloiddally prepared metal nanoparticle catalysts. *Dalton Trans* 47:5889–5915. <https://doi.org/10.1039/C7DT04728B>
- Rucinska E, Pattison S, Miedziak PJ et al (2020) Cinnamyl alcohol oxidation using supported bimetallic Au–Pd nanoparticles: an optimization of metal ratio and investigation of the deactivation mechanism under autoxidation conditions. *Top Catal* 63:99–112. <https://doi.org/10.1007/s11244-020-01231-0>
- Sadjadi S, Malmir M, Lazzara G et al (2020) Preparation of palladated porous nitrogen-doped carbon using halloysite as porogen: disclosing its utility as a hydrogenation catalyst. *Sci Rep* 10:2039. <https://doi.org/10.1038/s41598-020-59003-5>
- Safari J, Gandomi-Ravandi S (2014) Silver decorated multi-walled carbon nanotubes as a heterogeneous catalyst in the sonication of 2-aryl-2,3-dihydroquinazolin-4(1H)-ones. *RSC Adv* 4:11654–11660. <https://doi.org/10.1039/c3ra47811d>
- Safari J, Javadian L (2015) Ultrasound assisted the green synthesis of 2-amino-4H-chromene derivatives catalyzed by Fe<sub>3</sub>O<sub>4</sub>-functionalized nanoparticles with chitosan as a novel and reusable magnetic catalyst. *Ultrason Sonochem* 22:341–348. <https://doi.org/10.1016/j.ultsonch.2014.02.002>
- Sakon A, Ii R, Hamasaka G et al (2017) Detailed mechanism for hiyama coupling reaction in water catalyzed by linear polystyrene-stabilized PdO nanoparticles. *Organometallics* 36:1618–1622. <https://doi.org/10.1021/acs.organomet.7b00170>
- Salimi M, Esmaeli-nasrabadi F, Sandarous R (2020) Fe<sub>3</sub>O<sub>4</sub>@Hydroxycalcite-NH<sub>2</sub>-Co<sup>II</sup> NPs: a novel and extremely effective heterogeneous magnetic nanocatalyst for synthesis of the 1-substituted 1H–1, 2, 3, 4-tetrazoles. *Inorg Chem Commun* 122:108287. <https://doi.org/10.1016/j.inoche.2020.108287>
- Samsou D, Brahmaya M, Govindh B, Murthy YLN (2018) Green synthesis & catalytic study of sucrose stabilized Pd nanoparticles in reduction of nitro compounds to useful amines. *S Afr J Chem Eng* 25:110–115. <https://doi.org/10.1016/j.sajce.2017.11.006>
- Sankar M, He Q, Engel RV et al (2019) Role of the support in gold-containing nanoparticles as heterogeneous catalysts. *Chem Rev* 120:3890–3938. <https://doi.org/10.1021/acs.chemrev.9b00662>
- Santra S, Bagdi AK, Majee A, Hajra A (2013) Metal nanoparticles in “on-water” organic synthesis: one-pot nano CuO catalyzed synthesis of isoindolo[2,1-a]quinazolines. *RSC Adv* 3:24931–24935. <https://doi.org/10.1039/c3ra43917h>
- Sawoo S, Srimani D, Dutta P et al (2009) Size controlled synthesis of Pd nanoparticles in water and their catalytic application in C–C coupling reactions. *Tetrahedron* 65:4367–4374. <https://doi.org/10.1016/j.tet.2009.03.062>
- Sengupta D, Bhowmik K, De G, Basu B (2017) Ni nanoparticles on RGO as reusable heterogeneous catalyst: effect of Ni particle size and intermediate composite structures in C–S cross-coupling reaction. *Beilstein J Org Chem* 13:1796–1806. <https://doi.org/10.3762/bjoc.13.174>
- Seo YS, Ahn E, Park J et al (2017) Catalytic reduction of 4-nitrophenol with gold nanoparticles synthesized by caffeic acid. *Nanoscale Res Lett* 12:7. <https://doi.org/10.1186/s11671-016-1776-z>
- Shaker M, Elhamifar D (2021) Magnetic Ti-containing phenylene-based mesoporous organosilica: a powerful nanocatalyst with high recoverability. *Colloids Surf A* 608:125603. <https://doi.org/10.1016/j.colsurfa.2020.125603>
- Sharma N, Ojha H, Pathak DP, Sharma RK (2015) Preparation and catalytic applications of nanomaterials: a review. *RSC Adv* 5:53381–53403. <https://doi.org/10.1039/c5ra06778b>

- Sharma AS, Kaur H, Shah D (2016a) Selective oxidation of alcohols by supported gold nanoparticles: recent advances. *RSC Adv* 6:28688–28727. <https://doi.org/10.1039/C5RA25646A>
- Sharma RK, Dutta S, Sharma S et al (2016b) Fe<sub>3</sub>O<sub>4</sub> (iron oxide)-supported nanocatalysts: synthesis, characterization and applications in coupling reactions. *Green Chem* 18:3184–3209. <https://doi.org/10.1039/b000000x>
- Sharma AK, Josh H, Singh AK (2020) Catalysis with magnetically retrievable and recyclable nanoparticles layered with Pd(0) for C–C/C–O coupling in water. *RSC Adv* 10:6452–6459. <https://doi.org/10.1039/c9ra10618a>
- Sherborne GJ, Adomeit S, Menzel R et al (2017) Origins of high catalyst loading in copper(I)-catalysed Ullmann–Goldberg C–N coupling reactions. *Chem Sci* 8:7203–7210. <https://doi.org/10.1039/c7sc02859h>
- Shokouhimehr M (2015) Magnetically Separable and sustainable nanostructured catalysts for heterogeneous reduction of nitroaromatics. *Catalysts* 5:534–560. <https://doi.org/10.3390/catal5020534>
- Shokouhimehr M, Hong K, Lee TH et al (2018) Magnetically retrievable nanocomposite adorned with Pd nanocatalysts: efficient reduction of nitroaromatics in aqueous media. *Green Chem* 20:3809–3817. <https://doi.org/10.1039/C8GC01240G>
- Shokouhimehr M, Yek SM, Nasrollahzadeh M et al (2019) Palladium nanocatalysts on hydroxyapatite: green oxidation of alcohols and reduction of nitroarenes in water. *Appl Sci* 9:4183. <https://doi.org/10.3390/app9194183>
- Sravanthi K, Ayodhya D, Swamy PY (2019) Green synthesis, characterization and catalytic activity of 4-nitrophenol reduction and formation of benzimidazoles using bentonite supported zero valent iron nanoparticles. *Mater Sci Energy Technol* 2:298–307. <https://doi.org/10.1016/j.mset.2019.02.003>
- Srimani D, Sawoo S, Sarkar A (2007) Convenient synthesis of palladium nanoparticles and catalysis of hiyama coupling reaction in water. *Org Lett* 9:3639–3642
- Stankus DP, Lohse SE, Hutchison JE, Nason A (2011) Interactions between natural organic matter and gold nanoparticles stabilized with different organic capping agents. *Environ Sci Technol* 45:3238–3244. <https://doi.org/10.1021/es102603p>
- Stein M, Wieland J, Steurer P et al (2011) Iron Nanoparticles supported on chemically-derived graphene: catalytic hydrogenation with magnetic catalyst separation. *Adv Synth Catal* 353:523–527. <https://doi.org/10.1002/adsc.201000877>
- Su C, Zhao S, Wang P et al (2016) Synthesis and characterization of ultra fine palladium nanoparticles decorated on 2D magnetic graphene oxide nanosheets and their application for catalytic reduction of 4-nitrophenol. *J Environ Chem Eng* 4:3433–3440. <https://doi.org/10.1016/j.jece.2016.07.021>
- Subodh MNK, Chaudhary K et al (2018) Fur-imine-functionalized graphene oxide-immobilized copper oxide nanoparticle catalyst for the synthesis of xanthene derivatives. *ACS Omega* 3:16377–16385. <https://doi.org/10.1021/acsomega.8b01781>
- Sun X, Lin J, Chen Y et al (2019) Unravelling platinum nanoclusters as active sites to lower the catalyst loading for formaldehyde oxidation. *Commun Chem* 2:27. <https://doi.org/10.1038/s42004-019-0129-0>
- Sun B, Ning L, Zeng HC (2020) Confirmation of Suzuki–Miyaura cross-coupling reaction mechanism through synthetic architecture of nanocatalysts. *J Am Chem Soc* 142:13823–13832. <https://doi.org/10.1021/jacs.0c04804>
- Suramwar NV, Thakare SR, Khaty NT (2016) One pot synthesis of copper nanoparticles at room temperature and its catalytic activity. *Arab J Chem* 9:S1807–S1812. <https://doi.org/10.1016/j.arabjc.2012.04.034>
- Taheri-ledari R, Mirmohammadi SS, Valadi K et al (2020) Convenient conversion of hazardous nitrobenzene derivatives to aniline analogues by Ag nanoparticles, stabilized on a naturally magnetic pumice/chitosan substrate. *RSC Adv* 10:43670–43681. <https://doi.org/10.1039/d0ra08376c>
- Tahmasbi B, Ghorbani-Choghamarani A, Moradi P (2020) Palladium fabricated on boehmite as an organic–inorganic hybrid nanocatalyst for the C–C cross coupling and homoselective cycloaddition reactions. *New J Chem* 44:3717–3727. <https://doi.org/10.1039/C9NJ06129K>
- Tamoradi T, Ghadermazi M, Ghorbani-choghamarani A (2019) SBA-15@ABA-M (M = Cu, Ni and Pd): three efficient, novel and green catalysts for oxidative coupling of thiols under mild reaction conditions. *J Saudi Chem Soc* 23:846–855. <https://doi.org/10.1016/j.jscs.2019.02.003>
- Tang L, Guo X, Li Y et al (2013) Pt, Pd and Au nanoparticles supported on a DNA–MMT hybrid: efficient catalysts for highly selective oxidation of primary alcohols to aldehydes, acids and esters. *Chem Commun* 49:5213–5215. <https://doi.org/10.1039/c3cc41545g>
- Tanna JA, Chaudhary RG, Gandhare NV et al (2016) Copper nanoparticles catalysed an efficient one-pot multicomponents synthesis of chromenes derivatives and its antibacterial activity. *J Exp Nanosci* 11:884–900. <https://doi.org/10.1080/17458080.2016.1177216>
- Targhan H, Hassanpour A, Sohrabnezhad S, Bahrami K (2020) Palladium nanoparticles immobilized with polymer containing nitrogen-based ligand: a highly efficient catalyst for Suzuki–Miyaura and Mizoroki–Heck coupling reactions. *Catal Lett* 150:660–673. <https://doi.org/10.1007/s10562-019-02981-7>
- Thakore SI, Rathore PS (2015) Nanoparticle-assisted organic transformations. In: Aliofkhaezai M (ed) *Handbook of nanoparticles*. Springer International Publishing, Geneva, pp 1–28
- Thwin M, Mahmoudi B, Ivaschuk OA, Yousif QA (2019) An efficient and recyclable nanocatalyst for the green and rapid synthesis of biologically active polysubstituted pyrroles and 1,2,4,5-tetrasubstituted imidazole derivatives. *RSC Adv* 9:15966–15975. <https://doi.org/10.1039/c9ra02325a>
- Ulucan-altuntas K, Debik E (2020) Dechlorination of dichlorodiphenyltrichloroethane (DDT) by Fe/Pd bimetallic nanoparticles: comparison with nZVI, degradation mechanism, and pathways. *Front Environ Sci Eng* 14:17. <https://doi.org/10.1007/s11783-019-1196-2>
- Varma RS (2014) Nano-catalysts with magnetic core: sustainable options for greener synthesis. *Sustain Chem Process* 2:11
- Varma RS (2016) Greener and sustainable trends in synthesis of organics and nanomaterials. *ACS Sustain Chem Eng* 4:5866–5878. <https://doi.org/10.1021/acssuschemeng.6b01623>
- Veisi H, Karmakar B, Tamoradi T et al (2021) Bio-inspired synthesis of palladium nanoparticles fabricated magnetic Fe<sub>3</sub>O<sub>4</sub> nanocomposite over *Fritillaria imperialis* flower extract as an efficient recyclable catalyst for the reduction of nitroarenes. *Sci Rep* 11:4515. <https://doi.org/10.1038/s41598-021-83854-1>
- Venkatesan P, Santhanalakshmi J (2010) Designed synthesis of Au/Ag/Pd Trimetallic nanoparticle-based catalysts for sonogashira coupling reactions. *Langmuir* 26:12225–12229. <https://doi.org/10.1021/la101088d>
- Verma A, Shukla M, Sinha I (2019) Introductory chapter: salient features of nanocatalysis. In: Sinha I (ed) *Nanocatalysts*. IntechOpen, pp 1–8
- Wang D, Astruc D (2014) Fast-growing field of magnetically recyclable nanocatalysts. *Chem Rev* 114:6949–6985. <https://doi.org/10.1021/cr500134h>
- Wang H, Yan J, Chang W, Zhang Z (2009) Practical synthesis of aromatic amines by photocatalytic reduction of aromatic nitro compounds on nanoparticles N-doped TiO<sub>2</sub>. *Catal Commun* 10:989–994. <https://doi.org/10.1016/j.catcom.2008.12.045>



- Wang X, Ding X, Zou H (2020) Mesoporous silica nanosheets with tunable pore lengths supporting metal nanoparticles for enhanced hydrogenation reactions. *Catalysts* 10:12
- Woo H, Mohan B, Heo E et al (2013) CuO hollow nanosphere-catalyzed cross-coupling of aryl iodides with thiols. *Nanoscale Res Lett* 8:390
- Wu C, Chen D (2012) Spontaneous synthesis of gold nanoparticles on gum arabic-modified iron oxide nanoparticles as a magnetically recoverable nanocatalyst. *Nanoscale Res Lett* 3:317
- Wu L, Mendoza-garcia A, Li Q, Sun S (2016) Organic phase syntheses of magnetic nanoparticles and their applications. *Chem Rev* 116:10473–10512. <https://doi.org/10.1021/acs.chemrev.5b00687>
- Xiao J, Zhang H, Ejike AC et al (2021) Phenanthroline functionalized polyacrylonitrile fiber with Pd (0) nanoparticles as a highly active catalyst for the Heck reaction. *React Funct Polym* 161:104843. <https://doi.org/10.1016/j.reactfunctpolym.2021.104843>
- Xu S, Yang Q (2008) Well-dispersed water-soluble Pd nanocrystals: facile reducing synthesis and application in catalyzing organic reactions in aqueous media. *J Phys Chem C* 112:13419–13425
- Xu X, Wo J, Zhang J et al (2009) Catalytic dechlorination of p-NCB in water by nanoscale Ni/Fe. *Desalination* 242:346–354. <https://doi.org/10.1016/j.desal.2008.06.003>
- Yan Z, Xie X, Song Q et al (2020) Tandem selective reduction of nitroarenes catalyzed by palladium nanoclusters. *Green Chem* 22:1301–1307. <https://doi.org/10.1039/C9GC03957K>
- Yarmohammadi N, Ghadermazi M, Mozafari R (2021) Copper based on diamionaphthalene-coated magnetic nanoparticles as robust catalysts for catalytic oxidation reactions and C–S cross-coupling reactions. *RSC Adv* 11:9366–9380. <https://doi.org/10.1039/d1ra01029h>
- Zamani A, Marjani AP, Nikoo A et al (2018) Synthesis and characterization of copper nanoparticles on walnut shell for catalytic reduction and C–C coupling reaction. *Inorg Nanomet Chem* 48:176–181. <https://doi.org/10.1080/24701556.2018.1503676>
- Zeynizadeh B, Mohammadzadeh I, Shokri Z, Hosseini SA (2017) Synthesis and characterization of NiFe<sub>2</sub>O<sub>4</sub>@Cu nanoparticles as a magnetically recoverable catalyst for reduction of nitroarenes to arylamines with NaBH<sub>4</sub>. *J Colloid Interface Sci* 500:285–293. <https://doi.org/10.1016/j.jcis.2017.03.030>
- Zhang K, Suh JM, Choi J et al (2019a) Recent advances in the nanocatalyst-assisted NaBH<sub>4</sub> reduction of nitroaromatics in water. *ACS Omega* 4:483–495. <https://doi.org/10.1021/acsomega.8b03051>
- Zhang Q, Yang X, Guan J (2019b) Applications of magnetic nanomaterials in heterogeneous catalysis. *ACS Appl Nano Mater* 2:4681–4697. <https://doi.org/10.1021/acsnm.9b00976>
- Zhang K, Hwan J, Yeon S et al (2020) Pd modified prussian blue frameworks: multiple electron transfer pathways for improving catalytic activity toward hydrogenation of nitroaromatics. *Mol Catal* 492:110967. <https://doi.org/10.1016/j.mcat.2020.110967>
- Zhao J, Ge L, Yuan H et al (2019a) Heterogeneous gold catalysts for selective hydrogenation: from nanoparticles to atomically precise nanoclusters. *Nanoscale* 11:11429–11436. <https://doi.org/10.1039/c9nr03182k>
- Zhao J, Hernández WY, Zhou W et al (2019b) Selective oxidation of alcohols to carbonyl compounds over small size colloidal Ru nanoparticles. *ChemCatChem* 12:238–247. <https://doi.org/10.1002/cctc.201901249>
- Zhao B, Dong Z, Wang Q et al (2020a) Highly efficient mesoporous core-shell structured Ag@SiO<sub>2</sub> nanosphere as an environmentally friendly catalyst for hydrogenation of nitrobenzene. *Nanomaterials* 10:883. <https://doi.org/10.3390/nano10050883>
- Zhao M, Wu Y, Cao J-P (2020b) Carbon-based material-supported palladium nanocatalysts in coupling reactions: discussion on their stability and heterogeneity. *Appl Organomet Chem* 34:e5539. <https://doi.org/10.1002/aoc.5539>
- Zheng W, Tan R, Zhao L et al (2014) Mn<sup>2+</sup>/graphene oxide nanocomposite efficiently catalyzes the epoxidation of alkenes with H<sub>2</sub>O<sub>2</sub>. *RSC Adv* 4:11732–11739. <https://doi.org/10.1039/c3ra47183g>
- Zhi-tao W (2020) Cycloaddition of propargylic amines and CO<sub>2</sub> by Ni@Pd nanoclusters confined within metal-organic framework cavities in aqueous solution. *Catal Lett* 150:2352–2364. <https://doi.org/10.1007/s10562-019-03072-3>
- Zhou P, Li D, Jin S et al (2016) Catalytic transfer hydrogenation of nitro compounds into amines over magnetic graphene oxide supported Pd nanoparticles. *Int J Hydrogen Energy* 41:15218–15224. <https://doi.org/10.1016/j.ijhydene.2016.06.257>
- Zhu Q, Xu Q (2016) Immobilization of ultrafine metal nanoparticles to high-surface-area materials and their catalytic applications. *Chem* 1:220–245. <https://doi.org/10.1016/j.chempr.2016.07.005>
- Zhu J, Tao G, Liu H et al (2014) Aqueous-phase selective hydrogenation of phenol to cyclohexanone over soluble Pd nanoparticles. *Green Chem* 16:2664–2669. <https://doi.org/10.1039/c3gc42408a>

**Publisher's Note** Springer Nature remains neutral with regard to jurisdictional claims in published maps and institutional affiliations.